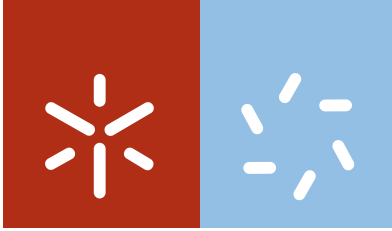**Universidade do Minho**

Escola de Ciências

Juan Alberto Panadero Pérez

**Biomaterials for cartilage tissue
engineering under mechanical stimulus**

julho de 2014

Universidade do Minho
Escola de Ciências

Juan Alberto Panadero Pérez

**Biomaterials for cartilage tissue
engineering under mechanical stimulus**

Tese de Doutoramento em Ciências
Especialidade de Física

Trabalho realizado sob a orientação do
Professor Doutor Senen Lanceros Méndez
e do
Professor Doutor José Luis Gómez Ribelles

julho de 2014

DECLARAÇÃO

Nome: Juan Alberto Panadero Pérez

Endereço electrónico: jualpanadero@gmail.com

 Título da tese: Biomaterials for cartilage tissue engineering under mechanical stimulus

Orientadores: Senen Lanceros Méndez, José Luis Gómez Ribelles

Ano de conclusão: 2014

Designação do Doutoramento: Doutoramento em Ciências, Especialidade de Física

Universidade do Minho, ___/___/_____

Assinatura: _____

Acknowledgements

This thesis would not be possible without the help and support of many people. First of all, I want to acknowledge to my supervisors, Senentxu, who gave me the opportunity to make the PhD, and supported me throughout all the steps until the end, and to José Luis, who not only helped us in developing all the work, but also introduced me in this area since my bachelor days.

To my fathers and the rest of my family, for the support, especially to my uncle Alberto, because he encouraged me in the worst moments.

To all my friends, the old ones from Valencia and the new ones from Portugal.

To my colleagues in Physics, for the advice in preparing this thesis, specially to Vitor Sencadas, for all the teaching of new concepts, and to Clarisse Ribeiro and Vitor Correia.

To Miguel Gama and all his group from DEB, especially João Pedro Silva, to allow to us to work in their lab and for the help provided, and to Carina Silva and Leon Kluskens from the same department, for allowing to use the qPCR equipments for the final chapter.

To Line Vikingsson, for all the help using equipment in Valencia, and to all the rest of the people from the Centro de Biomateriales e Ingeniería Tisular (CBIT)

Abstract

Tissue engineering is being explored as a suitable strategy to repair tissues that have no capability of regenerating by themselves, such as articular hyaline cartilage in the knee. This strategy involves the combination of cells and scaffold biomaterials, able to support the adhesion of cells and their guidance into differentiation. In the knee, the scaffolds have to bear cyclical stress and compressive loading. Therefore, the mechanical properties of the scaffolds are a key component to understand their performance in animal models and clinical trials. In this work, a new methodology has been developed to analyze the mechanical properties of scaffolds for cartilage tissue engineering by studying the fatigue behavior of macroporous poly-ε-caprolactone PCL scaffolds under cyclic loading in different conditions.

The PCL scaffolds in dry state were compared with scaffolds under immersion in water, in order to determine the hydrodynamic effects in resistance to fatigue by analyzing the evolution of the dissipated energy with the help of the Morrow's model. Moreover, the effect of fibrin hydrogel inside the pores was determined. This has been performed due to the fact that fibrin is a component in chirurgical interventions and can be a suitable matrix for cell differentiation in tissue engineering. It was found that water inside the pores plays a critical effect improving resistance to fatigue. On the other hand, the fibrin clot does not represent a relevant factor in determining the mechanical properties, when compared with water.

The same analysis was carried out in PCL scaffold combined with poly(vynil-alcohol) PVA hydrogel, an *in vitro* model of growing tissue inside the pores, in order to study how the addition of a third material resembling some aspects of tissue, can affect the mechanical response. It was concluded that the resistance to fatigue improved when the PVA hydrogel increased in stiffness. Further, the experimental data deviated from the model after few cycles, meaning that unknown effects were taking place inside the pores.

This methodology was also implemented in scaffolds with chondrogenic precursors seeded inside the pores in order to study the variations in the fatigue behavior due to the produced

extracellular matrix. To simulate some mechanical conditions during cell culture, a bioreactor was designed, capable of applying mechanical compression in multiple samples at the same time. The fabrication of the bioreactor implied the development of the corresponding electronics and mechanics suited to cell incubator environment, as well as sterility tests.

Thus, PCL scaffolds were seeded with chondrogenic precursor cells and fibrin and some of them were submitted to free swelling and others to cyclic loading in the bioreactor. All the samples were analyzed for fatigue. Moreover, some components of the extracellular matrix were identified. No differences were observed between samples undergoing free swelling or loading conditions, neither respect to matrix components nor to mechanical performance to fatigue. The extracellular matrix did not achieve in any case all the desired chondrogenic traits. However, an interesting fact was found: when compared with PCL and PCL with PVA under immersion, the extracellular matrix properties improved fatigue resistance, despite the fact that the measured elastic modulus at the first cycle was similar in all the cases. This is interesting as it corroborates the hypothesis that fatigue analysis in tissue engineering constructs can provide additional information missed with traditional measurements.

Different factors in these constructs, from the porosity – that influences, among others, water uptake - , to the characteristics of the hydrogel or cellular matrix within them, determine the evolution of fatigue resistance to specific cyclic loading. These effects should be considered for developing predictive models that provide information beyond the traditional mechanical measurements in cartilage tissue engineering.

Resumo

A engenharia de tecidos está a ser explorada como uma estratégia adequada para a reparação de tecidos que não possuem a capacidade de regenerarem-se, como por exemplo, a cartilagem hialina do joelho. Esta estratégia combina células e biomateriais (*scaffolds*), com a capacidade de suportar a adesão das células e a sua diferenciação. No joelho, os *scaffolds* têm de suportar tensões e cargas de compressão cíclica. Desta forma, as propriedades mecânicas dos *scaffolds* são um fator chave para perceber o seu desempenho em modelos animais e ensaios clínicos. Neste trabalho, foi desenvolvida uma nova metodologia para analisar as propriedades mecânicas dos *scaffolds* para engenharia de tecidos de cartilagem, através do estudo do comportamento de fadiga dos *scaffolds* macroporosos de poli-ε-caprolactona (PCL) sob cargas cíclicas em diferentes condições.

Os *scaffolds* de PCL secos foram comparados com *scaffolds* imersos em água para determinar os efeitos hidrodinâmicos na resistência à fadiga, analisando a evolução da energia dissipada com ajuda do modelo de Morrow. Além disso, o efeito de um hidrogel de fibrina no interior dos poros também foi determinado. A utilização da fibrina prende-se com o facto de esta ser um compoente usado em intervenções cirúrgicas, sendo também uma matriz adequada para a diferenciação celular em engenharia de tecidos. Verificou-se ainda que a água no interior dos poros possui um efeito crítico na melhoria da resistência à fadiga. Por outro lado, o coágulo de fibrina não representa um fator determinante nas propriedades mecânicas, quando comparado com a água.

A mesma análise foi realizada em *scaffolds* de PCL combinados com um hidrogel de poli(vinil-álcool) – PVA, um material que serve como modelo *in vitro* de tecido em crescimento dentro dos poros, de forma a estudar como a adição de um terceiro material, semelhante ao tecido, pode afetar a resposta mecânica. Assim, foi possível concluir que a resistência à fadiga melhora com o aumento da rigidez do hidrogel de PVA. Além disso, verificou-se que os dados experimentais sofreram um desvio relativamente aos dados do modelo teórico após poucos ciclos, o que significa que sucederam efeitos indeterminados no interior dos poros.

Esta metodologia foi também aplicada em *scaffolds* com precursores condrogênicos colocados no interior dos poros, com o objetivo de estudar as variações no comportamento de

fadiga causado pela matriz extracelular produzida. Para simular algumas das condições mecânicas durante o cultivo celular foi desenvolvido um bioreactor com a capacidade de aplicar uma compressão mecânica a múltiplas amostras ao mesmo tempo. O fabrico do bioreactor implicou o desenvolvimento das correspondentes partes eletrónica e mecânica, adequadas ao ambiente da incubadora de células, assim como aos testes de esterilização.

As células precursoras condrogênicas foram introduzidas nos *scaffolds* de PCL com fibrina, sendo parte deles submetidos a condições estáticas sem carga e outros com cargas cíclicas através da utilização do bioreactor. O comportamento de fadiga foi analisado para todas as amostras. Alguns componentes da matriz extracelular foram identificados. Verificou-se que comparando as amostras obtidas em condições estáticas e dinâmicas, nenhuma diferença foi encontrada quer para as propriedades mecânicas quer nas componentes da matriz. Além disso, constatou-se que a matriz extracelular não chegou a obter as características condrogênicas desejadas em nenhuma dessas amostras. Contudo, um facto interessante foi observado: aquando a comparação com as amostras de PCL em imersão com PVA, as propriedades da matriz extracelular melhoram a resistência à fadiga, apesar do módulo elástico medido no primeiro ciclo ser semelhante em todas as amostras. Isto é interessante uma vez que reforça a hipótese de que a análise da fadiga em engenharia de tecidos pode fornecer informações adicionais relativamente às medições tradicionais.

Os diferentes fatores nestas amostras, desde a porosidade – que influência, entre outros, o movimento da água no interior do scaffold – até às características do hidrogel ou da matriz no seu interior, determinam a evolução da resistência à fadiga para uma carga cíclica específica. Estes efeitos devem ser considerados para o desenvolvimento de modelos de previsão que forneçam informação para além das medições mecânicas tradicionais em engenharia de tecidos da cartilagem.

Table of contents

List of Acronyms

CryoSEM –Scanning Electron Microscopy. Cryo because sublimation of wáter it is used in vacuum after freezing the sample

DMEM – Dulbecco's Modified Eagle's Medium

DNA – Deoxyribonucleic acid

ECM – Extracellular matrix

FXIII – Factor XIII of caoagulation

ITS – Insulin Transferrin Selenium

KUM5 – Chondroprogenitor transformed cell line

mRNA – Messenger Ribonucleic Acid

MSC – Mesenchymal Stem Cell

PCL – Poly-ε-caprolactone

PEMA – Poly(ethyl methacrylate)

PVA – Poly(vinyl alcohol)

qPCR – Quantitative Polymerase Chain Reaction

TGF-β1 – Transforming Growth Factor – β1

UV – Ulta-Violet Radiation

List of Figures

List of Tables

Chapter 1: Introduction

1.1 Articular cartilage structure

1.1.1 Overview of articular hyaline cartilage in the knee

Cartilages are a group of connective tissues that exist in humans and other animals, distributed through the body. Three major types of cartilages exist: fibrocartilage, elastic cartilage and hyaline cartilage. Articular hyaline cartilage is an avascular and highly specialized tissue that provides low friction in joints and allows for efficient load bearing and distribution, namely in the knee.

Chondrocytes are the single cells in adult articular cartilage and conform less than 5% of the tissue total volume. They do not have any direct cell-to-cell contact and each one is enclosed in cavities called lacunae (Figure 1.1). These lacunae are formed by a highly hydrated extracellular matrix (ECM). Each isolated lacuna acts as an individual functional unit responsible for maintaining the ECM metabolically. The ECM produced by the chondrocytes consists on 45-50% of collagens (90% of which is collagen type II) and 20–25% consists of different proteoglycans (predominantly aggrecan, decorin, biglycan and fibromodulin), whose negatively charged glycosaminoglycans are responsible for swelling [1]. Water uptake of the solid ECM provides special viscoelastical properties to cartilage [2]. The fluid in ECM is also a reservoir of soluble macromolecules such as growth factors, chemokines and cytokines.

The organization of these components is not uniform through all cartilage. Thus, up to four different depth zones can be defined varying in relative content and structure of the matrix components (Figure 1.2) [3]
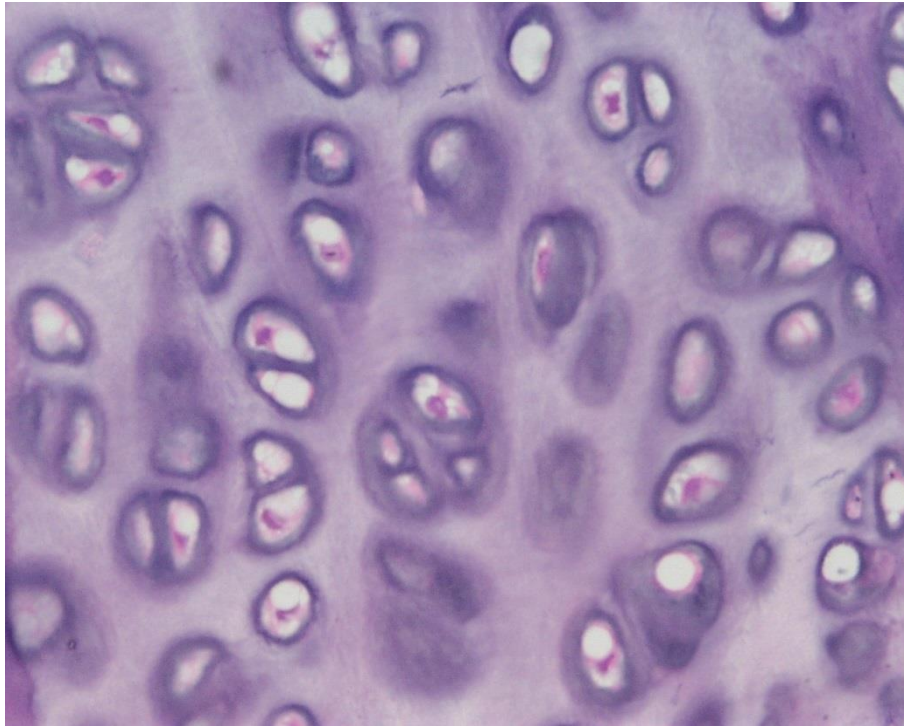
Figure 1.1 - Histological section of cartilage: Chondrocytes isolated in lacunae

1.1.2 Zonal Organization of Articular Hyaline Cartilage

The superficial zone, also known as the tangential or gliding zone, is exposed to the synovial fluid of the intraarticular space and represents 10–20% of articular cartilage thickness. In this zone elongated fusiform chondrocytes are positioned with their long axes parallel to the joint surface. The superficial zone contains the highest and lowest quantities of collagen and aggrecan, respectively. Collagen fibrils are thin and packed into fiber bundles situated parallel to both the articular surface and the long axes of the chondrocytes within this region. The superficial zone withstands shear stress and reduces friction. Further, the tensile strength of this zone is the largest of all articular cartilage zones.

Next, the middle or transitional zone comprises 40– 60% of the articular cartilage thickness, in which spherical and metabolically very active chondrocytes are randomly distributed. Like the cells inhabiting this zone, the collagen fibrils, which are the longest in all cartilage, are thicker in diameter, and more sparsely located than in the superficial zone, are randomly oriented. When articular cartilage is uncompressed, the collagen fibers arrange in a more vertical position. However, when articular cartilage is under compression, the collagen fibers reorient towards a horizontal position. Therefore, these properties make the transitional zone

able to withstand compression [3]. In this region of articular cartilage, aggrecan content reaches its maximal level.

The zone most distant from the articular surface, known as the deep, radial or radiate zone, comprises the remaining articular cartilage thickness and contains chondrocytes with ellipsoid morphology arranged in short, vertical columns. Large collagen fibrils from the deep zone spread until their insertion in the underlying calcified cartilage and subchondral cortical bone, where they are anchored. This leads to increase the shear resisting capacity of both this zone and articular cartilage as a whole. Finally, whereas the collagen content of the deep zone is similar to the midzone (67% collagen content by dry weight), aggrecan levels are significantly lower [2, 3] .

Another zone can be considered, and is the calcified zone, at the boundaries with subchondral bone, where chondrocytes become hyperthrophic chondrocytes, produce mineralization and contains high levels of collagen type X in the ECM.
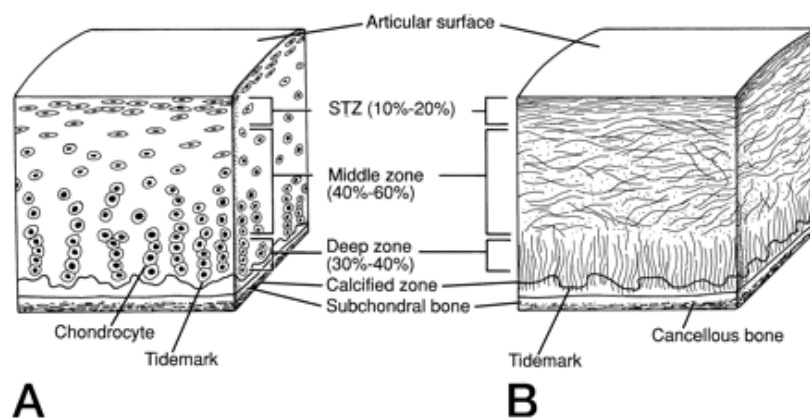
Figure 1.2 - Zones of cartilage: A) cell component, B) ECM organization. Image taken from Buckwalter et al. [4] with permission of the authors.

1.2 Embryonary and adult chondrogenesis of articular cartilage

During human embryogenesis cartilage is developed through condensation and differentiation of mesenchymal stem cells (MSCs) in limb primordia. First, undifferentiated MSCs migrate

19

to the sites of the developing cartilage. Then, MSCs assemble into compact cellular aggregates or condense through a specific combination of precartilage matrix and cell adhesion molecules, mainly N-cadherine and N-CAM [5]. This condensation allows essential cell–cell surface interactions and signaling events that conclude in differentiation to hyaline chondrocytes. Morphological changes take place in the chondrogenic progenitors, from their fibroblastic-like shape to the spherical morphology of hyaline chondrocytes, and start synthesis of transcription factors such as Sox9, which regulates the transcription and transduction of cartilage-specific ECM molecules such as collagen types II, IV, IX, and XI [6] and the highly-sulfated proteoglycan aggrecan [7]. When differentiation progresses, the expression of adhesion molecules decreases and the differentiated chondrocytes start to be isolated by the ECM. At this stage of development, there are two possible fates for hyaline chondrocytes: a) In endochondral bone development of long bones until adolescence, chondrocytes at the site of the growth plate become hypertrophic, produce alkaline phosphatase and collagen type X and are eventually reabsorbed while new bone is formed, being thus also called transient chondrocytes [8] and b) in the articular hyaline tissues, the chondrocytes remain with the mature phenotype for the rest of the lifespan of the organism, are separated in lacunae and maintain the ECM of persistent hyaline cartilage.[2] Although the mechanisms determining the two different fates remain unclear, the inhibition of N-cadherin and the route Wnt is a necessary step to differentiate into cartilage after condensation [9]

In adults, natural chondrogenesis is very limited or even practically inexistent. When a defect occurs, cartilage cannot heal spontaneously. One reason is the isolation of chondrocytes in lacunae, which hinders their migration to defect localization. The other is the lack of vascularization and innervations in cartilage - due to the limited supply of nutrients and oxygen, constrained to diffusion helped by compressive cyclic loading [10], mature chondrocytes show a low basic metabolism, and adult chondrocytes have little renewal. In some cartilage tissues a possible way to repair can be through precursor cells from the perichondrium layer, but in articular cartilage it is not possible as this layer does not exist.

Another well-known repair mechanism in articular cartilage occurs when deep cartilage defects reach down to the subchondral bone. This system is used in surgery microfracture

techniques, where a perforation of the subchondral bone initiates a contact between the blood vessels and cartilage what triggers bleeding to the defect site. A fibrin clot is formed and anchored to the bone by the increased surface roughness produced by the microperforations. This clot is capable of stimulating attraction, proliferation and differentiation of MSCs from bone marrow [10] . In the following weeks stem cells differentiate into cells with chondrocyte traits, as indicated by the high synthesis of proteoglycans. After several weeks the repair tissue is visually similar to hyaline cartilage, but really with decreased ECM content mismatching the strength and properties of normal articular cartilage. Finally, tissue undergoes degeneration to fibrocartilage with mechanical properties inadequate to keep the role of hyaline cartilage, mainly because the expression of collagen type I instead of type II [11].

This degeneration can be caused by several factors. The effect of fibrin, PDGF and other factors contained in a natural blood clot is highly chemoattractive for MSC in vitro, however, it is unclear if clot environment in vivo is optimal for chondrogenesis, as angiogenic growth factors and fibrogenic factors are predominant, situation which is different from chondrogenesis during embryogenesis, and some of them can have an antagonic effect to chondrogenic differentiation [12]. Another possible limitation is the relative low quantity of MSC in bone marrow. MSCS are only about 0.001–0.01% of the total mononucleated cells in bone marrow. If not concentrated through recruitment, only around 100 MSC would be contained in an initial clot of several milliliters, and even with factor recruitment, the number is not much higher, being typically 10^4-10^5 lower than the chondrocyte number before the defect. Finally, the resorption rate of the clot is fast and can disappear in a week , which is not enough time for the complete filling of the defect and to provide a stable environment for guiding differentiation [13]. Because all of these limitations, synthesis of appropriate ECM is mandatory.

Other approaches for regeneration are based in autologous cell source transplant. Autologous chondrocyte transplantation (ACT) consists on combined implantation of an autologous periosteal flap, taken from the same patient, and expanded harvested articular chondrocytes for posterior implantation in main defect [10]. This technique has some disadvantages such as the creation of new cartilage defects and the related morbidity, and the requirement of cell

expansion in order to obtain appropriate cell numbers to repair the defect. The latter is an important limitation because, besides low metabolic-rated chondrocytes which hinder proliferation, they also de-differentiate in monolayer culture and eventually prevent ectopic cartilage formation capacity after implantation, which can lead to fibrocartilage tissue formation. Also, the number of chondrocytes that can be extracted harmlessly is lower than the number of MSCs that can be extracted from one patient, and the extraction methods for chondrocytes are harder because require enzymatic digestion of the ECM. Cartilage Allografts have similar problems, plus immunologic rejection and disease transmission risks.

The most promising alternative therapies are thought to be found in the field of tissue engineering through the differentiation of autologous MSCs into chondrocytes in vitro. Tissue engineering approaches try to simulate the conditions found in cartilage development through growth factors, culture in 3D configuration, mostly in polymer supports, and more recently, additional epigenetic factors such as mechanical stimulation and hypoxia. All of these factors for chondrogenic differentiation will be addressed in the next sections. Many of the mechanisms of differentiation are not clear and therefore research in these systems in vitro is mandatory to understand the main phenomena involved in cartilage development in order to obtain new effective strategies for tissue repair.

A more complete insight in cartilage regeneration and cartilage tissue engineering can be found in some references [14-17]

1.3 Sources for Mesenchymal Stem Cells and culture in vitro

Bone marrow was the first tissue for obtaining MSCs and it is still the most common. The MSCs from bone marrow (bMSCs) are part of the adherent fraction from bone marrow aspirates that form round-shaped colonies composed of fibroblastoid cells, called Colony Forming Unit – fibroblasts (CFU-f) [18]. bMSCs proliferate maintaining their morphology and can differentiate into mature cells of mesenchymal lineages such as osteoblasts, chondrocytes, adipocytes, and even myoblasts (Figure 1.3) if proper signals are provided

[19]. Due to the ability of these cells to differentiate to tissues of the mesenchymal lineage, they were called mesenchymal stem or stromal cells [20]
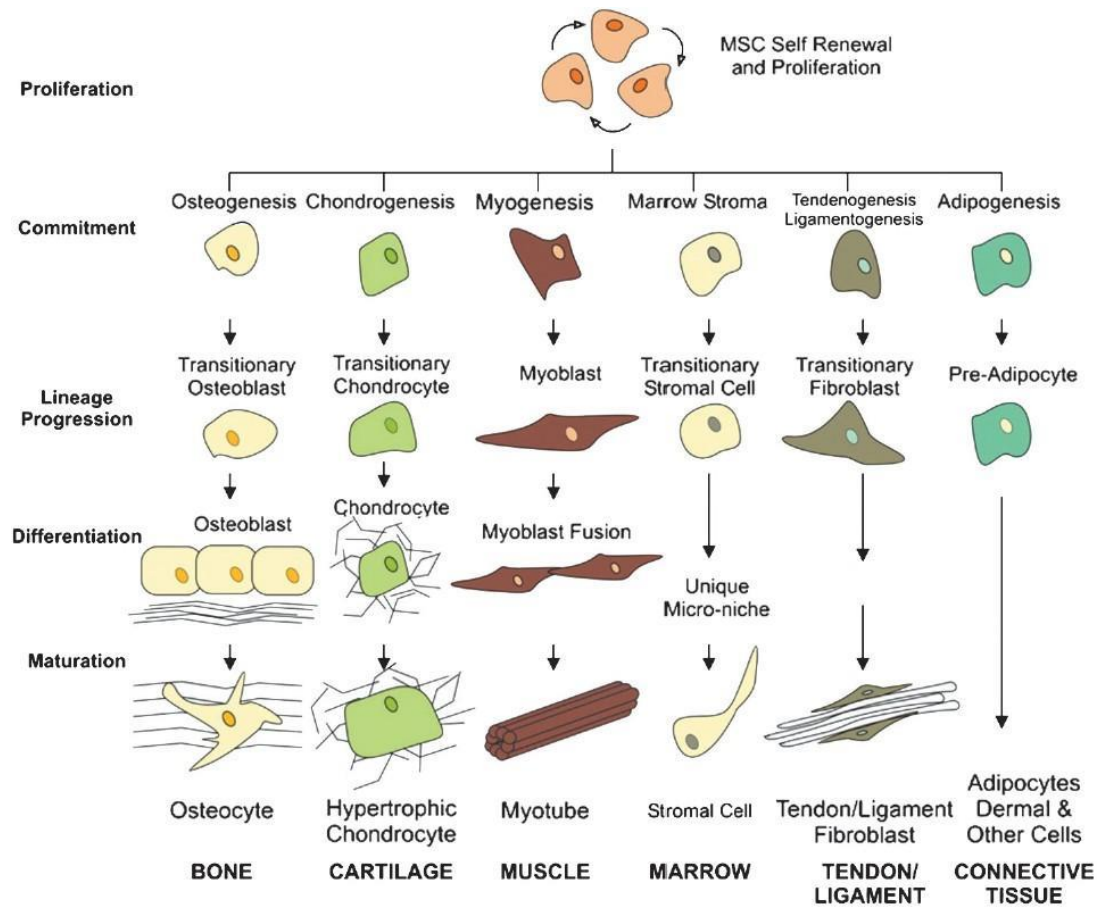
Figure 1.3 - Differentiation potential lineages of MSCs [21]

Mesenchymal stem cells have been discovered in almost all organs, being the bone marrow the most enriched MSCs reservoir. For chondrogenic differentiation, besides bone marrow MSCs, adipose tissue [22] and synovial fluid [23] MSCs have been also used, among others.

Bone marrow MSCs show also a large chondrogenic potential when compared with most of the other MSCs sources [24, 25], while often less when compared with those from synovial fluid. However, they are still the most commonly used because the simplicity in obtaining cells from bone marrow aspirates and the deep knowledge on them.

In 2006, the International Society for Cell Therapy proposed the following criteria for the minimal identification of human MSCs from any tissue source [26]: adherence to plastic in standard culture conditions; in vitro differentiation into osteocytes, adipocytes and

chondrocytes, among others (demonstrated by staining of in vitro cell culture); and, because the other two are not enough to distinguish from other precursor, the presence (+) or absence (-) of cell surface markers CD73+ CD34- CD19-, CD90+ , CD45- , HLA-DR- , CD14- or CD11b- , CD105+ , CD79a-,CD166+, CD44+ markers, assessed by FACS analysis. It is only possible to check these criteria after isolation and in vitro culture of MSCs, and not for their identification in vivo. They are overly dependent on culture conditions for derivation and expansion of MSC populations and, therefore, are unlikely to be extrapolated to native cells [13]. It is also not possible to distinguish subpopulations with more or less potential for differentiation into a specific lineage. Other problem is that most of these surface markers are still expressed in differentiated tissues and many are not exclusive of a differentiated lineage, thus usually do not serve to distinguish between undifferentiated and differentiated MSCs.

The different origins for MSCs introduce variation in biological properties. Even within each tissue source, single-cell-derived clonal MSC populations are known to be highly heterogeneous in their proliferative and differentiation potential. Due to this heterogeneity, which is fundamentally caused by a lack of complete profiles for each MSC subpopulation, even MSCs from the same source can have slight variations in their behavior for differentiation into a specific lineage. [13]

1.4 Chondrogenic medium

The two main factors in enhancing chondrogenic differentiation in vitro are close cell-to-cell contact, traditionally achieved by cell pellet or micromass culture, and the addition of chondrogenic bioactive factors, e.g. dexamethasone, ascorbate, transforming growth factor (TGF-β), bone morphogenetic proteins, BMPs, fibroblast growth factor (FGF) and insulin-like growth factor (IGF). Among them, dexamethasone, ascorbate and TGF-β have been shown to be most effective [27, 28]. The effects of these factors on MSCs will be discussed in more detail below.

TGF-β family molecules are the main factors to induce chondrogenesis in vitro. All TGF-β interact with a membrane heteromeric receptor that transforms their signals intracellularly

[29, 30]. Three subtypes form this family: TGF-β1, TGF-β2 and TGF-β3. It has been mostly concluded that any of the TGF-β subtypes are equally active chondrogenic factors and that there are more differences in a culture related to the batch rather than because the subtype [31]. Nevertheless, some recent studies reveal a better potential for TGF-β1 [32]. Chondrogenic fate is determined by TGF-β concentration: 10 ng·ml^{-1} TGF-β is enough for successful MSC differentiation in pellet culture and it is therefore the most used concentration in all culture systems [10]. Although TGF-β supports early- and intermediate-stage chondrogenesis, it is known to retain chondrocytes in the prehypertrophic state. Therefore TGF-β most likely represses terminal in vitro differentiation of MSCs as shown in very long-term cultures in their presence [33]

Glucocorticoids are used for in vitro differentiation of MSCs into multiple lineages. Glucocorticoid function is mediated by the cytoplasmic glucocorticoid receptor, which influences various differentiation processes by inducing transcriptional actions. The most used for chondrogenic differentiation is dexamethasone, a synthetic glucocorticoid, which upregulates gene expression and protein levels of several cartilage matrix markers, in particular collagen type XI [34]. Together with TGF-β, it is the main factor for chondrogenic differentiation media of MSCs. However, unlike TGF-β, dexamethasone alone has little effects on the expression of chondrogenic markers such as aggrecan and collagen type II. For human primary bone marrow-derived MSCs, successful chondrogenic differentiation was shown in medium containing 100 nM dexamethasone [10]

BMPs, also members of the TGF-β superfamily, are other growth factors that play an important role during bone morphogenesis by initiating chondroprogenitor cell determination and differentiation. BMP-2, BMP-4, BMP-6 and BMP-7 act synergistically with TGF-β by enhancing ECM deposition. However their supply without TGF-β and dexamethasone is not sufficient to stimulate in vitro chondrogenesis of human MSCs in conventional pellet culture [35, 36]. There is no consensus in which of the BMP has more chondrogenic potential [10, 37]

IGF is a circulating cytokine that reaches articular cartilage through the synovial fluid. IGF-1 is the most widely studied form with respect to cartilage. IGF-1 plays a key role in cartilage homeostasis, balancing proteoglycan synthesis and breakdown by the chondrocytes [38] . IGF also stimulates in vitro MSC proliferation, regulates cell apoptosis, increases the synthesis proteoglycans and promotes the survival, development and maturation of

chondrocytes [39, 40] Although some studies did not show any effect of isolated IGF application on in vivo MSC differentiation, others showed that IGF-1 can influence chondrogenesis independently of TGF- β1, but it seems that the more effective combination is when a synergism with TGF-β1 is involved. Indeed, the expression of the chondrogenic-specific transcription factor Sox9, the amounts of collagen type II and cartilage-specific proteoglycans in MSCs stimulated both with TGF- β1 and IGF-1 can be comparable to that of mature adult chondrocytes [40, 41]

In vitro treatment of MSCs with FGF, increased pellet content of collagen type II and glycosaminoglycans as well as mRNA expression of aggrecan, but also needs the presence of TGF-β [42]

Ascorbate and its derivative Ascorbate-2-Phosphate cause hydroxylation of proline and lysine amino acids –that is necessary to produce the triple helix conformation of all collagens and make them functional. Its addition to the culture medium leads to increased MSC proliferation and enhances production of collagen type II.

PDGF can favor chondrogenesis, but it is thought to be an indirect effect, because inhibition of its receptor does not result in a total inhibition of chondrogenic differentiation [42]

1.5 Differentiation in 3D without mechanical stimulus: Micromass and pellet cultures

The necessity of studying and obtaining strategies to grow chondrocytes in vitro for tissue repair led to focus in models that mimic as much as possible the conditions in vivo. Cell culture in 2D do not resemble the in vivo situation, and it is known that mature chondrocytes de-differentiate [43, 44]. Further, MSCs in specific medium is not appropriate for all chondrogenic differentiation, the cells developing a fibrous phenotype, at the most resembling only the chondrocytes of the articular surface. 2D enhances the natural tendency of MSCs to express collagen type I due to the flattened morphology [45]. Moreover levels of GAG and collagen II expression are lower than in most of three-dimensional (3D) supports.

The first strategies for MSC differentiation toward chondrogenic in 3D were designed to mimic the conditions during stem cell condensation: pellet and micromass cultures (Figure 1.4). Pellet cultures consist on centrifuging the MScs in a conical tube and then incubation.

After 24h in culture, the cells aggregate and form a round cell pellet. MSCs are capable of chondrogenic differentiation in pellet culture using serum-free medium containing glucocorticoids and TGF-β family [46] . However, it is hard to obtain a satisfactory cartilage in pellet culture. Cells are often found undifferentiated or necrotized in the central region of the pellet and only the outside layer cells undergo chondrogenic differentiation [47-49]. Additionally, MSCs in pellet culture show induced fibrocartilage-like features such as expression of collagen I and hypertrophy , as shown by upregulation of collagen X [48]

In micromass cultures, a droplet of cell suspension is carefully placed in the center of each well of a multiwell plate. Cells are allowed to adhere at 37 ^{o}C for some hours, followed by the addition of chondrogenic medium. After 24 h, the cells in every droplet merge and form a spherical mass. All chondrogenic cultures are performed for more than 21 days.

It has been reported that micromass culture systems enhance chondrogenesis more than standard pellet systems [50]. When compared with pellet cultures, in the micromass cultures the cartilage-like tissue is more homogenous and enriched in collagen II, decreasing the expression of fibrocartilage collagen I (more fibrocartilage features) and collagen X (hypertrophic features). One reason for the existence of collagen type I and type X can be the lack of time regulation of the adhesion molecules typical from condensation, what can result in cells remaining in pre-cartilage stage. The nutrients and the oxygen reach more easily the central zone of the micromasses than the pellets, which usually leads to necrotized tissue.
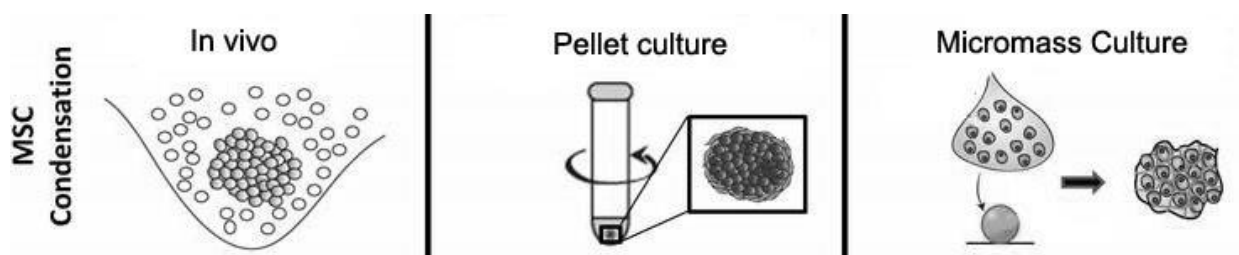
Figure 1.4 - Schematics of condensation in vivo, in pellet culture and in micromass.

1. 6 Regulation of differentiation by cell shape: interaction between the cells and the Extracellular Matrix

Micromass and pellet cultures have been useful to show that cell and nuclear shape are strong regulators of cell growth and physiology and, in particular, differentiation of adult or embryonic stem cells into a chondrocytic phenotype requires a rounded cell shape [46, 51, 52]. In bone-marrow-derived MSCs it is shown that a more rounded nuclear shape was associated to the larger expression of molecular chondrogenic markers [53].

The biophysical interaction between integrins and cadherins with matrix molecules initiate intracellular signal mediated by the three cytoskeletal networks: actin microfilaments, intermediate filaments and microtubules. [54] These cytoskeletal filaments are polymerized and reorganized with signal propagation from adhesion sites and transmit signals by linking to the nucleus, resulting in the control of protein expression and post-translational modifications. Thus, as the adhesion to environment molecules determines the morphology of the cell and cytoskeleton structure, it also regulates chondrogenic differentiation. In developing limbs, MSCs aggregate, resulting in increased cell density and cell–cell contact. As these cells undergo chondrogenesis they acquire a distinct spherical morphology and initiate expression of, Sox5, Sox6 and Sox9, that are transcription factors for chondrogenic ECM components like collagen type II and aggrecan, in particular Sox9 [55]. In micromass systems, direct disruption of actin cytoskeleton with chemical agents leads to chondrogenic differentitation [56] [57]. Further, inhibition of RhoA is a negative F-actin cytoskeleton-regulating protein, whose usual downstream target is Rho-associated protein kinase (ROCK). Although inhibition of RhoA in chick limb (similar cells to MSCs) micromass enhances chondrogenesis, inhibition of ROCK does not, suggesting that there are unknown alternative pathways [58]

1.7 Differentiation in 3D without mechanical stimulus: Scaffolds

Although micromass culture is able to mimic some of the conditions for chondrogenesis during development being therefore a suitable as model, it has two main problems as a therapy: it is not suitable for implantation and produce necrotic problems, the later attributed to too close contact, as it should be reminded that in adults, chondrocytes are physically

separated to each other through lacunae, and even in avascular conditions, there is some diffusion of oxygen and nutrients.

Thus, the most common solution is to embed the cell suspension in a surrounding environment capable to retain the cells. Two kind of biomaterial supports are employed: hydrogels, formed by suspension of cells within a solution that encapsulates them, and macroporous scaffolds. Both can improve some limitations of micromass and pellet systems. These scaffolds must be evaluated first in vitro to comprehend their effects in differentiation. 3D systems for in vitro culture provide more surface for cell adhesion and proliferation. In vivo, scaffolds prevent the diffusion of transplanted cells and can improve integration.

A broad set of different materials have been used to produce hydrogels for cartilage tissue engineering [59]: proteins as collagen type I or collagen type II [60-62], fibrin [63-65] , elastin-like polypeptides [66], polysacharides as hyaluronic acid [67-69] , chitosan [70-72] , chondroitin sulphate [68]; agar gel, gellan gum [73], synthetic hydrogels as crosslinked poly(ethylene glycol) [74], poly(vynil alcohol) [75] and others. Hydrogels are formed by cross-linking of fiber molecules, normally encapsulating the cells at the beginning of the culture. Hydrogels show several interesting characteristics such as the possibility of obtaining highly swollen structures approaching to similar condition than cartilage natural ECM and also the possibility of obtaining cell homogeneous distributions.

Other non-hydrogel scaffolding systems are produced for cartilage issue engineering, mainly semicrystalline polymers such as hydrophobous biodegradable polyesters, as well as the series of polymers and copolymers based on biodegradable polyesters such as polylactide [76], polyglicolide [77], poly-ε-caprolactone (PCL) [78-80], biodegradable poly(ether ester) multiblock copolymers [81], poly(3-hydroxybutyrateco-3-hydroxyhexanoate) [82], and also biostable acrylic polymers [83, 84]   among others [85]. Many combinations of these hydrogels with polymer scaffolds can exist, for example fibrin with PCL [27], semycristalline polymers providing a broader set of structures due to the extended plethora of processing methods [86] .

In this thesis, poly-ε-caprolactone (PCL) was the the selected material, as it has been proven be an interesting material for cartilage tissue engineering, due to its viscoelastic properties,

and the capability of being tuned with different pore geometry and bioactive coatings [80, 87-90]. It has been already used in animal models [91, 92]

As cell shape is a factor of differentiation, the effect of scaffolds on chondrogenesis is mainly regulated by cell interactions with the matrix and the morphologic configuration acquired as a consequence [93, 94]. There is a consensus in that adhesion in monolayer cultures to film biomaterials (2D) is not capable of suitable chondrogenic differentiation, MSCs taking a spread morphology to only one surface and acquiring a fibrous phenotype characterized by high expression of collagen type I relative to collagen type II. Three-dimensional cultures do not only provide more surface for cell adhesion and proliferation, but also the structural cues to affect morphology and attachment to ECM. The importance of 3D environment configuration for chondrogenesis is such that MSCs cultured in decellularized cartilage are capable of chondrogenic differentiation without addition of exogenous factors [95].

For example, encapsulation of MSCs in non-adherent hydrogels, such as PEG or alginate, can induce a rounded cell shape, what favors expression of chondrogenic markers, similarly to inhibition of cytoskeleton. In gels that favor integrin binding, like fibrin, MSCs adopt a spread morphology in 3D and differentiate spontaneously towards myocites [96]. An example of different morphologies of chondrocytes in different 3D substrates is shown in Figure 1.5. It should be remarked that spreading in 3D is different from the spread morphology obtained in 2D. In 3D environments the existence of more binding points for adhesion produce a contractile tension in all directions, while in 2D contractile is biased towards the adhesion surface. When compared 2D and 3D spreading, 3D spreading results in more chondrocytic phenotype. Generally, when no other factors are influencing, chondrogenic differentiation is favored, from worst to best, in the following order: 2D spread 3D, non-adherence 3D.

Macroporous sponges fabricated from molecules found in ECMs (e.g. collagens, GAG) or analogue molecules provide direct adhesion properties to cell ligands, mainly integrins and cadherins. However, processing methods for these materials are more limited and few structures can be designed. Thus, other non-bioactive materials are also used and the cell response to their surface is not mediated by a direct contact, but rather through an interfacial

layer formed on material surface once it is in contact with a physiological environment. Such a layer is created as result of non-specific adsorption of ECM proteins, like fibronectin, laminin and vitronectin, which interact with surface integrins [97]. This protein deposition not only is fundamental for cell adhesion [98], but also influences posterior cell events like proliferation, migration and differentiation [99]. Usually, layer formation is controlled in some manner through functionalization with specific protein and allowing non-specifical attaching before cell culture [100]. Scaffold chemistry influences surface properties such as morphology, hydrophilicity, surface energy and charge, which control this protein adsorption [101]. Thus, by tuning these parameters through suitable physico-chemical modifications, the creation of this layer can be guided. Moreover, surfaces can be modified to attach specific proteins in desired conformations, through grafting specific peptid ligands, physically or covalently, such as RGD sequences [93]. In these sponges, when pore diameters are significantly larger than the cell diameter (more than 100 micrometers), the surface presented to cells ranges in the micrometric scale and it is thought that cells adhere in a manner resembling cell adhesion on 2D substrates [90, 93]. Reducing fiber diameter to nanoscale can enhance the chondrogenic differentiation of mesenchymal stem when compared with the same material as a sponge of thicker fibers [102, 103]. It is reasonable, as more binding points can be established with a high porosity, interconnectivity and permeability, parameters that influence differentiation through fluid flow, cell migration, cell-cell contact and nutrient and soluble factors local concentration [104-107]

Signaling complexity in 3D also increases with respect to 2D. There are several metabolic pathways involved in differentiation in both 2D and 3D systems. However, the differences in these pathways between the two systems have not been identified yet [108]
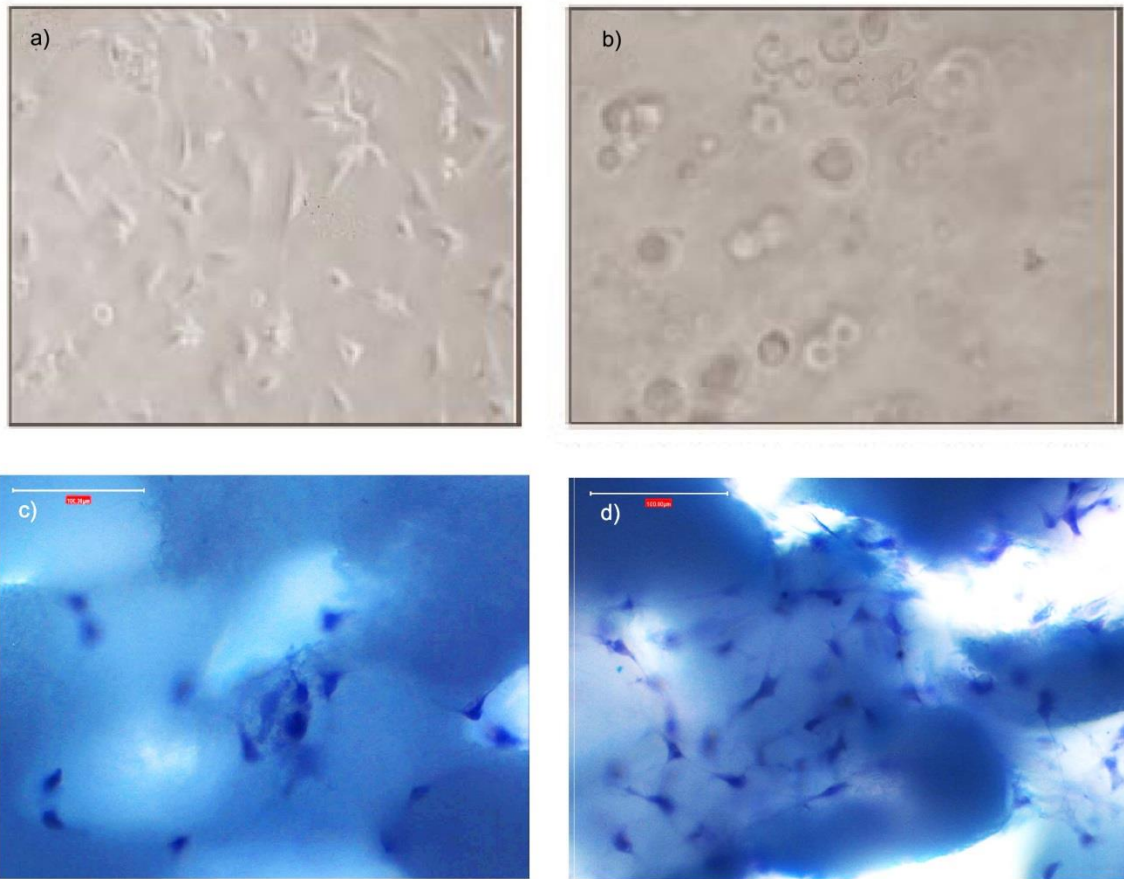
Figure 1.5 - Contrast phase microphotographies of human chondrocytes: a) in standard culture plate, after 2 weeks, dedifferentiated and with fibroblastoid spread morphology, b) encapsulated in non-adherent alginate gel, with round morphology. The images c) and d) correspond to Masson's trichromic stain of chondrocytes after 28 days of cell culture in PCL macroporous 3D sponges in which cells where initially seeded with adherent hydrogel fibin (c), and without fibrin (d). Chondrocytes in (d) adhere to the pore walls and take a similar morphology to that of standard 2D cell culture (a). Despite the degradation of fibrin, the cells in (c) retain a morphology with less protrusions than (a) and (d), indicating the presence of an adherent matrix (not visible). However, morphology is not truly rounded as in (b). Images a) and b) were taken from Bettencourt et al. [109] with permission of the authors.

1. 8 Differentiation in 3D: mechanical loading effects

1.8.1 Mechanobiology of cartilage

Other relevant aspects in the effect of the scaffold on differentiation are elasticity and mechanical properties. In native hyaline cartilage, organization of collagen, GAG and other matrix components provides mechanical stiffness able to resist mechanical loadings caused by joint movement and weight bearing, uniform compressive normal stresses ranging from 3 to 10 MPa and frequencies between 0.1 and 10 Hz [110, 111]. From a materials science point of view, the cartilage behaves as a viscoelastic material that deforms easily at small strains but stiffens while strain is increased.

The mechanical forces acting in the knee are varying within the articular zones, due to differences in composition and structure. In the superficial zone, the highest strains can be found (up to 50%) as well as the highest fluid flow, being also the most resistant zone to shear stress. This is the only zone where the interstitial fluid can flow out of the cartilage when it squeezes, through the surface, and the hydrostatic pressure is the lowest of all cartilage. Also, this zone sustains shear stress resulting from angular displacement of the two sides of the joint. In the middle zone the strains range between 10 and 20% and there is less fluid flow and, from this zone to the lower parts, it is limited to inside the cartilage matrix, as subchondral bone and adjacent tissue confine these zones. In the deep zone, the strains are 0 to 5% and practically does not exist fluid movement. In this zone, there are found the higher hydrostatic pressures [111]. This difference in loads results in anisotropic mechanical properties through the cartilage, with the elastic modulus of hyaline cartilage increasing with depth. For example in bovine, values of modulus are 0.08 MPa at the surface and 2.1 MPa in the deep zone. The apparent modulus of the whole cartilage is 0.38 MPa [112].

Not only the mechanical properties of ECM allow the cartilage to accomplish its function, but they also regulate the transmission of loads to the cells. There is a feedback situation between loads and matrix synthesis, because the loads which must sustain the matrix act as epigenetic signaling factor to the expression and production of its components, which provide at the same time the mechanical properties of cartilage. Mechanical loading is thus essential for proper musculoskeletal development [55]. Therefore, the knowledge on mechanical

properties of tissue environment and the ways in which loadings are transmitted to cells is fundamental.

Although the macroscopic effects of mechanical loading in vivo are well established [55], the molecular mechanisms still remain unclear. Recent research is unraveling that the mechanotransduction in chondrocytes in vivo is mediated through mechanoreceptors in the plasma membrane, mainly integrins, associated with stretch-activated ion channels and voltage-gated calcium channels, like TRPV4 [113]. As indicated before, integrins are binding proteins to ECM, thus, the pericellular matrix plays an important role in the transmission of loading. The biochemical transduction is mediated through the cytoskeleton also, as integrins interact with focal adhesion kinase and the cytoskeleton. For example, vimentin intermediate filaments are thought to play a role in mechanosensing, specifically to strain deformations [114]. It has been also identified an immotile primary cilium on human mesenchymal stem cells, on arthritic chondroprogenitor cells (CPCs) and on chondrocytes [115], which is directly associated with many of the mechanorreceptors mentioned previously (Figure 1.6), and current focus identify it as one of the main mechanosensors in chondrocytes. This microtubule is important because it is related to the expression of factors like PKA, what is a recent route of mechanical transduction, through a cascade resulting in activation of sox9 transcription factor [116]. Other pathways found to intervene in the chondrogenic differentiation in absence of mechanical loading are also regulated by the loading, like those related with the TGF- receptors: the TGF-β/activin/nodal pathway. It was shown that mechanical strain upregulates TGF- β 1, Activin A, Nodal and SMAD2/3 phosphorylation in undifferentiated embryonic stem cells, whereas inhibition of the TGFb/Activin/Nodal receptor stimulated differentiation.
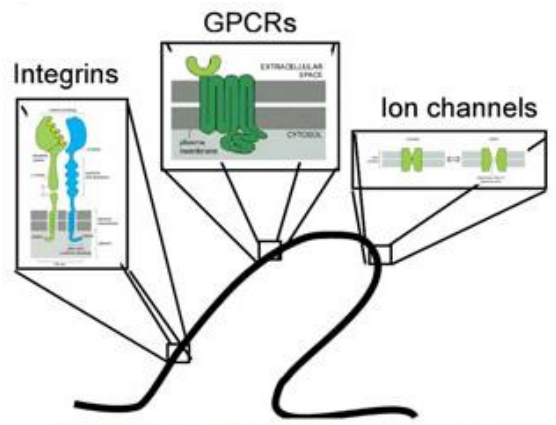
Figure 1.6 - Types of mechanosensor receptors contained in primary cilium. Image taken from H. Muhammad, Y. Rais et al. [115], with permission of the authors

It should be noted that chondrocytes in the different zones of cartilage show different morphology: The typical round shape found in the literature corresponds to the chondrocytes from the middle and deep radial zone, but in the superficial zone, the chondrocytes are more spread. These spreading chondrocytes can express collagen type I and lower amounts of collagen type II relative to proteoglycans than the round chondrocytes. These differences are probably related to the different loading profiles in the different zones and the varying matrix composition and structure. However, there is no evidence that dynamic loading transforms the cell shape in vitro and it is difficult to identify all the relations among the three parameters –cell shape, ECM and mechanical loading – and to categorize each one as cause or consequence of the other, due to the feed-back nature of the interactions in cartilage [111]

1.8.2 Mechanical considerations for biomaterials

Matrix elasticity is an extremely important factor in cell differentiation [117]. Thus, elasticity of the scaffolds is also a sensitive regulator of matrix proteins expression and controls the mechanical properties of new synthesized matrix. Little is known about the accurate mechanisms of stiffness effect in 3D scaffolds for chondrogenesis. For example, increasing cross-linking of PEG, and thus, increasing stiffness, improves differentiation of MSCs to chondrocytes [106]

Mechanical properties of the scaffolds are tuned by modifying pore size and the solid part simultaneously. Pore architecture and hydrodynamics influence mechanical properties, for example in cartilage, where flow-dependent viscoelastic response has a major contribution [118-120]. Likewise, both characteristics are related to the material and therefore to the processing methods, allowing to adjust geometric and mechanical properties.

The scaffold should have sufficient mechanical strength during in vitro culturing to maintain the spaces required for cell growth and matrix formation. Moreover, it must provide sufficient temporary mechanical support, matching the mechanical properties of the host tissue as closely as possible, to bear in vivo stresses and loading, until the newly grown tissue would be able to support loads and stresses [101]. If the scaffold is too stiff, it can shield the cells to sense the mechanical environment, hindering important mechanical signals. If it is too soft, it can fail with mechanical loading [121]. Thus, scaffold stiffness should be within a specific range of elasticity. However there is not a consensus in the exact values for this range is specific applications, probably because the gradient nature of the cartilage and canbe also because the difficulty in tailoring all relevant properties of the scaffolds. It should be remarked that scaffolds should resist the harsh mechanical environment (cyclic strain and shear stress), and hence, any research of biomaterials should focus in the long-term behavior of the implants.

1.8.3 Mechanical loading in vitro

As previously stated, mechanical loading is an important signaling factor for the correct regulation of ECM in vivo. To investigate its effects in vitro, external mechanical stresses have been applied through bioreactor devices, first in micromass cultures [122] and hydrogels with mature chondrocytes and more recently with mesenchymal stem cells. Different ways of providing mechanical stresses have been used: unconfined uniaxial compression (Figure 1.7) [123-125], direct shear stress [126-128] and perfusion (shear stress) [129-131] and hydrostatic pressure [132-135]. Each one of these mechanical solicitations simulate one or

some of the different components of mechanical stress in vivo and each one matches more closely to the conditions given in the different zones of cartilage. Unconfined compression resembles the conditions found in the upper zones of the cartilage with higher medium flow, low hydrostatic pressure, high stresses (in displacement control) or low strains (in force control). Direct shear stress can be combined with unconfined compression. Hydrostatic pressure resembles better the condition in the deeper zones. Ideally, semi-confined compression would resemble all the zones at the same time but it is hard to perform for cell culture, as it requires a permeable load plate over the load zone and impermeable boundaries around the rest of the scaffold [111].

Figure 1.7- Example of bioreactor device for unconfined compression. Image taken from G.D. Nicodemus and S.J. Bryant [125], with permission of the authors.

Effects of compression and hydrostatic pressure have been extensively studied for chondrogenic differentiation. It is known that for both compression and hydrostatic pressure in hydrogels, intermittent or dynamic application of mechanical stresses [136, 137] produces higher expressions of collagen II and proteoglycan expression than static loading [138, 139] and better mechanical properties in mature chondrocytes in explants and hydrogels. This is reasonable because loading in vivo is intermittent. Success of application of dynamic loads

depends on the frequency of application [126], typically 1 Hz and it is necessary the addition of repose periods. The period of continuous cycling loading in knee rarely excess 1h and are dispersed through all day with resting periods, which reach at least 16 h [111].

In non-adherent hydrogels under cyclic hydrostatic pressure [140] and cyclic compression, the presence of a pericellular matrix –formed by the cells or artificially recreated with coating -, is mandatory for the differentiation of MSCs. Although MSCs cyclic loading are capable to express chodrogenic markers and to produce ECM in non-adherent hydrogels, they need a pre-differentiation step and some initial pericellular matrix in order to sustain the same dynamic loads than differentiated chondrocytes for cultures until 21-28 days [123, 141]. This effect is more noticeable in cultures until 42 days with daily loadings, where levels of markers can drop below free-swelling conditions [142]. If a pericellular matrix is allowed to be generated for at least two weeks, higher expression and matrix synthesis is obtained.

In adherent hydrogels, direct mechanical loading can override the effects of adhesion in chondrogenic differentiation described in section 1.7. For example, in fibrin gels, when cyclic loading is applied, MSCs first keep un-differentiated traits, but in long-term culture, increase expression of chondrogenic markers compared to unloaded gels and inhibits myogenic markers [143], even when loads are applied from the first day. As the adhesive structure can resemble some aspects of a pericellular matrix, not allowing the cells to generate their own could not be as critical. MSCs in adherent hydrogels accumulate more GAG and reduce collagen type I under the effects of dynamic hydrostatic pressure than non-adherent hydrogels, where hydrostatic pressure has little effect [140]

These results can seem contradictory with the results obtained without mechanical loading, whose inhibition of cytoskeleton, either by chemical agents or non-formation by non-adherent hydrogels, produces a more rounded shape and induces expression and accumulation of chondrogenic markers. Introduction of mechanical loading introduces new effects that modify the effect of cell shape. It seems reasonable that fibers interacting with cells are a right cue for chondrogenesis when cyclic loads are applied, because it is closer to the situation in adult cartilage, where chondrocytes are attached by ligands to the surrounding

ECM that transmits the loads. There are no studies determining the effect of decreased size of fibers and thus the grade of adhesion and spreading, combined with mechanical loading.

The mechanosensors of totally differentiated chondrocytes can be other than those in undifferentiated cells, which have to be formed during differentiation. Actually, measurements of mechanical properties in individual cells find that undifferentiated MSCs have higher elastic modulus than mature chondrocytes, as a consequence of the stronger cytoskeleton [144] . Thus, they should sustain mechanical loadings in a different way. Without mechanical loading, the effect of a rounded cell shape can resemble the situation of MSC in the pre-condensation step, a stage of the development when the mechanical cues are not present. It has been suggested that dynamic compression can inhibit N-cadherin activity, the main binding protein during condensation [143]. Without loading, spreading increases N-cadherin expression, leading to the up-regulation of myogenic genes. Like in vivo, the expression of N-cadherin is necessary at the beginning but it is reduced as chondrogenesis progress, thus in an in vitro culture the expression should be reduced at the end. If this is correct, it could explain the lack of differentiation response of MSCs to myogenic and chondrogenic lineage at the beginning of the culture, but it would mean that chondrogenesis would be induced by skipping the condensation step, or simulating the final steps of condensation to mature cartilage.

The response of MSCs to mechanical loading seems also conditioned by other factors. For instance, under the same mechanical and surrounding structure conditions, MSCs responds better with lower concentrations of TGF-β than in non-loaded cultures [145] , what suggests that mechanical loading act via similar pathways, and because of it, higher concentration of TGF-β mask the effects of mechanical loading.

1.8.4 Measurement of chondrogenic differentiation – biochemical and mechanical analysis

Mechanical properties correlate with ECM markers in vitro until some extent. In some studies differences in mechanical properties are found when there are not significant differences in

analyzed ECM components [124] . Most of the experiments analyze the predominant ECM markers (collagen type II, aggrecan, sox9,…) and its association with mechanical properties, but neglect other components as collagens IX and XI and others, whose contribution to cartilage development is completely necessary, as could be seen in knock-out mices [146], where the depletion of the expression of these genes leads to loss of function.

Only recent studies include transcriptomic analysis of gene upregulation during chondrogenesis [147, 148], but none of them have correlated these expression profiles with mechanical properties yet, especially because the large amount of generated data and the difficulty in discerning the relation of all differentially expressed genes with the mechanical properties of the whole construct. Therefore, by the moment, only one main method remains to evaluate and predict if the constructs can match the conditions and provide a similar function to cartilage: by measuring their mechanical properties directly.

There have been efforts to separate the effects of matrix components in cartilage by bottom-up approaches of measuring single ECM components [149], but integration of these data in a coherent model is defying . Hitherto, the study of mechanical properties of cartilage and constructs treat them as materials with two components, a fluid part and a solid matrix, considering it as a whole. The parameters used are common parameters in materials science: compressive modulus, elastic modulus, dynamic modulus, Poisson ratio or aggregate modulus, presented in Table 1.1. In cartilage, if the values of these parameters are calculated for the whole cartilage, they are apparent values. When constructs are analyzed, usually their properties are compared with these apparent values, and usually the properties of the different cartilage zones are not considered.

Table 1.1 – Usual parameters measured in cartilage and constructs for tissue engineering

Parameter	Meaning	Formula
Young modulus or elastic modulus(E)	Stiffness, as ratio of the stress along an axis over the strain along that axis in the range of stress in which Hooke's law is valid	$E = \dfrac{\sigma}{\varepsilon}$
Poisson ratio (v)	Negative ratio of transverse to axial strain	$v = -\dfrac{\varepsilon_{trans}}{\varepsilon_{long}}$
Aggregate modulus (H$_a$)	Stiffness when fluid has stopped flowing	$H_a = \dfrac{E(1-v)}{[(1+v)(1-2v)]} =$
Shear modulus (G)	Ratio of the shear stress to shear strain	$G = \dfrac{\tau}{\gamma}$
Storage and loss modulus (E' and E'')	The storage modulus is a measure of the energy stored elastically during deformation, and the loss modulus is a measure of the energy converted to heat; in cyclical motions of strain and stress	
Dynamic compressive modulus (E*)	Ratio of stress to strain under vibratory conditions	$E^* = E' + iE''$

Mechanical fatigue is a known effect in all materials [150], but it has not been discussed properly for biomaterials and ECM yet. Fatigue in material sciences is understood as the irreversible structural damage produced in a material that is subjected to cyclic loading. Fracture-related failure has been assessed in cartilage and in some hydrogels with techniques that evaluate resistance to a crack generated in purpose, that grows depending the test, analogous to a series of standard methodology in material science [151]. Further, the materials fabrication processes themselves introduce imperfections that can act as stress accumulators, which can initiate fatigue effects, when subjected to cyclic loadings and permanent deformation. Compression to failure in hydrogels or other biomaterials have been barely studied [152] and never under cyclic loading.

1.9 Objectives

Before a correlation between all relevant components of ECM under mechanical loading is found, it is important to ensure the proper knowledge on the mechanical properties of the biomaterials and their relationship to overall cell response. This thesis is a contribution to understand the variation of the mechanical properties of PCL scaffold-cell systems over time and to find suitable methodologies to obtain proper information on cell culture and the response of the growing tissues inside the scaffolds

The specific goals are:

- To find a methodology to assess and predict mechanical fatigue under cyclic compression in PCL scaffolds, suitable for samples in aqueous media.

- To evaluate models in vitro for simulating ECM via a PVA viscoelastic hydrogel.

- To design a bioreactor for dynamic compression able for chondrogenic differentiation of multiple samples and easily operable in sterile conditions.

- To evaluate the effects of an in vitro generated ECM in the resistance to fatigue of PCL constructs.

1.10 Structure of the tesis

Chapter 1 provides a general introduction to the main relevant topics of this area of research. The main objectives of this work area stated and the structure of the thesis oulined.

In Chapter 2, the PCL scaffolds in dry state will be compared with scaffolds under immersion in water, in order to determine the hydrodynamic effects in resistance to fatigue by analyzing evolution of the dissipated energy under cyclic loading. The effect of fibrin hydrogel inside the pores will be determined.

In Chapter 3, the same analysis is performed in PCL scaffolds combined with PVA hydrogel as an vitro model of growing tissue inside the pores. It is studied how the addition of a third material, resembling some aspects of tissue, affects the mechanical response.

In Chapter 4, the design of a mechanical bioreactor is presented, that will be used in the final cell culture tests under mechanical stimulus.

Chapter 5 shows the results of PCL scaffolds seeded with chondrogenic precursor cells and submitted to free swelling and cyclic loading in the bioreactor. All the samples were analyzed for fatigue.

Finally, Chapter 6 describes the general conclusions and indications for further work

1.11 References

1.   Csaki, C., P.R. Schneider, and M. Shakibaei, *Mesenchymal stem cells as a potential pool for cartilage tissue engineering.* Ann Anat, 2008. **190**(5): p. 395-412.

2.   Bobick, B.E., et al., *Regulation of the chondrogenic phenotype in culture.* Birth Defects Res C Embryo Today, 2009. **87**(4): p. 351-71.

3.   Schulz, R.M. and A. Bader, *Cartilage tissue engineering and bioreactor systems for the cultivation and stimulation of chondrocytes.* Eur Biophys J, 2007. **36**(4-5): p. 539-68.

4.   Buckwalter, J.A., V.C. Mow, and A. Ratcliffe, *Restoration of Injured or Degenerated Articular Cartilage.* J Am Acad Orthop Surg, 1994. **2**(4): p. 192-201.

5.   DeLise, A.M., et al., *Embryonic limb mesenchyme micromass culture as an in vitro model for chondrogenesis and cartilage maturation.* Methods Mol Biol, 2000. **137**: p. 359-75.

6.   Hoffman, L.M., A.D. Weston, and T.M. Underhill, *Molecular mechanisms regulating chondroblast differentiation.* J Bone Joint Surg Am, 2003. **85-A Suppl 2**: p. 124-32.

7.   Woods, A., G. Wang, and F. Beier, *Regulation of chondrocyte differentiation by the actin cytoskeleton and adhesive interactions.* J Cell Physiol, 2007. **213**(1): p. 1-8.

8.   Beier, F., *Cell-cycle control and the cartilage growth plate.* J Cell Physiol, 2005. **202**(1): p. 1-8.

9.   Oberlender, S.A. and R.S. Tuan, *Spatiotemporal profile of N-cadherin expression in the developing limb mesenchyme.* Cell Adhes Commun, 1994. **2**(6): p. 521-37.

10.   Richter, W., *Mesenchymal stem cells and cartilage in situ regeneration.* J Intern Med, 2009. **266**(4): p. 390-405.

11.   Hunziker, E.B., *Articular cartilage repair: basic science and clinical progress. A review of the current status and prospects.* Osteoarthritis Cartilage, 2002. **10**(6): p. 432-63.

12.   Caplan, A.I., *Adult mesenchymal stem cells for tissue engineering versus regenerative medicine.* J Cell Physiol, 2007. **213**(2): p. 341-7.

13.   Augello, A., T.B. Kurth, and C. De Bari, *Mesenchymal stem cells: a perspective from in vitro cultures to in vivo migration and niches.* Eur Cell Mater, 2010. **20**: p. 121-33.

14.   Temenoff, J.S. and A.G. Mikos, *Review: tissue engineering for regeneration of articular cartilage.* Biomaterials, 2000. **21**(5): p. 431-440.

15.   Darling, E.M. and K.A. Athanasiou, *Articular cartilage bioreactors and bioprocesses.* Tissue Eng, 2003. **9**(1): p. 9-26.

16.   Beris, A.E., et al., *Advances in articular cartilage repair.* Injury, 2005. **36 Suppl 4**: p. S14-23.

17.   Chung, C. and J.A. Burdick, *Engineering cartilage tissue.* Adv Drug Deliv Rev, 2008. **60**(2): p. 243-62.

18.   Friedenstein, A.J., R.K. Chailakhjan, and K.S. Lalykina, *The development of fibroblast colonies in monolayer cultures of guinea-pig bone marrow and spleen cells.* Cell Tissue Kinet, 1970. **3**(4): p. 393-403.

19.   Friedenstein, A.J., *Precursor cells of mechanocytes.* Int Rev Cytol, 1976. **47**: p. 327-59.

20.   Caplan, A.I., *Mesenchymal stem cells.* J Orthop Res, 1991. **9**(5): p. 641-50.

21.   Firth, A.L. and J.X. Yuan, *Identification of functional progenitor cells in the pulmonary vasculature.* Pulm Circ, 2012. **2**(1): p. 84-100.

22.   Zuk, P.A., et al., *Human adipose tissue is a source of multipotent stem cells.* Mol Biol Cell, 2002. **13**(12): p. 4279-95.

23.   Jones, E.A., et al., *Enumeration and phenotypic characterization of synovial fluid multipotential mesenchymal progenitor cells in inflammatory and degenerative arthritis.* Arthritis Rheum, 2004. **50**(3): p. 817-27.

24.   Seda Tigli, R., et al., *Comparative chondrogenesis of human cell sources in 3D scaffolds.* J Tissue Eng Regen Med, 2009. **3**(5): p. 348-60.

25.   Yoshimura, H., et al., *Comparison of rat mesenchymal stem cells derived from bone marrow, synovium, periosteum, adipose tissue, and muscle.* Cell Tissue Res, 2007. **327**(3): p. 449-62.

26.   Dominici, M., et al., *Minimal criteria for defining multipotent mesenchymal stromal cells. The International Society for Cellular Therapy position statement.* Cytotherapy, 2006. **8**(4): p. 315-7.

27.   Ho, S.T., et al., *The influence of fibrin based hydrogels on the chondrogenic differentiation of human bone marrow stromal cells.* Biomaterials, 2010. **31**(1): p. 38-47.

28.   Curran, J.M., R. Chen, and J.A. Hunt, *The guidance of human mesenchymal stem cell differentiation in vitro by controlled modifications to the cell substrate.* Biomaterials, 2006. **27**(27): p. 4783-93.

29.   Miyazono, K., *Positive and negative regulation of TGF-beta signaling.* J Cell Sci, 2000. **113 (Pt 7)**: p. 1101-9.

30.   Lee, J.W., et al., *Chondrogenic differentiation of mesenchymal stem cells and its clinical applications.* Yonsei Med J, 2004. **45 Suppl**: p. 41-7.

31.   Barry, F., et al., *Chondrogenic differentiation of mesenchymal stem cells from bone marrow: differentiation-dependent gene expression of matrix components.* Exp Cell Res, 2001. **268**(2): p. 189-200.

32.   James, A.W., et al., *Differential effects of TGF-beta1 and TGF-beta3 on chondrogenesis in posterofrontal cranial suture-derived mesenchymal cells in vitro.* Plast Reconstr Surg, 2009. **123**(1): p. 31-43.

33.   Zhang, X., et al., *Primary murine limb bud mesenchymal cells in long-term culture complete chondrocyte differentiation: TGF-beta delays hypertrophy and PGE2 inhibits terminal differentiation.* Bone, 2004. **34**(5): p. 809-17.

34. Derfoul, A., et al., *Glucocorticoids promote chondrogenic differentiation of adult human mesenchymal stem cells by enhancing expression of cartilage extracellular matrix genes.* Stem Cells, 2006. **24**(6): p. 1487-95.

35. Xu, D., et al., *Potential involvement of BMP receptor type IB activation in a synergistic effect of chondrogenic promotion between rhTGFbeta3 and rhGDF5 or rhBMP7 in human mesenchymal stem cells.* Growth Factors, 2006. **24**(4): p. 268-78.

36. Hennig, T., et al., *Reduced chondrogenic potential of adipose tissue derived stromal cells correlates with an altered TGFbeta receptor and BMP profile and is overcome by BMP-6.* J Cell Physiol, 2007. **211**(3): p. 682-91.

37. Sekiya, I., et al., *Comparison of effect of BMP-2, -4, and -6 on in vitro cartilage formation of human adult stem cells from bone marrow stroma.* Cell Tissue Res, 2005. **320**(2): p. 269-76.

38. Schmidt, M.B., E.H. Chen, and S.E. Lynch, *A review of the effects of insulin-like growth factor and platelet derived growth factor on in vivo cartilage healing and repair.* Osteoarthritis Cartilage, 2006. **14**(5): p. 403-12.

39. Luyten, F.P., et al., *Insulin-like growth factors maintain steady-state metabolism of proteoglycans in bovine articular cartilage explants.* Arch Biochem Biophys, 1988. **267**(2): p. 416-25.

40. Longobardi, L., et al., *Effect of IGF-I in the chondrogenesis of bone marrow mesenchymal stem cells in the presence or absence of TGF-beta signaling.* J Bone Miner Res, 2006. **21**(4): p. 626-36.

41. Vater, C., P. Kasten, and M. Stiehler, *Culture media for the differentiation of mesenchymal stromal cells.* Acta Biomater, 2011. **7**(2): p. 463-77.

42. Ng, F., et al., *PDGF, TGF-beta, and FGF signaling is important for differentiation and growth of mesenchymal stem cells (MSCs): transcriptional profiling can identify markers and signaling pathways important in differentiation of MSCs into adipogenic, chondrogenic, and osteogenic lineages.* Blood, 2008. **112**(2): p. 295-307.

43. Ma, B., et al., *Gene expression profiling of dedifferentiated human articular chondrocytes in monolayer culture.* Osteoarthritis Cartilage, 2013. **21**(4): p. 599-603.

44. Schulze-Tanzil, G., *Activation and dedifferentiation of chondrocytes: implications in cartilage injury and repair.* Ann Anat, 2009. **191**(4): p. 325-38.

45. Huebsch, N., et al., *Harnessing traction-mediated manipulation of the cell/matrix interface to control stem-cell fate.* Nat Mater, 2010. **9**(6): p. 518-26.

46. Johnstone, B., et al., *In vitro chondrogenesis of bone marrow-derived mesenchymal progenitor cells.* Exp Cell Res, 1998. **238**(1): p. 265-72.

47. Kafienah, W., et al., *Three-dimensional cartilage tissue engineering using adult stem cells from osteoarthritis patients.* Arthritis Rheum, 2007. **56**(1): p. 177-87.

48. Mueller, M.B. and R.S. Tuan, *Functional characterization of hypertrophy in chondrogenesis of human mesenchymal stem cells.* Arthritis Rheum, 2008. **58**(5): p. 1377-88.

49. Murdoch, A.D., et al., *Chondrogenic differentiation of human bone marrow stem cells in transwell cultures: generation of scaffold-free cartilage.* Stem Cells, 2007. **25**(11): p. 2786-96.

50. Zhang, L., et al., *Chondrogenic differentiation of human mesenchymal stem cells: a comparison between micromass and pellet culture systems.* Biotechnol Lett, 2010. **32**(9): p. 1339-46.

51. Erickson, G.R., et al., *Chondrogenic potential of adipose tissue-derived stromal cells in vitro and in vivo.* Biochem Biophys Res Commun, 2002. **290**(2): p. 763-9.

52. Hoben, G.M., E.J. Koay, and K.A. Athanasiou, *Fibrochondrogenesis in two embryonic stem cell lines: effects of differentiation timelines.* Stem Cells, 2008. **26**(2): p. 422-30.

53. McBride, S.H., T. Falls, and M.L. Knothe Tate, *Modulation of stem cell shape and fate B: mechanical modulation of cell shape and gene expression.* Tissue Eng Part A, 2008. **14**(9): p. 1573-80.

54. Zanetti, N.C. and M. Solursh, *Induction of chondrogenesis in limb mesenchymal cultures by disruption of the actin cytoskeleton.* J Cell Biol, 1984. **99**(1 Pt 1): p. 115-23.

55. Kelly, D.J. and C.R. Jacobs, *The role of mechanical signals in regulating chondrogenesis and osteogenesis of mesenchymal stem cells.* Birth Defects Res C Embryo Today, 2010. **90**(1): p. 75-85.

56. Titushkin, I. and M. Cho, *Modulation of cellular mechanics during osteogenic differentiation of human mesenchymal stem cells.* Biophys J, 2007. **93**(10): p. 3693-702.

57. Yourek, G., M.A. Hussain, and J.J. Mao, *Cytoskeletal changes of mesenchymal stem cells during differentiation.* ASAIO J, 2007. **53**(2): p. 219-28.

58. Kim, M.J., et al., *Inhibition of RhoA but not ROCK induces chondrogenesis of chick limb mesenchymal cells.* Biochem Biophys Res Commun, 2012. **418**(3): p. 500-5.

59.   Kim, I.L., R.L. Mauck, and J.A. Burdick, *Hydrogel design for cartilage tissue engineering: a case study with hyaluronic acid.* Biomaterials, 2011. **32**(34): p. 8771-82.

60.   Noth, U., et al., *Chondrogenic differentiation of human mesenchymal stem cells in collagen type I hydrogels.* J Biomed Mater Res A, 2007. **83**(3): p. 626-35.

61.   Vickers, S.M., L.S. Squitieri, and M. Spector, *Effects of cross-linking type II collagen-GAG scaffolds on chondrogenesis in vitro: dynamic pore reduction promotes cartilage formation.* Tissue Eng, 2006. **12**(5): p. 1345-55.

62.   Zscharnack, M., et al., *Low oxygen expansion improves subsequent chondrogenesis of ovine bone-marrow-derived mesenchymal stem cells in collagen type I hydrogel.* Cells Tissues Organs, 2009. **190**(2): p. 81-93.

63.   Ahmed, T.A., E.V. Dare, and M. Hincke, *Fibrin: a versatile scaffold for tissue engineering applications.* Tissue Eng Part B Rev, 2008. **14**(2): p. 199-215.

64.   Eyrich, D., et al., *Long-term stable fibrin gels for cartilage engineering.* Biomaterials, 2007. **28**(1): p. 55-65.

65.   Peretti, G.M., et al., *Review of injectable cartilage engineering using fibrin gel in mice and swine models.* Tissue Eng, 2006. **12**(5): p. 1151-68.

66.   Hrabchak, C., et al., *Assessment of biocompatibility and initial evaluation of genipin cross-linked elastin-like polypeptides in the treatment of an osteochondral knee defect in rabbits.* Acta Biomater, 2010. **6**(6): p. 2108-15.

67.   Chung, C., et al., *Influence of gel properties on neocartilage formation by auricular chondrocytes photoencapsulated in hyaluronic acid networks.* J Biomed Mater Res A, 2006. **77**(3): p. 518-25.

68.   Nguyen, L.H., et al., *Unique biomaterial compositions direct bone marrow stem cells into specific chondrocytic phenotypes corresponding to the various zones of articular cartilage.* Biomaterials, 2011. **32**(5): p. 1327-38.

69.   Tan, H., et al., *Injectable in situ forming biodegradable chitosan-hyaluronic acid based hydrogels for cartilage tissue engineering.* Biomaterials, 2009. **30**(13): p. 2499-506.

70.   Cho, J.H., et al., *Chondrogenic differentiation of human mesenchymal stem cells using a thermosensitive poly(N-isopropylacrylamide) and water-soluble chitosan copolymer.* Biomaterials, 2004. **25**(26): p. 5743-51.

71.   Jin, R., et al., *Injectable chitosan-based hydrogels for cartilage tissue engineering.* Biomaterials, 2009. **30**(13): p. 2544-51.

72. Sa-Lima, H., et al., *Stimuli-responsive chitosan-starch injectable hydrogels combined with encapsulated adipose-derived stromal cells for articular cartilage regeneration.* Soft Matter, 2010. **6**(20): p. 5184-5195.

73. Oliveira, J.T., et al., *Gellan gum: a new biomaterial for cartilage tissue engineering applications.* J Biomed Mater Res A, 2010. **93**(3): p. 852-63.

74. Bryant, S.J., et al., *Crosslinking density influences the morphology of chondrocytes photoencapsulated in PEG hydrogels during the application of compressive strain.* J Orthop Res, 2004. **22**(5): p. 1143-9.

75. Maher, S.A., et al., *Nondegradable hydrogels for the treatment of focal cartilage defects.* J Biomed Mater Res A, 2007. **83**(1): p. 145-55.

76. Antunes, J.C., et al., *Novel poly(L-lactic acid)/hyaluronic acid macroporous hybrid scaffolds: characterization and assessment of cytotoxicity.* J Biomed Mater Res A, 2010. **94**(3): p. 856-69.

77. López-Ruiz, E., et al., *Chondrocytes extract from patients with osteoarthritis induces chondrogenesis in infrapatellar fat pad-derived stem cells.* Osteoarthritis and Cartilage, 2013. **21**(1): p. 246-258.

78. Garcia-Giralt, N., et al., *A porous PCL scaffold promotes the human chondrocytes redifferentiation and hyaline-specific extracellular matrix protein synthesis.* J Biomed Mater Res A, 2008. **85**(4): p. 1082-9.

79. Ivirico, J.L., et al., *Proliferation and differentiation of goat bone marrow stromal cells in 3D scaffolds with tunable hydrophilicity.* J Biomed Mater Res B Appl Biomater, 2009. **91**(1): p. 277-86.

80. Izquierdo, R., et al., *Biodegradable PCL scaffolds with an interconnected spherical pore network for tissue engineering.* J Biomed Mater Res A, 2008. **85**(1): p. 25-35.

81. Malda, J., et al., *The effect of PEGT/PBT scaffold architecture on the composition of tissue engineered cartilage.* Biomaterials, 2005. **26**(1): p. 63-72.

82. Wang, Y., et al., *Evaluation of three-dimensional scaffolds prepared from poly(3-hydroxybutyrate-co-3-hydroxyhexanoate) for growth of allogeneic chondrocytes for cartilage repair in rabbits.* Biomaterials, 2008. **29**(19): p. 2858-68.

83. Barry, J.J., et al., *Porous methacrylate scaffolds: supercritical fluid fabrication and in vitro chondrocyte responses.* Biomaterials, 2004. **25**(17): p. 3559-68.

84. Diego, R.B., et al., *Acrylic scaffolds with interconnected spherical pores and controlled hydrophilicity for tissue engineering.* J Mater Sci Mater Med, 2005. **16**(8): p. 693-8.

85. Diego, R.B., J.L.G. Ribelles, and M.S. Sánchez, *Pore collapse during the fabrication process of rubber-like polymer scaffolds.* Journal of Applied Polymer Science, 2007. **104**(3): p. 1475-1481.

86. Weigel, T., G. Schinkel, and A. Lendlein, *Design and preparation of polymeric scaffolds for tissue engineering.* Expert Rev Med Devices, 2006. **3**(6): p. 835-51.

87. Lebourg, M., et al., *Biodegradable polycaprolactone scaffold with controlled porosity obtained by modified particle-leaching technique.* J Mater Sci Mater Med, 2008. **19**(5): p. 2047-53.

88. Gamboa-Martínez, T.C., J.L. Gómez Ribelles, and G. Gallego Ferrer, *Fibrin coating on poly (L-lactide) scaffolds for tissue engineering.* Journal of Bioactive and Compatible Polymers, 2011. **26**(5): p. 464-477.

89. Lebourg, M., et al., *Different hyaluronic acid morphology modulates primary articular chondrocyte behavior in hyaluronic acid-coated polycaprolactone scaffolds.* J Biomed Mater Res A, 2013. **101**(2): p. 518-27.

90. Olmedilla, M.P., et al., *In vitro 3D culture of human chondrocytes using modified epsilon-caprolactone scaffolds with varying hydrophilicity and porosity.* J Biomater Appl, 2012. **27**(3): p. 299-309.

91. Martinez-Diaz, S., et al., *In vivo evaluation of 3-dimensional polycaprolactone scaffolds for cartilage repair in rabbits.* Am J Sports Med, 2010. **38**(3): p. 509-19.

92. Lebourg, M., et al., *Cell-free cartilage engineering approach using hyaluronic acid-polycaprolactone scaffolds: a study in vivo.* J Biomater Appl, 2014. **28**(9): p. 1304-15.

93. Wheeldon, I., et al., *Nanoscale tissue engineering: spatial control over cell-materials interactions.* Nanotechnology, 2011. **22**(21): p. 212001.

94. Guilak, F., et al., *Control of Stem Cell Fate by Physical Interactions with the Extracellular Matrix.* Cell Stem Cell, 2009. **5**(1): p. 17-26.

95. Pei, M., et al., *A review of decellularized stem cell matrix: a novel cell expansion system for cartilage tissue engineering.* Eur Cell Mater, 2011. **22**: p. 333-43; discussion 343.

96. Gao, L., R. McBeath, and C.S. Chen, *Stem cell shape regulates a chondrogenic versus myogenic fate through Rac1 and N-cadherin.* Stem Cells, 2010. **28**(3): p. 564-72.

97. Geiger, B., et al., *Transmembrane crosstalk between the extracellular matrix and the cytoskeleton.* Nat Rev Mol Cell Biol, 2001. **2**(11): p. 793-805.

98. Garcia, A.J., *Get a grip: integrins in cell-biomaterial interactions.* Biomaterials, 2005. **26**(36): p. 7525-9.

99. Streuli, C.H., *Integrins and cell-fate determination.* J Cell Sci, 2009. **122**(Pt 2): p. 171-7.

100. Reyes, C.D., et al., *Biomolecular surface coating to enhance orthopaedic tissue healing and integration.* Biomaterials, 2007. **28**(21): p. 3228-35.

101. Puppi, D., et al., *Polymeric materials for bone and cartilage repair.* Progress in Polymer Science, 2010. **35**(4): p. 403-440.

102. Schagemann, J.C., et al., *Chondrogenic differentiation of bone marrow-derived mesenchymal stromal cells via biomimetic and bioactive poly-epsilon-caprolactone scaffolds.* J Biomed Mater Res A, 2013. **101**(6): p. 1620-8.

103. Holmes, B., et al., *Enhanced human bone marrow mesenchymal stem cell functions in novel 3D cartilage scaffolds with hydrogen treated multi-walled carbon nanotubes.* Nanotechnology, 2013. **24**(36): p. 365102.

104. Lee, J., M.J. Cuddihy, and N.A. Kotov, *Three-dimensional cell culture matrices: state of the art.* Tissue Eng Part B Rev, 2008. **14**(1): p. 61-86.

105. Yamane, S., et al., *Effect of pore size on in vitro cartilage formation using chitosan-based hyaluronic acid hybrid polymer fibers.* J Biomed Mater Res A, 2007. **81**(3): p. 586-93.

106. Erickson, I.E., et al., *Macromer density influences mesenchymal stem cell chondrogenesis and maturation in photocrosslinked hyaluronic acid hydrogels.* Osteoarthritis Cartilage, 2009. **17**(12): p. 1639-48.

107. Karande, T.S., J.L. Ong, and C.M. Agrawal, *Diffusion in musculoskeletal tissue engineering scaffolds: design issues related to porosity, permeability, architecture, and nutrient mixing.* Ann Biomed Eng, 2004. **32**(12): p. 1728-43.

108. McMahon, L.A., P.J. Prendergast, and V.A. Campbell, *A comparison of the involvement of p38, ERK1/2 and PI3K in growth factor-induced chondrogenic differentiation of mesenchymal stem cells.* Biochem Biophys Res Commun, 2008. **368**(4): p. 990-5.

109. Bittencourt, R.A.d.C., et al., *Cultura de condrócitos em arcabouço tridimensional: hidrogel de alginato.* Acta Ortopédica Brasileira, 2009. **17**: p. 242-246.

110. Elder, B.D. and K.A. Athanasiou, *Hydrostatic pressure in articular cartilage tissue engineering: from chondrocytes to tissue regeneration.* Tissue Eng Part B Rev, 2009. **15**(1): p. 43-53.

111.   Wong, M. and D.R. Carter, *Articular cartilage functional histomorphology and mechanobiology: a research perspective.* Bone, 2003. **33**(1): p. 1-13.

112.   Schinagl, R.M., et al., *Depth-dependent confined compression modulus of full-thickness bovine articular cartilage.* J Orthop Res, 1997. **15**(4): p. 499-506.

113.   O'Conor, C.J., et al., *TRPV4-mediated mechanotransduction regulates the metabolic response of chondrocytes to dynamic loading.* Proc Natl Acad Sci U S A, 2014. **111**(4): p. 1316-21.

114.   Langelier, E., et al., *The Chondrocyte Cytoskeleton in Mature Articular Cartilage: Structure and Distribution of Actin, Tubulin, and Vimentin Filaments.* Journal of Histochemistry & Cytochemistry, 2000. **48**(10): p. 1307-1320.

115.   Muhammad, H., et al., *The primary cilium as a dual sensor of mechanochemical signals in chondrocytes.* Cell Mol Life Sci, 2012. **69**(13): p. 2101-7.

116.   Juhasz, T., et al., *Mechanical loading stimulates chondrogenesis via the PKA/CREB-Sox9 and PP2A pathways in chicken micromass cultures.* Cell Signal, 2014. **26**(3): p. 468-82.

117.   Engler, A.J., et al., *Matrix elasticity directs stem cell lineage specification.* Cell, 2006. **126**(4): p. 677-89.

118.   Setton, L.A., W. Zhu, and V.C. Mow, *The biphasic poroviscoelastic behavior of articular cartilage: role of the surface zone in governing the compressive behavior.* J Biomech, 1993. **26**(4-5): p. 581-92.

119.   Mow, V.C., et al., *Biphasic creep and stress relaxation of articular cartilage in compression? Theory and experiments.* J Biomech Eng, 1980. **102**(1): p. 73-84.

120.   Armstrong, C.G., W.M. Lai, and V.C. Mow, *An analysis of the unconfined compression of articular cartilage.* J Biomech Eng, 1984. **106**(2): p. 165-73.

121.   Mouw, J.K., et al., *Dynamic compression regulates the expression and synthesis of chondrocyte-specific matrix molecules in bone marrow stromal cells.* Stem Cells, 2007. **25**(3): p. 655-63.

122.   Tran, S.C., A.J. Cooley, and S.H. Elder, *Effect of a mechanical stimulation bioreactor on tissue engineered, scaffold-free cartilage.* Biotechnol Bioeng, 2011. **108**(6): p. 1421-9.

123.   Huang, A.H., et al., *Long-term dynamic loading improves the mechanical properties of chondrogenic mesenchymal stem cell-laden hydrogel.* Eur Cell Mater, 2010. **19**: p. 72-85.

124. Lima, E.G., et al., *The beneficial effect of delayed compressive loading on tissue-engineered cartilage constructs cultured with TGF-beta3.* Osteoarthritis Cartilage, 2007. **15**(9): p. 1025-33.

125. Nicodemus, G.D. and S.J. Bryant, *The role of hydrogel structure and dynamic loading on chondrocyte gene expression and matrix formation.* J Biomech, 2008. **41**(7): p. 1528-36.

126. Li, Z., et al., *Chondrogenesis of human bone marrow mesenchymal stem cells in fibrin-polyurethane composites is modulated by frequency and amplitude of dynamic compression and shear stress.* Tissue Eng Part A, 2010. **16**(2): p. 575-84.

127. Garcia Cruz, D.M., M. Salmeron-Sanchez, and J.L. Gomez-Ribelles, *Stirred flow bioreactor modulates chondrocyte growth and extracellular matrix biosynthesis in chitosan scaffolds.* J Biomed Mater Res A, 2012. **100**(9): p. 2330-41.

128. Gamboa-Martínez, T.C., et al., *Chondrocytes Cultured in an Adhesive Macroporous Scaffold Subjected to Stirred Flow Bioreactor Behave Like in Static Culture.* Journal of Biomaterials and Tissue Engineering, 2013. **3**(3): p. 312-319.

129. Xie, L., et al., *In vitro mesenchymal trilineage differentiation and extracellular matrix production by adipose and bone marrow derived adult equine multipotent stromal cells on a collagen scaffold.* Stem Cell Rev, 2013. **9**(6): p. 858-72.

130. Goncalves, A., et al., *Effect of flow perfusion conditions in the chondrogenic differentiation of bone marrow stromal cells cultured onto starch based biodegradable scaffolds.* Acta Biomater, 2011. **7**(4): p. 1644-52.

131. Mahmoudifar, N. and P.M. Doran, *Chondrogenic differentiation of human adipose-derived stem cells in polyglycolic acid mesh scaffolds under dynamic culture conditions.* Biomaterials, 2010. **31**(14): p. 3858-67.

132. Angele, P., et al., *Cyclic hydrostatic pressure enhances the chondrogenic phenotype of human mesenchymal progenitor cells differentiated in vitro.* J Orthop Res, 2003. **21**(3): p. 451-7.

133. Miyanishi, K., et al., *Effects of hydrostatic pressure and transforming growth factor-beta 3 on adult human mesenchymal stem cell chondrogenesis in vitro.* Tissue Eng, 2006. **12**(6): p. 1419-28.

134. Zeiter, S., P. Lezuo, and K. Ito, *Effect of TGF beta1, BMP-2 and hydraulic pressure on chondrogenic differentiation of bovine bone marrow mesenchymal stromal cells.* Biorheology, 2009. **46**(1): p. 45-55.

135. Rodenas-Rochina, J., et al., *Compositional changes to synthetic biodegradable scaffolds modulate the influence of hydrostatic pressure on chondrogenesis of mesenchymal stem cells* To be submitted, 2014.

136. Demarteau, O., et al., *Dynamic compression of cartilage constructs engineered from expanded human articular chondrocytes.* Biochem Biophys Res Commun, 2003. **310**(2): p. 580-8.

137. De Croos, J.N., et al., *Cyclic compressive mechanical stimulation induces sequential catabolic and anabolic gene changes in chondrocytes resulting in increased extracellular matrix accumulation.* Matrix Biol, 2006. **25**(6): p. 323-31.

138. Steinmeyer, J. and S. Knue, *The proteoglycan metabolism of mature bovine articular cartilage explants superimposed to continuously applied cyclic mechanical loading.* Biochem Biophys Res Commun, 1997. **240**(1): p. 216-21.

139. Wong, M., et al., *Chondrocyte biosynthesis correlates with local tissue strain in statically compressed adult articular cartilage.* J Orthop Res, 1997. **15**(2): p. 189-96.

140. Steward, A.J., et al., *Cell-matrix interactions regulate mesenchymal stem cell response to hydrostatic pressure.* Acta Biomater, 2012. **8**(6): p. 2153-9.

141. Thorpe, S.D., et al., *Dynamic compression can inhibit chondrogenesis of mesenchymal stem cells.* Biochem Biophys Res Commun, 2008. **377**(2): p. 458-62.

142. Terraciano, V., et al., *Differential response of adult and embryonic mesenchymal progenitor cells to mechanical compression in hydrogels.* Stem Cells, 2007. **25**(11): p. 2730-8.

143. Thorpe, S.D., et al., *European Society of Biomechanics S.M. Perren Award 2012: the external mechanical environment can override the influence of local substrate in determining stem cell fate.* J Biomech, 2012. **45**(15): p. 2483-92.

144. Mathieu, P.S. and E.G. Loboa, *Cytoskeletal and focal adhesion influences on mesenchymal stem cell shape, mechanical properties, and differentiation down osteogenic, adipogenic, and chondrogenic pathways.* Tissue Eng Part B Rev, 2012. **18**(6): p. 436-44.

145. Li, Z., et al., *Mechanical load modulates chondrogenesis of human mesenchymal stem cells through the TGF-beta pathway.* J Cell Mol Med, 2010. **14**(6A): p. 1338-46.

146. Opolka, A., et al., *Collagen IX is indispensable for timely maturation of cartilage during fracture repair in mice.* Matrix Biol, 2007. **26**(2): p. 85-95.

147.   Henrionnet, C., et al., *Expression of chondrogenic genes by undifferentiated vs. differentiated human mesenchymal stem cells using array technology.* Biomed Mater Eng, 2010. **20**(3): p. 175-81.

148.   Yoo, H.J., et al., *Gene expression profile during chondrogenesis in human bone marrow derived mesenchymal stem cells using a cDNA microarray.* J Korean Med Sci, 2011. **26**(7): p. 851-8.

149.   Han, L., A.J. Grodzinsky, and C. Ortiz, *Nanomechanics of the Cartilage Extracellular Matrix.* Annual Review of Materials Research, 2011. **41**(1): p. 133-168.

150.   Manson, S.S. and G.R. Halford, *Fatigue and Durability of Structural Materials. Chapters 1, 3, 10 and 12.* 2006.

151.   Xiao, Y., et al., *Mechanical testing of hydrogels in cartilage tissue engineering: beyond the compressive modulus.* Tissue Eng Part B Rev, 2013. **19**(5): p. 403-12.

152.   DeKosky, B.J., et al., *Hierarchically designed agarose and poly(ethylene glycol) interpenetrating network hydrogels for cartilage tissue engineering.* Tissue Eng Part C Methods, 2010. **16**(6): p. 1533-42.

Chapter 2: Fatigue Prediction on Poly-ε-caprolactone Macroporous Scaffolds - Influence of water and fibrin

.
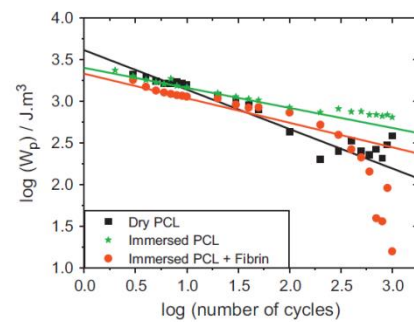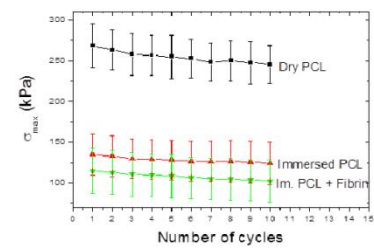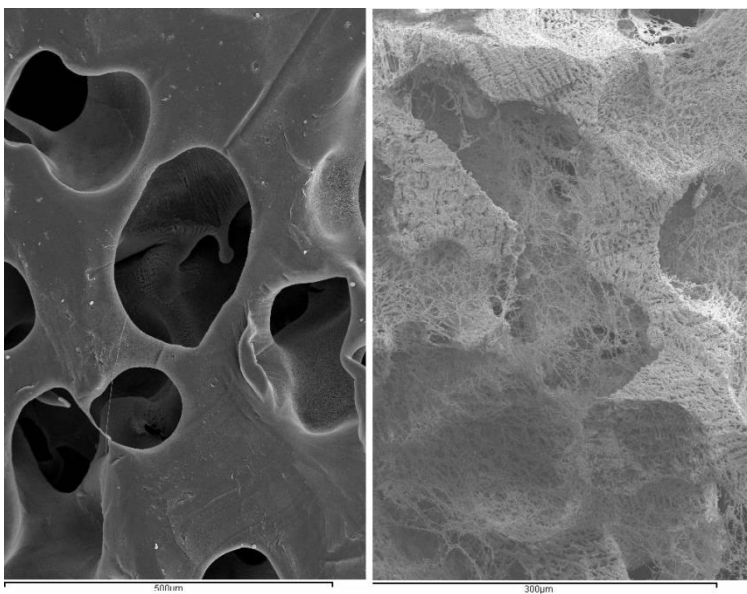
This chapter is based on the published paper: **Panadero, J.A., Vikingsson, L., Gomez Ribelles, J.L., Sencadas, V., Lanceros-Mendez, S.** *Fatigue prediction in fibrin poly-ε-caprolactone macroporous scaffolds.* **J Mech Behav Biomed Mater, 2013. 28: p. 55-61.**

2.1 Introduction

Tissue engineering has arisen as a therapy for regenerating damaged or diseased tissues. The most common strategy relies in the use of three-dimensional (3D) scaffolds, in combination with a cell source and signaling factors [1]. The scaffold should provide the architecture to guide new tissue formation, allowing cell-cell and cell-matrix interactions [2]. In order to achieve this purpose scaffold morphology should have a geometry of interconnected pores to allow cell seeding, proliferation, extracellular matrix (ECM) formation, diffusion of physiological nutrients and removal of metabolic waste products [3].

Scaffold mechanical properties are an important issue concerning tissue and biomedical engineering, as in addition to protect the cells when their extracellular matrix is still not developed, they regulate the biomechanical environment that offers stimulatory cues providing a better integration with the surrounding tissue. In particular in the regeneration of musculoskeletal tissues, like cartilage and bone, supported loads provide cues for the right gene expression and synthesis of ECM [4-7].

Polymer materials with a wide range of mechanical stiffness and viscoelastic properties can be prepared and polymer scaffolds can be designed to match the mechanical properties of living musculoskeletal tissues [8]. The evolution of mechanical properties of scaffold-cells culture during culture, due to the formation of synthetized ECM is an important parameter characterizing cell growth and differentiation [9]. The right production of ECM "in vitro" might require to perform culture under dynamic loading conditions. This has been performed by the development of a broad plethora of bioreactors which induce mechanical stimulus in different ways, such as confined or unconfined compression and hydrostatic pressure, among others [10-12]. It was found that cyclic applications of these stimuli generally produce higher differentiation responses due to a cascade of signaling events that has been called mechanotransduction [13-16].

Prediction of the mechanical behavior, ultimate properties and fatigue resistance of a polymer scaffolds implanted in the host tissue is an important issue that has been addressed insufficiently in the literature. The properties of the dry scaffold are not representative of that of the scaffold with the pores filled by a growing tissue or simply by a fluid. In dry scaffolds, mechanical properties mainly depend on its inner morphology, in particular pore size, geometry and interconnectivity [17]. However, in the scaffold immersed in a liquid medium

other factors can influence the mechanical properties as well, such as the hydrodynamics and permeability inside the scaffold. Since compressibility of water is low, any factor limiting water permeation through the material is expected to increase apparent scaffold stiffness, in particular under cyclic loading, which means that the influence of liquid media, such as cell culture medium cannot be disregarded. Nevertheless, to our knowledge, only few investigations deal with the description of the mechanical behavior of polymer scaffolds under liquid environment [18, 19] and none under cyclic loading in aqueous media.

The resistance of the material to mechanical fatigue can be influenced by several factors such as mechanical loading history, environmental conditions, polymer composition and to certain aspects of stress-strain constitutive behavior [20]. Few works concerning fatigue testing of polymeric materials are found in the literature. However, well validated research into metals has related fatigue results with atomic and molecular processes [21] and several models have been proposed to predict fatigue life cycle such as Coffin–Manson, Smith-Watson-Topper (SWT) or Morrow models [22]. Coffin-Manson model is based on the plastic strain range measured by subtracting the elastic strain range from the total strain range from the middle of the mechanical hysterics loop ($\Delta\varepsilon_t$), while SWT model assumes that the fatigue life cycle for any situation of mean stress depends on the product of the maximum stress (σ_{max}) and $\Delta\varepsilon_t$ [23]. Moreover, Morrow developed a model to predict fatigue life cycle of metals based on the plastic strain energy density that can be physically interpreted as the distortion energy associated to the change in shape of a volume element and can be related to failure, in particular under conditions of ductile behavior [24]. Testing of a scaffold in conditions that simulate in some extent the situation during cell culture seems therefore to be an important issue for a correct interpretation of stress transmission to the cells cultured in bioreactors.

In vivo ECM provides generally mechanical resistance by the capability of ECM components of retaining water, articular cartilage being a good example [11]. This phenomenon will appear as well in cells cultured "in vitro" inside the pores of the scaffold, seeded alone or encapsulated in fibrin, collagen and others [25]. In the present work, fatigue life cycle of a poly-ε-caprolactone, PCL, scaffold with and without fibrin as filler of the pore structure was characterized both dry and immersed in liquid water; in order to provide some insight in the fatigue behavior of the scaffolds for application in cell cultures under dynamic loading.

2.2 Materials and methods

2.2.1 Materials

Poly-ε-caprolactone (PCL, molecular weight of 43-50 kDa) and dioxan were purchased from *Sigma-Aldrich*. Poly(ethyl methacrylate) (PEMA - Elvacite 2043) in the shape of spheres with mean diameter of 200 □m was purchased from *Lucite*. Fibrinogen from human plasma 50-70% protein (≥80% of protein is clottable) and thrombin from human plasma lyophilized powder, ≥2,000 NIH units/mg protein (E1%/280, 18.3) were purchased from *Sigma-Aldrich* and glutaraldehyde (50 % H_2O) was purchased from *Panreac*.

2.2.2 Sample preparation

PCL was dissolved in dioxan (25% w/v) and this solution was mixed with PEMA microspheres (1:1 w/w). Then, the mixture was placed in Teflon Petri dishes and submerged in liquid nitrogen for a minute. Dioxan was extracted from the frozen plates with ethanol at -20 ^{0}C for three days, changing ethanol every day. Porogen leaching was performed in ethanol at 40 ^{0}C for one day. The porous samples were cut into cylinders with 6 mm diameter and a thickness of approximately of 2 mm. To achieve a complete removal of the porogen, further leaching for each cylinder was performed in ethanol at 40 ºC for nine more days, with daily change of ethanol.

A fibrinogen solution with concentration of 20 μg/ml in saline solution and a thrombin solution of 10 U/ml in TBS with 20 mM of $CaCl_2$ were prepared. Two chromatography syringes with beveled needles were prepared containing 20 μl of fibrinogen or thrombin solutions each. Finally, both solutions were injected in the PCL scaffold and fibrin was allowed to coagulate for 1 h at 37 ^{0}C and subsequently kept in distilled water for no more than 24 hours before the tests.

2.2.3 Characterization

Sample overall porosity, ϕ, was calculated by weighing the scaffolds after complete filling the pores with ethanol. The sample was sealed in a container under high vacuum in which ethanol was injected. Porosity was determined by:

$$\phi = \frac{V_p}{V_p + V_{PCL}}$$

$$V_p = \frac{(m_w - m_d)}{\rho_{EtOH}}$$

$$V_{PCL} = \frac{m_d}{\rho_{PCL}} \tag{1}$$

where m_d is the dry weight of the sample, m_w the weight with the sample filled in ethanol, V_p the volume of pores, V_{PCL} the volume occupied by the polymer and $\rho_{EtOH} = 0.785$ g/cm^3 and $\rho_{PCL} = 1.135$ g/cm^3 are the densities of ethanol and PCL at room temperature. Porosity values are the average of 5 measurements.

Sample microstructure was assessed by scanning electron microscopy. PCL filled with fibrin was fixed with a 2.5% glutaraldehyde (GA) solution for 1 h at 4 ^{0}C. CryoSEM was performed in a *JEOL JSM-5410* equipment. Water was sublimated at 5 kV, -50 ^{0}C for 20 min, and carbon-sputtered inside SEM chamber before analyses. PCL pristine samples were coated with a thin gold layer using a sputter coating (*Polaron,* model SC502) and their morphology was analyzed using aforementioned equipment.

Mechanical experiments were performed on cylindrical samples with 6 mm diameter and a height of ~2 mm in a *Shimadzu AG-IS* universal testing machine in compression mode at a test velocity of 1 mm.min^{-1} and at room temperature. In fatigue experiment, samples were submitted at a compressive-strain cycle load up to 1000 cycles at a strain of 15%. Mechanical parameters were obtained on an average of three measurements. The mechanical experiments were performed in dry PCL samples and in PCL and PCL filled with fibrin samples immersed in deionized water.

2.3 Results and Discussion

2.3.1 Electron Microscopy

The pore architecture of the PCL scaffolds consists in a double porosity: macropores obtained with the porogen spheres with diameters in the order of 200 microns and pores in the order of few microns produced by the freeze extraction technique (Figure 2.1) that interconnect the bigger ones. This double pore structure allows producing scaffolds with quite high porosity that have been previously proposed for cartilage and bone engineering [26-28]. Microporosity favors permeability of the scaffold to nutrients and waste products of cell metabolism and can be used to retain different active components [29-31]. Nevertheless, the apparent stiffness of the scaffold becomes significantly smaller than in similar sponges lacking microporosity, also used in cartilage engineering [32, 33].
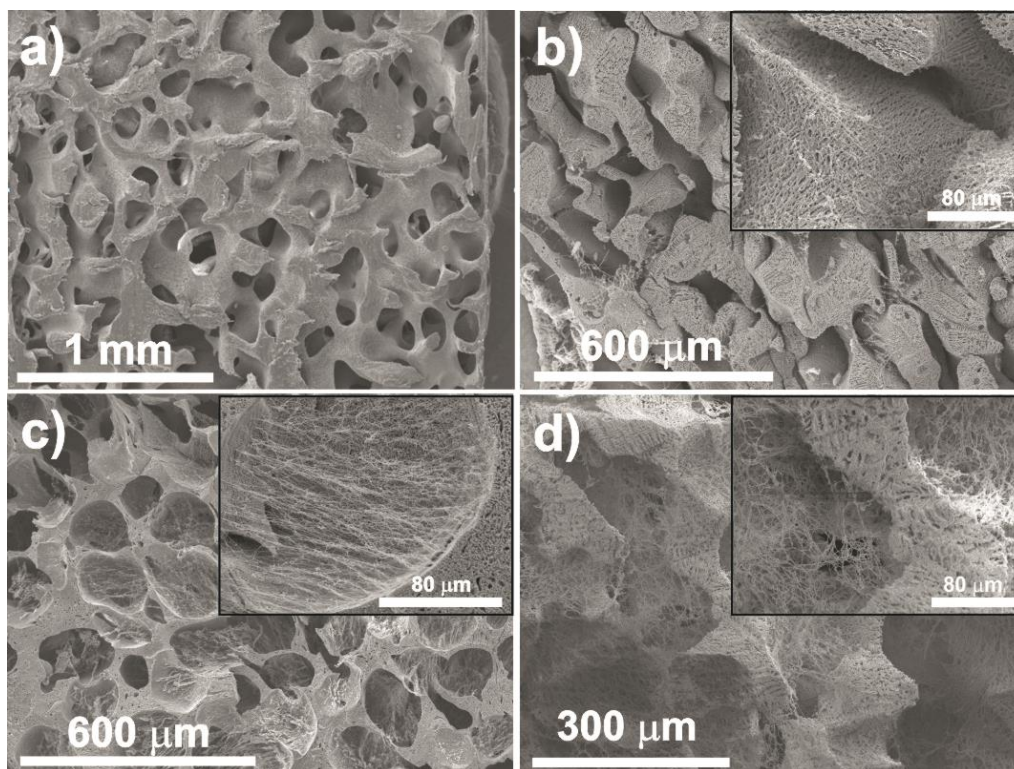
Figure 2.1 - PCL microstructure: a) dry pristine sample, b) dry PCL sample after 10 cycles, c) PCL with fibrin filling the pore structure and d) PCL with fibrin after 10 load-recovery cycles.

2.3.2 Mechanical analysis

These samples with and without fibrin were submitted to cyclic mechanical loading under compressive mode up to a 15% strain, which is a typical deformation in experiments with bioreactors for chondrogenic differentiation [34-36]. Stress-strain curves in 10 consecutive loading-unloading cycles are shown in Figure 2.2a for the dry sample. The difference between the first and second cycle indicates that some of the PCL trabecullae suffer permanent deformation during the first compression ramp. In successive cycles, the continuous increase of irreversible processes leding to permanent deformation is reflected in a slight decrease of the maximum stress reached in each stress-strain loop (Figure 2.2c) and in the continuous narrowing of the mechanical hysteresis cycle. It is also worth noticing that zero stress is reached in the recovering ramp for strains around 5% what is the range of permanent deformation after each load-recovery cycle. The effect of this permanent deformation on sample morphology is observed in the SEM microphotographs of Figure 2.1b obtained after 10 load-recovery cycles. Macropores partially collapse although an interconnected pore structure still remains, with the open macropores presenting a more oval shape. The micropore structure, on the other hand, do not seems to be affected (see the inset in Figure 2.2b) in this situation.

PCL is quite hydrophobous with a contact angle of ~ 92º [37] and filling the pores of the sponge with water requires the application of high vacuum to extract completely air form the micropores before introducing water. Simultaneous injection of fibrinogen and thrombin solutions into the pores and further coagulation allows producing a fibrin gel homogeneously distributed in the whole pore volume. This gel has a nanofibrillar structure, as observed in CryoSEM (Figure 2.2c) after sublimating the water from the sample. Filling the pores with fibrin facilitates water diffusion through the scaffold.

The mechanical behavior of the samples evaluated in immersion in an aqueous liquid media is quite different to that of the dry tested samples. On the one hand, in spite to be hydrophobous, PCL absorbs a small amount of water [33] that significantly affects the mechanical behavior of PCL trabecullae. This fact results on the scaffold becoming more compliant and the maximum stress reached for 15% strain is smaller in ~50% in immersion tests than in the dry sample, as shown in Figure 2.2b for the scaffold filled with fibrin and

tested in immersion in PBS (the behavior of the unfilled PCL sponge is similar. Data not shown). The shape of the stress-strain plot reveals a larger curvature of the recovery curve up to zero strain with respect to the dry sample, indicating a lower degree of permanent deformation. This fact is supported by the SEM images shown in Figure 2.1d, showing the macropores nearly unaffected by the mechanical compression experiment. After 10 loading-unloading cycles it was observed that the fibrin starts to lose its characteristic fibrillar structure, suggesting a weak bonding between the fibrin and the PCL scaffold (Figure 2.1d). The small but continuous decrease of the maximum stress in the successive load-recovery cycles is also apparent in the samples tested in immersion (Figure 2.2c)
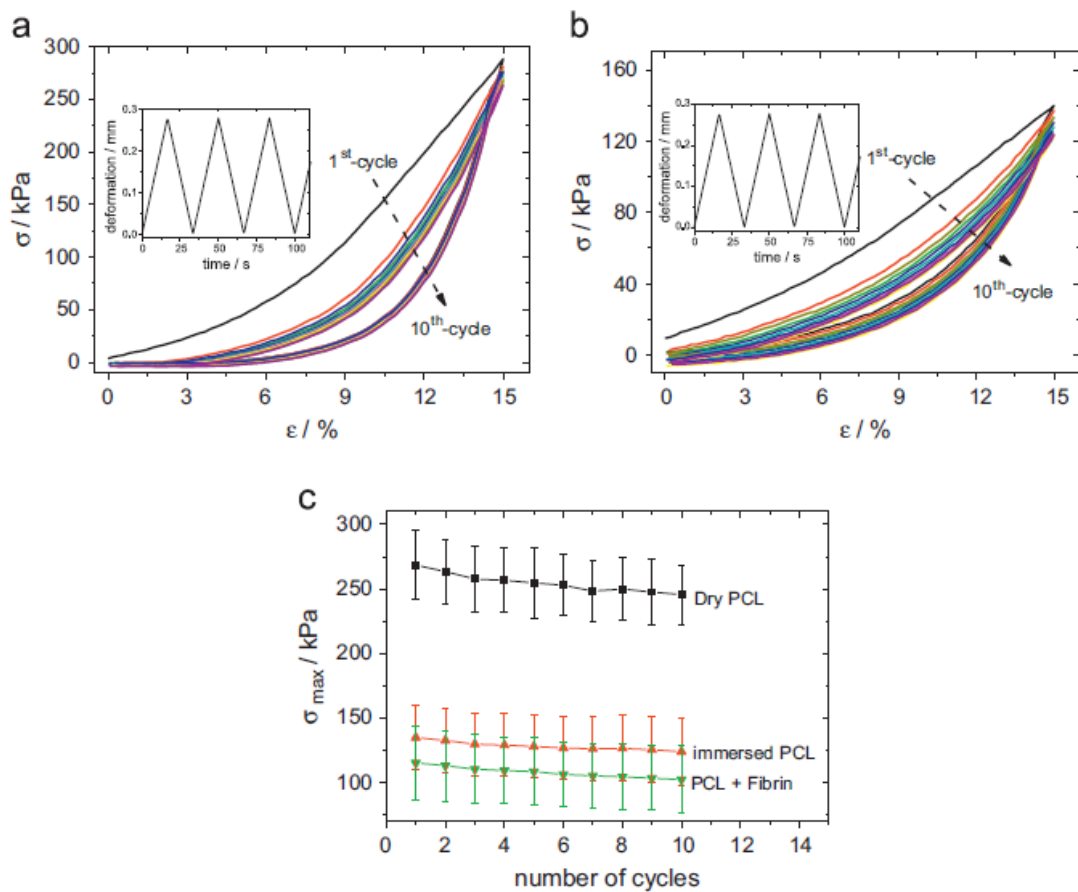
Figure 2.2 - Characteristic hysteresis loops obtained for: a) dry PCL and b) PCL with fibrin filler measured in a PBS solution at room temperature and c) typical peak tensile stress obtained up to 10 complete cycles for the PCL samples.
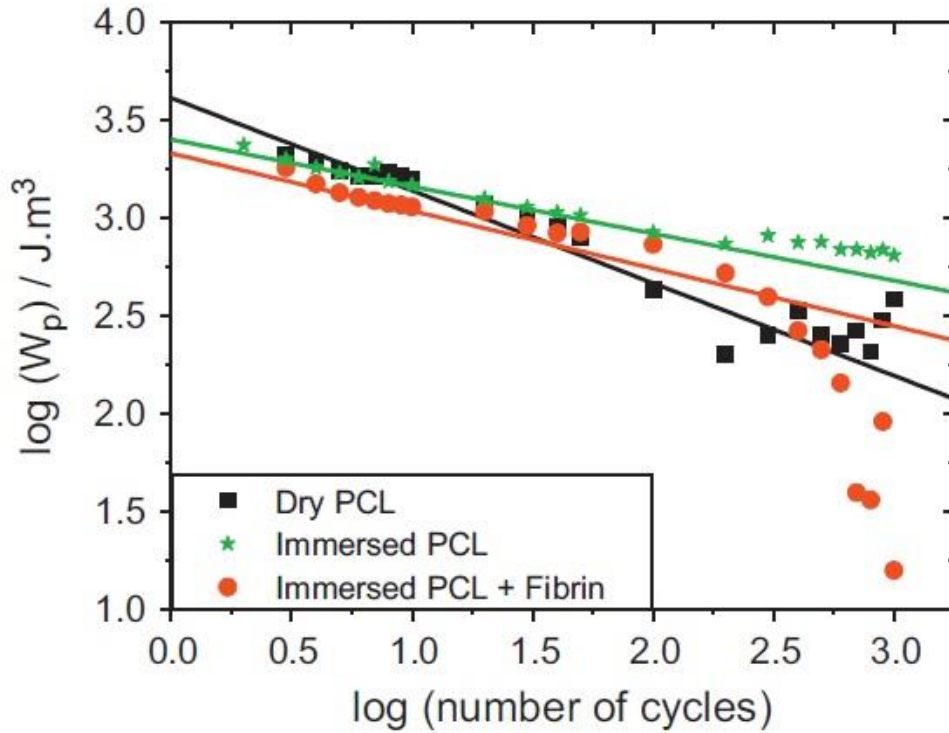
2.3.3 Morrow Energy Model: Plastic Strain Energy Density–Life Model

The plastic strain energy density can be physically interpreted as distortion energy associated to the change in shape of a volume element and related to permanent deformation, particularly under conditions of ductile behavior. It can be evaluated as the inner area (W_p) of the stress-strain hysteresis loop for a compressive experiments. Morrow's model describes fatigue behavior in terms of the plastic strain energy density [38, 39]:

$$N_f^m W_p = C \tag{2}$$

where, W_p is the plastic strain energy density, N_f is the fatigue life, and m and C are the fatigue exponent and coefficient, respectively.

Fatigue life for dry PCL and immersed PCL with fibrin samples submitted to compressive strain load is presented in Figure 2.3. Morrow's model predicts a linear relationship between $\log(N_f)$ and $\log(W_p)$, equation (2), The plot of Figure 2.3, shows that Morrow model can predict with accuracy the fatigue behavior of PCL scaffolds at least up to 100 deformation cycles The experimental results were fitted to equation (2) in this initial range of the curves to characterize fatigue behavior before collapse of the samples. The calculated lines are also represented in Figure 2.3 together with the experimental data. Morrow´s model fitting parameters are presented in table 1. It is observed a general decrease of the fatigue exponent and coefficient for the samples immersed in water with and without fibrin with respect to the sample tested under dry conditions (Table 2.1). Moreover, the m value found for the immersed PCL and immersed PCL with fibrin are quite similar, which suggests that the main contribution for samples fatigue behavior is giving, as expected, by water. Deviation from the straight line predicted by Morrows equation is considered the fatigue failure criterion [38]. Dry PCL collapses before 100 cycles but when immersed in water it seems to deviate from Morrow's straight line after 500 cycles. A similar behavior was found for the samples immersed in water with fibrin fibers distributed within the porous structure. This behavior reflects the relevant role of the aqueous filling in the fatigue behavior of PCL scaffolds, promoting a homogeneous distribution of the applied mechanical stress and diminishing stress concentration in the PCL trabecullae which is the main reason for the premature collapse of the dry scaffold.

Figure 2.3 - Relationship between the overall equivalent behavior similar to plastic strain energy density and number of load- recovery cycles of PCL samples.

Table 2.1 - Fitting results after Morrow's model for the PCL scaffolds.

Sample	m	C
Dry PCL	0.32 ± 0.01	3500 ± 650
Immersed PCL	0.24 ± 0.05	2500 ± 600
PCL + Fibrin	0.27 ± 0.04	2100 ± 660

Based on the experimental data and in the fitting parameters obtained from Morrow's fatigue model (Table 2.1), fatigue life was calculated and compared to the experimental results. The calculated life for the different samples are shown plotted versus the experimental lives in

Figure 2.4. In this figure, perfect correlation would be represented by data points lying on the solid diagonal line. It is clear from Figure 2.4 that Morrow´s plastic strain energy model can successfully predict the fatigue lives of the pristine dry and immersed PCL specimens both with and without fibrin. Further, it is possible to observe that the main contribution for the increase of number of cycles before permanent deformation of PCL scaffolds is due to the presence of water that occupies the scaffolds due to the more uniform distribution of the applied stress along the sample. When the porous scaffold is filled with air, local distribution of the stress occurs and, due to the porous nature of the scaffolds and the different geometry and dimensions of the pore walls s (Figure 2.1), a heterogeneous distribution of the applied mechanical stress occurs that leads to the collapse of the structure after just 100 cycles, whereas for the sample immersed in water stability is strongly increases with fatigue failure occurring only after 500 cycles.
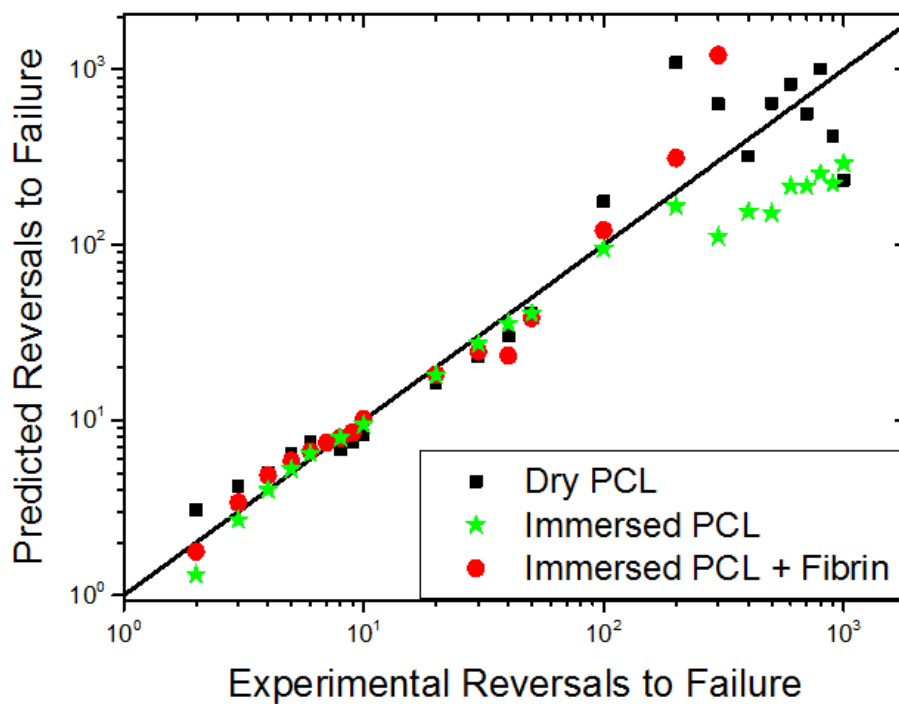
Figure 2.4 - Comparison of experimental and predicted fatigue behaviors, calculated according to Morrow's model

2.4 Conclusions

The mechanical stability of the scaffold is strongly important for tissue engineering applications and, in particular, in situations in which mechanical solicitations are applied. Fatigue life cycle of poly-ε-caprolactone scaffolds has been studied both with and without fibrin as filler of the pore structure and under dry and immersed in liquid water conditions. It has been proven that collapse of the samples occur after 100 cycles under dry conditions and the number of cycles increase to 500 i in the samples tested in immersed conditions. This fact is due to the more uniform stress distributions within the samples when the samples filled with water. It is also observed that the fibrin loading does not play a relevant role in the mechanical performance of the scaffolds.

2.5 References

1.   Nerem, R.M., *Chapter Two - The challenge of imitating nature*, in *Principles of Tissue Engineering (Third Edition)*, L. Robert, et al., Editors. 2007, Academic Press: Burlington. p. 7-14.

2.   Chen, Q., S. Liang, and G.A. Thouas, *Elastomeric biomaterials for tissue engineering.* Progress in Polymer Science, 2013. **38**(3–4): p. 584-671.

3.   Mikos, A.G., et al., *Prevascularization of porous biodegradable polymers.* Biotechnol Bioeng, 1993. **42**(6): p. 716-723.

4.   Kelly, D.J. and C.R. Jacobs, *The role of mechanical signals in regulating chondrogenesis and osteogenesis of mesenchymal stem cells.* Birth Defects Res C Embryo Today, 2010. **90**(1): p. 75-85.

5.   Huang, A.H., M.J. Farrell, and R.L. Mauck, *Mechanics and mechanobiology of mesenchymal stem cell-based engineered cartilage.* J Biomech, 2010. **43**(1): p. 128-36.

6.   McCullen, S.D., C.M. Haslauer, and E.G. Loboa, *Musculoskeletal mechanobiology: interpretation by external force and engineered substratum.* J Biomech, 2010. **43**(1): p. 119-27.

7. Riehl, B.D., et al., *Mechanical stretching for tissue engineering: two-dimensional and three-dimensional constructs.* Tissue Eng Part B Rev, 2012. **18**(4): p. 288-300.

8. Puppi, D., et al., *Polymeric materials for bone and cartilage repair.* Progress in Polymer Science, 2010. **35**(4): p. 403-440.

9. Khatiwala, C.B., S.R. Peyton, and A.J. Putnam, *Intrinsic mechanical properties of the extracellular matrix affect the behavior of pre-osteoblastic MC3T3-E1 cells.* American Journal of Physiology - Cell Physiology, 2006. **290**(6): p. C1640-C1650.

10. Wong M Fau - Carter, D.R. and D.R. Carter, *Articular cartilage functional histomorphology and mechanobiology: a research perspective.* Bone, 2003. **33**(8756-3282 (Print)): p. 1-13.

11. Schulz, R.M. and A. Bader, *Cartilage tissue engineering and bioreactor systems for the cultivation and stimulation of chondrocytes.* Eur Biophys J, 2007. **36**(4-5): p. 539-68.

12. Knecht, S., B. Vanwanseele, and E. Stussi, *A review on the mechanical quality of articular cartilage - implications for the diagnosis of osteoarthritis.* Clin Biomech (Bristol, Avon), 2006. **21**(10): p. 999-1012.

13. Mahmoudifar, N. and P.M. Doran, *Chondrogenic differentiation of human adipose-derived stem cells in polyglycolic acid mesh scaffolds under dynamic culture conditions.* Biomaterials, 2010. **31**(14): p. 3858-67.

14. Huang, A.H., et al., *Long-term dynamic loading improves the mechanical properties of chondrogenic mesenchymal stem cell-laden hydrogel.* Eur Cell Mater, 2010. **19**: p. 72-85.

15. De Croos, J.N., et al., *Cyclic compressive mechanical stimulation induces sequential catabolic and anabolic gene changes in chondrocytes resulting in increased extracellular matrix accumulation.* Matrix Biol, 2006. **25**(6): p. 323-31.

16. Chen, A., et al., *Twenty-four well plate miniature bioreactor system as a scale-down model for cell culture process development.* Biotechnol Bioeng, 2009. **102**(1): p. 148-60.

17. Spiller, K.L., et al., *Superporous hydrogels for cartilage repair: Evaluation of the morphological and mechanical properties.* Acta biomaterialia, 2008. **4**(1): p. 17-25.

18. Hutmacher, D.W., et al., *Mechanical properties and cell cultural response of polycaprolactone scaffolds designed and fabricated via fused deposition modeling.* J Biomed Mater Res, 2001. **55**(2): p. 203-16.

19. Blasi, P., et al., *Plasticizing effect of water on poly(lactide-co-glycolide).* J Control Release, 2005. **108**(1): p. 1-9.

20. Mars, W.V., *Factors that affect the fatigue life of a rubber: a literature survey.* Journal of Rubber Chemistry and Technology, 2004. **77**(3): p. 391-412.

21. T. Alshuth and F. Abraham, *Parameter dependence and prediction of fatigue properties of elastomer products.* Rubber chemistry and technology, 2002. **75**(4): p. 635-642.

22. Ince, A. and G. Glinka, *A modification of Morrow and Smith–Watson–Topper mean stress correction models.* Fatigue & Fracture of Engineering Materials & Structures, 2011. **34**(11): p. 854-867.

23. Bourago, N.G., A.B. Zhuravlev, and I.S. Nikitin, *Models of multiaxial fatigue fracture and service life estimation of structural elements.* Mechanics of Solids, 2011. **46**(6): p. 828-838.

24. Morrow, J.D., *Internal Friction, Damping, and Cyclic Plasticity*, in *ASTM-STP 378*1965: Philadelphia.

25. Lee, K.Y. and D.J. Mooney, *Hydrogels for Tissue Engineering.* Chemical Reviews, 2001. **101**(7): p. 1869-1880.

26. Santamaría, V.A., et al., *Influence of the macro and micro-porous structure on the mechanical behavior of poly(l-lactic acid) scaffolds.* Journal of Non-Crystalline Solids, 2012. **358**(23): p. 3141-3149.

27. Gamboa-Martínez, T.C., J.L. Gómez Ribelles, and G. Gallego Ferrer, *Fibrin coating on poly (L-lactide) scaffolds for tissue engineering.* Journal of Bioactive and Compatible Polymers, 2011. **26**(5): p. 464-477.

28. Izal, I., et al., *Culture of human bone marrow-derived mesenchymal stem cells on of poly(L: -lactic acid) scaffolds: potential application for the tissue engineering of cartilage.* Knee Surg Sports Traumatol Arthrosc, 2012.

29. Lebourg, M., J. Suay Anton, and J.L. Gomez Ribelles, *Hybrid structure in PCL-HAp scaffold resulting from biomimetic apatite growth.* J Mater Sci Mater Med, 2010. **21**(1): p. 33-44.

30. Lebourg, M., J. Suay Antón, and J.L. Gomez Ribelles, *Characterization of calcium phosphate layers grown on polycaprolactone for tissue engineering purposes.* Composites Science and Technology, 2010. **70**(13): p. 1796-1804.

31. Deplaine, H., J.L.G. Ribelles, and G.G. Ferrer, *Effect of the content of hydroxyapatite nanoparticles on the properties and bioactivity of poly(l-lactide) – Hybrid membranes.* Composites Science and Technology, 2010. **70**(13): p. 1805-1812.

32. Martinez-Diaz, S., et al., *In vivo evaluation of 3-dimensional polycaprolactone scaffolds for cartilage repair in rabbits.* Am J Sports Med, 2010. **38**(3): p. 509-19.

33. Olmedilla, M.P., et al., *In vitro 3D culture of human chondrocytes using modified epsilon-caprolactone scaffolds with varying hydrophilicity and porosity.* J Biomater Appl, 2012. **27**(3): p. 299-309.

34. Nicodemus, G.D. and S.J. Bryant, *The role of hydrogel structure and dynamic loading on chondrocyte gene expression and matrix formation.* Journal of Biomechanics, 2008. **41**(7): p. 1528-1536.

35. Michalopoulos, E., et al., *Development of methods for studying the differentiation of human mesenchymal stem cells under cyclic compressive strain.* Tissue Eng Part C Methods, 2012. **18**(4): p. 252-62.

36. Appelman, T.P., et al., *The differential effect of scaffold composition and architecture on chondrocyte response to mechanical stimulation.* Biomaterials, 2009. **30**(4): p. 518-25.

37. Little, U., et al., *Surface modification of poly(ε-caprolactone) using a dielectric barrier discharge in atmospheric pressure glow discharge mode.* Acta biomaterialia, 2009. **5**(6): p. 2025-2032.

38. Kallmeyer, A.R. and R.I. Stephens, *Constant and Variable Amplitude Fatigue Behavior and Modeling of an SRIM Polymer Matrix Composite.* Journal of Composite Materials, 1995. **29**(12): p. 1621-1648.

39. Kanchanomai, C. and Y. Mutoh, *Low-cycle fatigue prediction model for pb-free solder 96.5Sn-3.5Ag.* Journal of Electronic Materials, 2004. **33**(4): p. 329-333.

Chapter 3: Fatigue Prediction on Poly-ε-caprolactone Macroporous Scaffolds - Influence of pore filling by a poly(vinyl alcohol) gel.
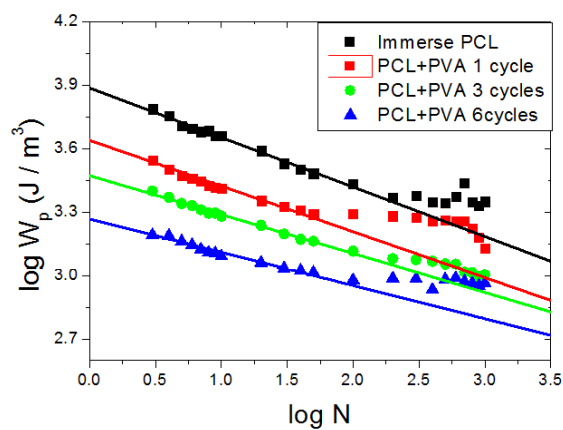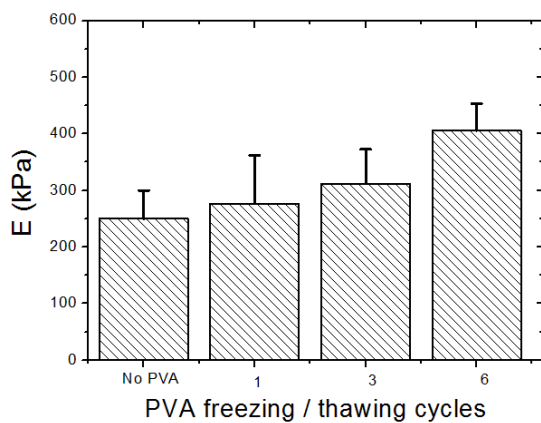
3.1 Introduction

Macroporous biodegradable polyesters are interesting scaffolds for cartilage tissue engineering applications, since they are able to sustain the mechanical loading produced in the joint during motion, which in turn produce suitable signals for the development of the extracellular matrix (ECM). The interconnected pores can provide a structure suitable for cell attachment, proliferation and fluid flow for nutrients and waste transport [1, 2]. The overall mechanical properties of the scaffold are determined by material mechanical properties, permeability and pore structure. These properties regulate load transfer and evolution of the ECM in a feedback process where the growing ECM matrix changes with time together with the aforementioned properties. Thus, prediction of the scaffolds mechanical behavior, in particular when a cyclic load is applied, is necessary for the proper understanding of the mechanical effect on cell response.

The retrieval of scaffolds after implantation in animals for measuring mechanical properties is hard, expensive and raises ethical issues. On the other hand, the measurement of the mechanical performance of scaffolds during *in vitro* experiments involves the use of growth factors and bioreactors to stimulate ECM synthesis, needing also large experimental time to obtain information concerning material mechanical performance. Therefore, finding a model capable to predict material behavior during *in vitro* and *in vivo* experiments is an important challenge for tissue and biomedical engineering.

Mechanical fatigue behavior of polymer scaffolds have been barely assessed in the literature [3, 4], despite their large importance in actual applications. The mechanical properties of dry scaffold are not representative of the behavior of the material when immersed in cell culture media or during *in vivo* experiments, as the porous will be filled with aqueous media and/or growing tissue that will strongly contribute to the scaffold mechanical response. For dry scaffolds, the mechanical properties will depend mainly on the inner morphology, in particular, pore size and polymer wall thickness and interconnectivity [5]. On the other hand, when the scaffold is immersed in an aqueous media, there are other factors that contribute for scaffold mechanical behavior as well, such as hydrodynamics and permeability inside the porous structure [5, 6]. Water is known for its low compressibility and any factor limiting water permeation through the material will increase apparent scaffold stiffness and therefore

the influence of liquid media cannot be disregarded, as was seen in the previous chapter [6]. However, only few investigations mention the mechanical behavior of polymer scaffolds under liquid environment [7, 8] and none of them under cyclic loading in aqueous media.

In this work a micro and macro porous poly-ε-caprolactone (PCL) scaffold has been employed, it is a semicrystalline hydrophobic polymer and has a degradation time of 2-4 years "in vivo", raising interest in cartilage tissue engineering [9, 10]. By combining a freeze extraction process and the use of porogen microparticles a scaffold structure that is characterized by large interconnected spherical pores with microporous walls can be synthetized. [11-13]

Fatigue behavior of materials can be influenced by several factors such as thermal and mechanical loading history, environmental conditions, polymer composition and other aspects of stress-strain constitutive behavior [14]. Several mathematical models have been developed mainly to predict fatigue life cycle of metallic materials, including the Coffin–Manson, Smith-Watson-Topper (SWT) and Morrow models [15, 16]. The Coffin-Manson model is based on the plastic strain amplitude and number of elapsed cycles, while in the SWT model[17] the product of maximum stress (σ_{max}) and $\Delta\varepsilon_t$ is assumed to control the fatigue life cycle for any given situation[18]. The model used in this wok, the Morrow model, describes evolution of fatigue as changes in the plastic strain energy density, under conditions of ductile behavior [19].

It has been shown in the previous chapter [6] that fatigue life cycle of poly-ε-caprolactone (PCL) scaffolds, with and without fibrin within the porous structure strongly depends on the presence of water, the fatigue life cycle increasing from 100 up to 500 loading cycles in samples tested under dry and immersed conditions, respectively. This effect was attributed to a more homogeneous stress distribution promoted by water within the samples. On the other hand, the presence of fibrin inside the macroporous structure plays just a minor role in the mechanical performance of the scaffolds.

Poly(vinyl alcohol) (PVA) gels are often applied as cartilage substitutes as they can mimic the elastic modulus of cartilage [20, 21], as they offer the possibility of formation of physical cross-links during freezing/thawing cycles without the need of toxic monomers used typically

in chemically cross-linked gels[22] such as gelatin[23] or chitosan[24]. During exposure to cold temperatures promoting water freezing, phase separation leads to regions of high PVA concentration, hydrogen bonding and crystallite formation due to the higher packing of the PVA chains[25]. These interactions remain intact before thawing and create a non-degradable three-dimensional hydrogel network. Increasing the number of freezing/thawing cycles, the degree of polymer phase separation, hydrogen bonding and crystallite formation can be increased leading to tailored mechanical properties by controlling the freeze/thaw process and the number of cycles[26].

In a previous study a macro and micro porous PCL scaffold was filled with an aqueous solution of PVA and exposed to up to 6 cycles of freezing and thawing. The mechanical properties of the PCL and PVA construct reached values of natural articular cartilage and meniscus . The PCL and PVA construct is then considered suitable as an in vitro model for simulating the growing cartilage inside of the scaffold of the PCL scaffold [27] In the present work the same protocol was applied to obtain PCL – PVA constructs, whose fatigue mechanical properties were measured. These properties are critical for the use of these scaffolds in cell cultures under dynamic loading.

3.2 Materials and methods

3.2.1 Materials

Poly-ε-caprolactone (PCL, 43-50 kDa) and 1,4-dioxan were purchased from *Sigma-Aldrich*. Poly(ethyl methacrylate) (PEMA - Elvacite 2043) spheres (mean diameter of 200 μm) were purchased from *Lucite*. Poly (vinyl alcohol) with Mw 13 kDa and >99% hydrolyzed was obtained from Sigma-Aldrich.

3.2.2 Sample preparation

PCL scaffolds were prepared as described in the previous chapter. [6]. Briefly, PCL was dissolved in dioxane (25% w/v) and this solution was mixed with PEMA microspheres (1:1

w/w). Then, the mixture was placed in Teflon Petri dishes and submerged in liquid nitrogen for a minute. Dioxan was extracted from the frozen plates with ethanol at - 20 ^{0}C for three days, changing ethanol every day. Porogen leaching was performed in ethanol at 40 ^{0}C for one day. The porous samples were cut into cylinders with 6 mm diameter and a thickness of approximately of 2 mm. Further leaching for each cylinder was performed in ethanol at 40 ℃ for nine days, changing ethanol daily.

In order to ensure the maximum water uptake for measurements in immersion, after complete porogen leaching, all samples were immersed in a distilled water bath and placed in a chamber (Vacuum-Temp from Selecta) under 10^{-2} mmHg conditions until the samples dropped to the bottom of the bath

PVA was dissolved in water (10% w/v) at 90 °C for 1 hour. After the solution was obtained it was allowed to cool to room temperature. The viscous solution was introduced into PCL scaffolds by syringe vacuum. All PCL scaffolds under immersion were placed inside a syringe with 10 ml of PVA solution 10%, at room temperature. The syringe barrel was closed with a syringe cap and vacuum was made by moving the piston alternately at maximum (50 ml) and minimum to displace and substitute the air inside the pores by PVA. The operation was repeated 30 times. The remaining PVA in the external surface of the scaffolds was removed. Hydrogels of different stiffness were obtained by freezing PCL-PVA constructs at - 20 °C for 16 hours and then thawed back to room temperature for 8 hours in humid environment. Three series of samples were prepared with 1, 3 or 6 freeze-thawing cycles respectively.

3.2.3 Sample characterization

Sample morphology and gel construct was assessed by scanning electron microscopy using a *JEOL JSM-5410* apparatus equipped with a cryogenic device. Images were taken at an accelerating voltage of 10 kV. Samples were previously immersed in water during 24 h and then frozen at -80 ℃. Then, the samples were cryo-fractured and water was sublimated during 40 min before coating with a gold thin layer.

Mechanical experiments were performed on cylindrical samples with 6 mm diameter and a height of ~2 mm in a *Shimadzu AG-IS* universal testing machine in compression mode at a test velocity of 1 mm.min^{-1} and at room temperature. In fatigue experiment, samples were submitted to a compressive-strain cycle load at a strain of 15% and up to 1000 cycles, which is typically the strain range of interest considered to be the maximum magnitude physiological deformation suffered for articular cartilage [28, 29]. Strain deformation was measured by machine cross-head displacement. Mechanical stress and strain parameters were obtained after an average of five sample replicas for each set of constructs (PCL with PVA after 1,3 and 6 freeze-thawing cycles) . All mechanical experiments were performed after sample immersion in deionized water.

3.3 Results and discussion

3.3.1 Morphology, morphology variation and mechanical response

It was observed that PCL porous architecture consists on a double porosity: macropores ranging from 120 up to 200 μm obtained from the leaching of the porogen spheres and micropores resulting from dioxane crystals formed during the freeze extraction process that interconnect the bigger ones (examples indicated with arrows in Figure 3.1a and b). This double porous structure results in and overall high porosity (83.4±2.6%[6]) and has been previously proposed for cartilage and bone replacement[30-32]. Such structure favors scaffold permeability to nutrients and waste products of cell metabolism and can be used to retain active components [11, 33, 34]. However, apparent scaffold stiffness becomes smaller than in similar sponges lacking microporosity [13, 35]. Further, when PVA solution is introduced in PCL scaffolds in which the air has been extracted from the pores, it is able to fill both the macropores and the micropores. On crosslinking by freeze-thawing cycles, PVA forms a continuous polymer network filling the pore structure. The continuity of the PVA phase between the micropores and macropores even made it difficult to identify the interphases with PCL in SEM pictures. Only small discontinuities can barely be found in particular points of the SEM pictures (area in Figure 3.1c) Due to the viscosity of PVA solution some micropores can remain empty, an example can be observed in the inset of Figure 3.1c. Small detachments at the interphase between PVA and PCL appear in some points in but they could be produced during cryofracture in sample preparation (inset of

Figure 3.1c). Scaffolds observed after cyclic mechanical loading for 1000 cycles show that the PCL macropores collapse and their shape changed from circular to a more ellipsoid one (Figure 3.1 a and b). In the case of the samples filled with PVA after fatigue testing (Figure 3.1d) cryogenic fracture shows increased roughness with respect to the smooth surface observed before fatigue (Figure 3.1c) and the shape of macropores is not clear.
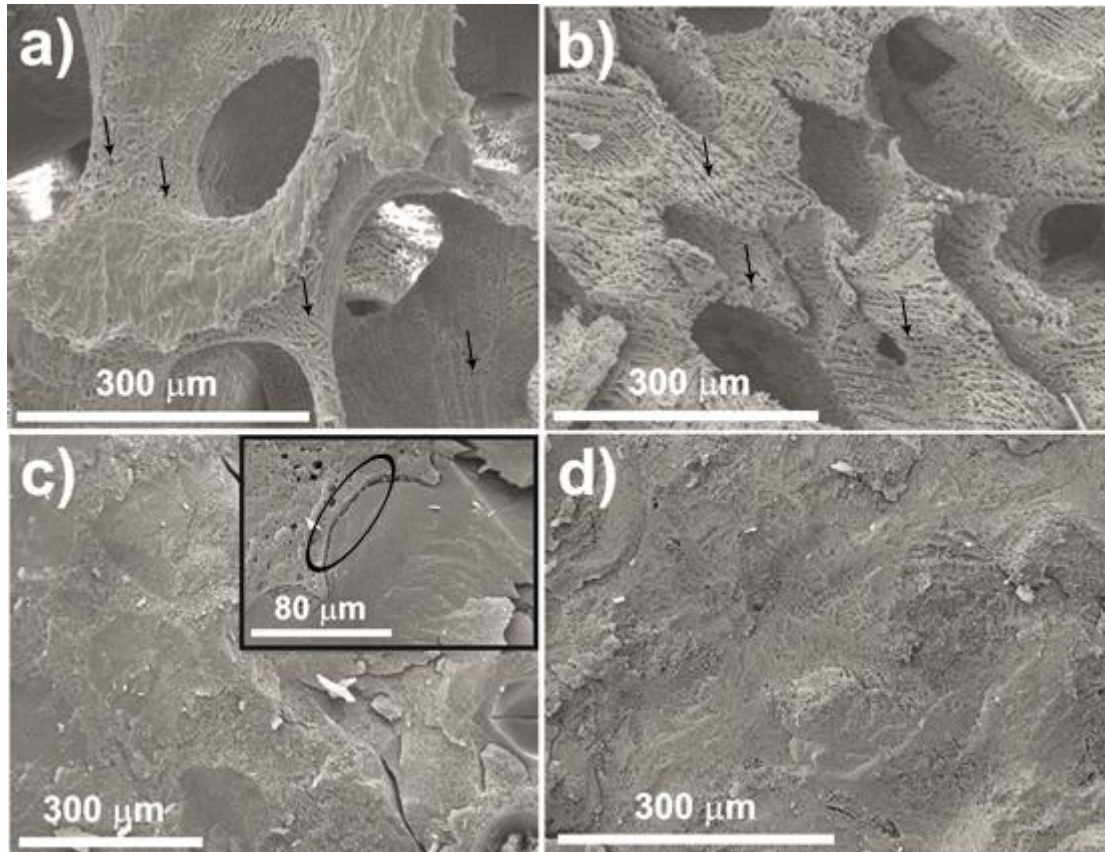
Figure 3.1 - PCL microstructure: a) pristine scaffold, b) after applied cyclic mechanical loading for 1000 cycles, c) PCL – PVA sample after 6 freeze/thawing cycles before and d) after applied cyclic mechanical loading for 1000 cycles. Arrows and areas indicate elements described in the text.

3.3.2 Mechanical analysis

Mechanical performance of PCL and PCL – PVA samples obtained from the evaluation of the elastic modulus for the first cycle determined at $\varepsilon = 5\%$ show that PVA contributes for

an increase of the elastic modulus, especially for the samples submitted to higher freezing/thawing cycles (Figure 3.2a). Further, the incorporation of PVA inside of the PCL porous matrix leads to an increase of the maximum stress when compared to the pristine polymer (Figure 3.2b). Such behavior is ascribed to the increase in the degree of crystallinity present in the PVA hydrogel that promotes a homogenous distribution of the stress among the sample crystalline regions [25, 26].
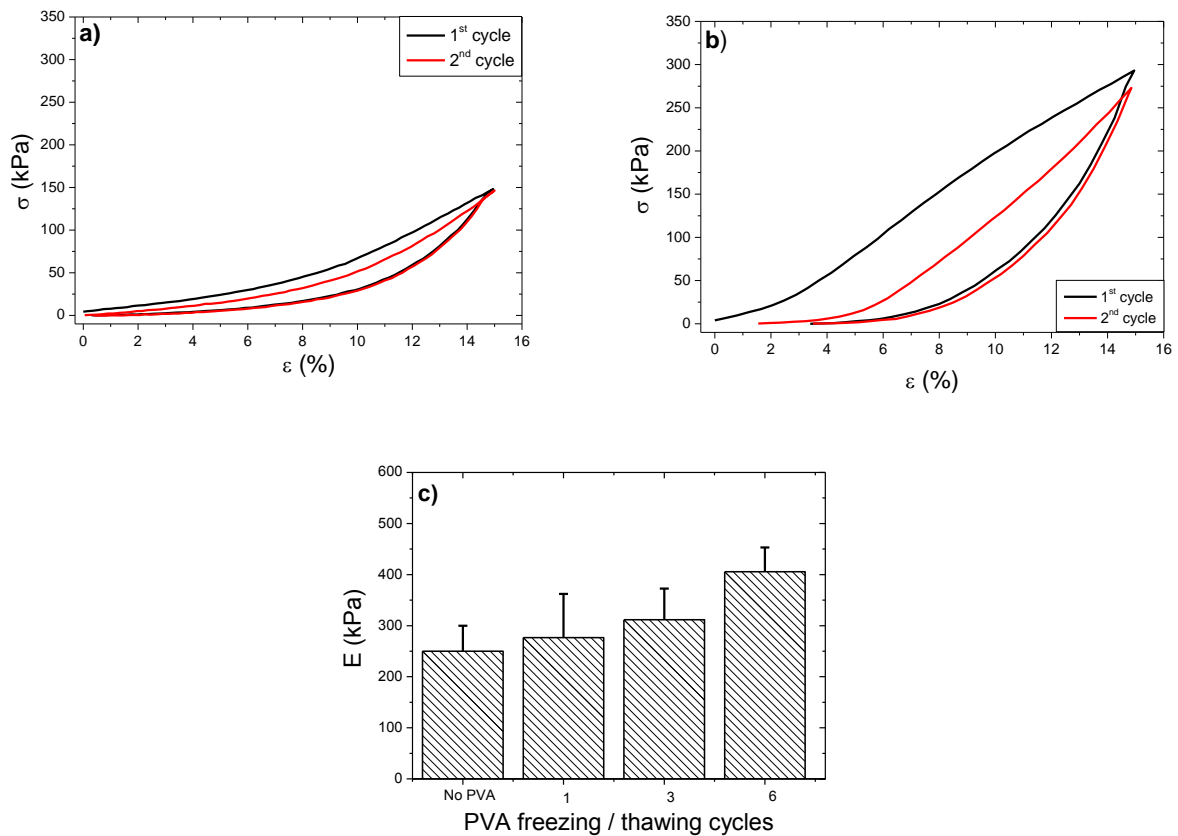
Figure 3.2 - Hysteresis of first and second loop for a) pristine immerse PCL and b) immerse PCL-PVA after 6 freezing/thawing samples c) Elastic moduli obtained for first cycle in PCL and PCL-PVA samples (1, 3 and 6 freezing/thawing cycles), calculated from first 5% of strain.

Moreover, the maximum stress decreases after each cycle, suggesting that the material undergoes permanent deformation with increasing the number of loading cycles during the

first ~40 cycles, stabilizing after that (Figure 3.3). Initial maximum stress is higher while PVA freezing/thawing cycles are increased.
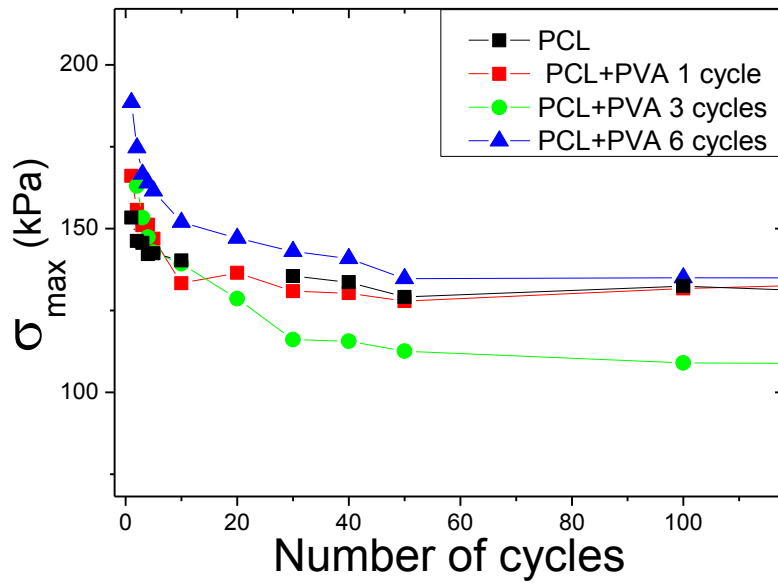
Figure 3.3 - Average maximum tensile stress as a function of the number of cycles for PCL and PCL - PVA samples.

3.3.3 Morrow energy model: plastic strain energy density-life model

Hysteresis loops behave differently when PVA is added, especially after 6 freeze/thawing cycles (Figure 3.4). Cyclic loading has a major impact for immerse PCL without PVA. These differences can be observed in detail with fatigue analysis.
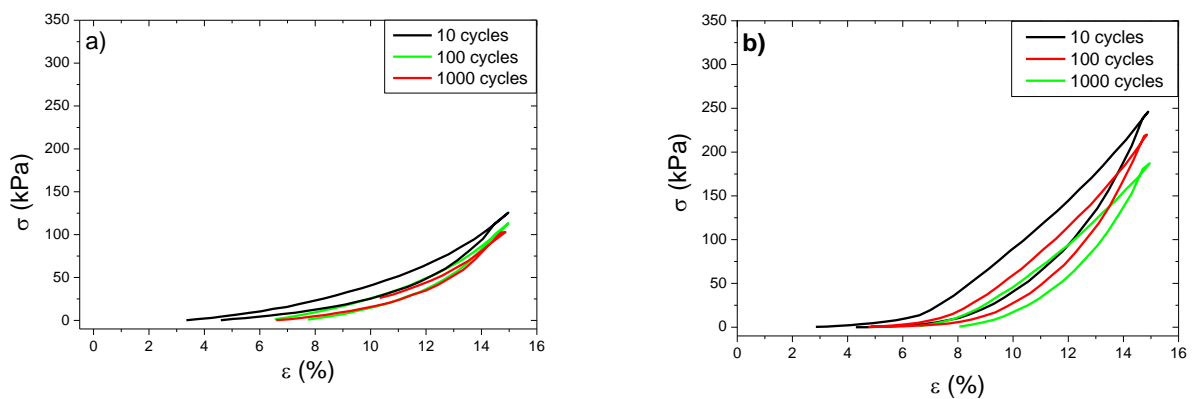
Figure 3.4 - Hysteresis loops after 10, 100 and 1000 loading cycles, for a) immerse pristine PCL and b) immerse PCL with PVA after 6 freeze/thawing cycles.

82

Under cyclic loading, the plastic strain energy per cycle is considered a measure of the amount of fatigue damage per cycle. The amount of plastic strain by the material and the hysteresis energy absorbed during cyclic loading has been postulated as a basis for failure analysis. According to Morrow´s model [19], the relation between plastic strain energy density and the fatigue life can be expressed as:

$$N_f^m W_p = C \qquad (1)$$

where W_p is the overall equivalent behavior similar to plastic strain energy density; N_f is the fatigue life and m and C are the fatigue exponent and coefficient, respectively.

Experimental data were fitted with equation 1 to evaluate the material behavior in response to cyclic mechanical loading before ample collapse with R > 0.98. The fitting results are represented in Figure 3.5 as solid lines, together with the experimental data points, and the fitting parameters are presented in Table 3.1. A general decrease of the fatigue exponent (slope in Figure 3.5) and coefficient (y-intercept) for all samples was observed, with respect to the pristine porous PCL sample, which means a lower decrease in dissipated and energy suggests that the PVA is attached to the porous PCL walls and some mechanical loading is supported by PVA gel. According to ANOVA with Tukey test, the slopes are significantly different between PCL samples without PVA and after 6 freezing-thawing cycles.
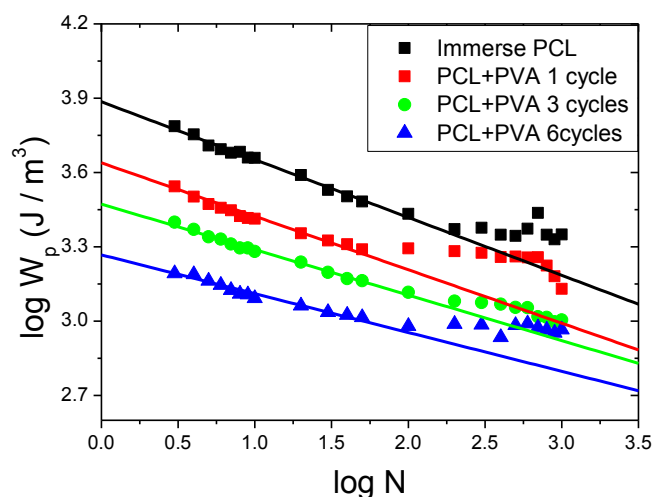
Figure 3.5 - Relationship between the overall equivalent behavior similar to plastic strain energy density and the number of load-recovery cycles of PCL and PCL-PVA samples.

Table 3.1 - Fitting results with equation 1 for the different immersed PCL and PCL with PVA samples.

Sample	m	C
PCL	0.24 ± 0.05	2500 ± 600
PCL+PVA 1 Cycle	0.23 ± 0.03	4564 ± 293
PCL+PVA 3 Cycles	0.18 ± 0.01	1830 ± 1600
PCL+PVA 6 Cycles	0.16 ± 0.04	1865 ± 170

It has been reported [36] that freezing/thawing promotes a decrease in the number of hydroxyl groups available for hydrogen bonding caused by an increase of entanglement which hinders other hydrogen bonding formation from weakening of physical network. Further, decreasing of the glass transition also occurs with increasing number of freezing/thawing cycles.

For higher freezing/thawing cycles, the volume of the PVA increases as well as the degree of crystallinity [22, 25], and the material can support partially the mechanical load that is transferred from water and from PCL matrix, leading to more stable distribution of the applied mechanical loading and consequently to higher fatigue life cycle behavior.

Based on the fitting parameters (Table 3.1), mechanical life cycle behavior was calculated and compared to the experimental data. The calculated number of cycles to reach scaffolds plastic deformation for PCL and the different PCL – PVA samples are plotted *vs* the experimental load-recovery cycles (Figure 3.6). Good correlation is represented by experimental data points lying on the solid diagonal line with deviations lower than 10 % from the theoretical line [37]. Figure 3.6 shows thus that Morrow´s model can successfully predict the load recovery cycles behavior for the PCL and PCL-PVA samples, at least until 200 cycles, when intrinsic properties change and the constructs does not respond equally to cyclic loads [16, 37].
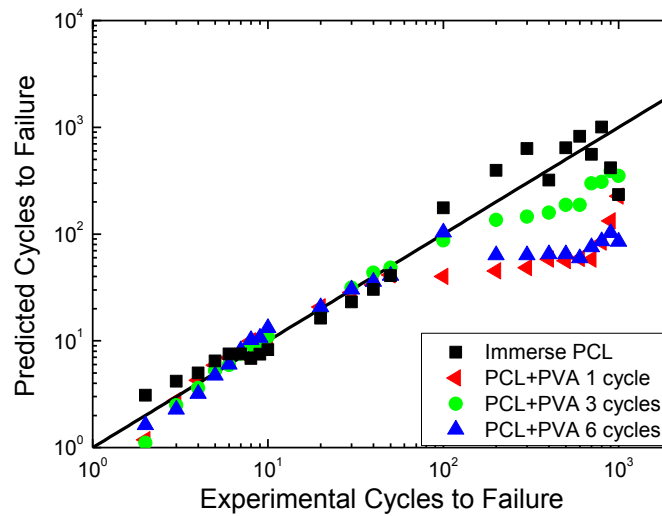
Figure 3.6 - Comparison of experimental and theoretically predicted fatigue behavior, according to Morrow's model for PCL and PCL-PVA samples

3.4 Discussion

PCL porous scaffolds, with and without PVA inside the porous structure has been submitted to cyclic mechanical compression until a 15% deformation. When PVA solution is introduced in PCL scaffolds and after crosslinking by freeze-thawing cycles, a continuous polymer network filling the matrix pore structure was observed (Figure 3.1). It has been reported [36] that freezing/thawing promotes a decrease in the number of hydroxyl groups available for hydrogen bonding caused by an increase of entanglement which hinders other hydrogen bonding formation from weakening of physical network. Further, decreasing of the glass transition also occurs with increasing number of freezing/thawing cycles.

For higher freezing/thawing cycles, the volume of the PVA increases as well as the degree of crystallinity[22, 25], and the material can support partially the mechanical load that is transferred from water and from PCL matrix, leading to more stable distribution of the applied mechanical loading and consequently to higher fatigue life cycle behavior. Similar behavior was observed for PCL scaffolds immersed in water [6].

Finally, Morrow's fitting parameters presented in Table 3.1 allowed to compare experimental and predicted PCL scaffolds fatigue life cycle and a truthful correlation was obtained up to 200 loading-unloading cycles and for larger number of cycles deviation occurs both for dry and pristine PCL[6] samples.

3.5 Conclusions

The mechanical stability of polymer scaffolds is a key issue for tissue and biomedical engineering applications, particularly, when the materials are immersed in aqueous media and submitted to cycle mechanical loading in conditions resembling their application environment. In this way, PVA gel has been introduced within the PCL macroporous scaffolds aiming to simulate the growing tissue. It is demonstrated that the presence of PVA increases the elastic modulus of the scaffolds, this effect being more pronounced with increasing the number of freeze/thawing cycles. Increasing the number of freeze/thawing for PVA improves the resistance to fatigue, being only noticeably for higher freeze/thawing cycles, which better resemble the conditions of a growing extracellular matrix. However, accurate fitting to the Morrow´s energy model is just possible up to 200 loading-unloading cycles. The deviation for larger number of cycles occurs both for dry and pristine PCL [6] samples. This fact, should be related to complex changes in the porous structure and local interactions among the different phases (PCL, PVA and water). In future works these results will be compared with the effect of cartilage-like ECM generated *in vitro* inside the macropores, in order to further validate the model and to delve in the mechanical integration of ECM and scaffolds, and its effects in fatigue resistance of the overall construct.

3.6 References

1. Mikos, A.G., et al., *Prevascularization of porous biodegradable polymers.* Biotechnol Bioeng, 1993. **42**(6): p. 716-723.
2. Chen, Q., S. Liang, and G.A. Thouas, *Elastomeric biomaterials for tissue engineering.* Progress in Polymer Science, 2013. **38**(3–4): p. 584-671.

3. Ergun, A., et al., *Unitary Bioresorbable Cage/Core Bone Graft Substitutes for Spinal Arthrodesis Coextruded from Polycaprolactone Biocomposites.* Annals of Biomedical Engineering, 2012. **40**(5): p. 1073-1087.

4. Amin Yavari, S., et al., *Fatigue behavior of porous biomaterials manufactured using selective laser melting.* Materials Science and Engineering: C, 2013. **33**(8): p. 4849-4858.

5. Spiller, K.L., et al., *Superporous hydrogels for cartilage repair: Evaluation of the morphological and mechanical properties.* Acta biomaterialia, 2008. **4**(1): p. 17-25.

6. Panadero, J.A., et al., *Fatigue prediction in fibrin poly-epsilon-caprolactone macroporous scaffolds.* J Mech Behav Biomed Mater, 2013. **28**: p. 55-61.

7. Hutmacher, D.W., et al., *Mechanical properties and cell cultural response of polycaprolactone scaffolds designed and fabricated via fused deposition modeling.* J Biomed Mater Res, 2001. **55**(2): p. 203-16.

8. Blasi, P., et al., *Plasticizing effect of water on poly(lactide-co-glycolide).* J Control Release, 2005. **108**(1): p. 1-9.

9. Valonen, P.K., et al., *In vitro generation of mechanically functional cartilage grafts based on adult human stem cells and 3D-woven poly(epsilon-caprolactone) scaffolds.* Biomaterials, 2010. **31**(8): p. 2193-200.

10. Kim, H.J., J.H. Lee, and G.I. Im, *Chondrogenesis using mesenchymal stem cells and PCL scaffolds.* J Biomed Mater Res A, 2010. **92**(2): p. 659-66.

11. Lebourg, M., J. Suay Anton, and J.L. Gomez Ribelles, *Hybrid structure in PCL-HAp scaffold resulting from biomimetic apatite growth.* J Mater Sci Mater Med, 2010. **21**(1): p. 33-44.

12. Lebourg, M., et al., *Different hyaluronic acid morphology modulates primary articular chondrocyte behavior in hyaluronic acid-coated polycaprolactone scaffolds.* J Biomed Mater Res A, 2013. **101**(2): p. 518-27.

13. Martinez-Diaz, S., et al., *In vivo evaluation of 3-dimensional polycaprolactone scaffolds for cartilage repair in rabbits.* Am J Sports Med, 2010. **38**(3): p. 509-19.

14. Mars, W.V., *Factors that affect the fatigue life of a rubber: a literature survey.* Journal of Rubber Chemistry and Technology, 2004. **77**(3): p. 391-412.

15. Ince, A. and G. Glinka, *A modification of Morrow and Smith–Watson–Topper mean stress correction models.* Fatigue & Fracture of Engineering Materials & Structures, 2011. **34**(11): p. 854-867.

16. Milne, I., R.O. Ritchie, and B.L. Karihaloo, *Comprehensive Structural Integrity: Cyclic loading and fatigue*. 2003: Elsevier/Pergamon.

17. Smith, K.N., P. Watson, and T.H. Topper, *A stress-strain function for the fatigue of metals.* Journal of Materials, 1970. **4**: p. 767-778.

18. Bourago, N.G., A.B. Zhuravlev, and I.S. Nikitin, *Models of multiaxial fatigue fracture and service life estimation of structural elements.* Mechanics of Solids, 2011. **46**(6): p. 828-838.

19. Morrow, J.D., *Internal Friction, Damping, and Cyclic Plasticity*, in *ASTM-STP 378*1965: Philadelphia.

20. Spiller, K.L., et al., *Design of semi-degradable hydrogels based on poly(vinyl alcohol) and poly(lactic-co-glycolic acid) for cartilage tissue engineering.* J Tissue Eng Regen Med, 2011. **5**(8): p. 636-47.

21. Li, F., et al., *Comparison of Human Articular Cartilage and Polyvinyl Alcohol Hydrogel as Artificial Cartilage in Microstructure Analysis and Unconfined Compression.* Advanced Materials Research, 2009. **87-88**: p. 188-193.

22. Hickey, A.S. and N.A. Peppas, *Mesh size and diffusive characteristics of semicrystalline poly(vinyl alcohol) membranes prepared by freezing/thawing techniques.* Journal of Membrane Science, 1995. **107**(3): p. 229-237.

23. Correia, D.M., et al., *Thermal and hydrolytic degradation of electrospun fish gelatin membranes.* Polymer Testing, 2013. **32**(5): p. 995-1000.

24. Sencadas, V., et al., *Physical-chemical properties of cross-linked chitosan electrospun fiber mats.* Polymer Testing, 2012. **31**(8): p. 1062-1069.

25. Vladimir, I.L., *Cryotropic gelation of poly(vinyl alcohol) solutions.* Russian Chemical Reviews, 1998. **67**(7): p. 573.

26. Holloway, J.L., A.M. Lowman, and G.R. Palmese, *Mechanical evaluation of poly(vinyl alcohol)-based fibrous composites as biomaterials for meniscal tissue replacement.* Acta Biomaterialia, 2010. **6**(12): p. 4716-4724.

27. Vikingsson, L., et al., *An "in vitro" experimental model to predict the mechanical behavior of macroporous scaffolds implanted in articular cartilage.* Journal of the Mechanical Behavior of Biomedical Materials, 2014. **32**(0): p. 125-131.

28. Wong, B.L. and R.L. Sah, *Effect of a focal articular defect on cartilage deformation during patello-femoral articulation.* Journal of Orthopaedic Research, 2010. **28**(12): p. 1554-1561.

29. Guilak, F., A. Ratcliffe, and V.C. Mow, *Chondrocyte deformation and local tissue strain in articular cartilage: A confocal microscopy study.* Journal of Orthopaedic Research, 1995. **13**(3): p. 410-421.

30. Santamaría, V.A., et al., *Influence of the macro and micro-porous structure on the mechanical behavior of poly(l-lactic acid) scaffolds.* Journal of Non-Crystalline Solids, 2012. **358**(23): p. 3141-3149.

31. Gamboa-Martínez, T.C., J.L. Gómez Ribelles, and G. Gallego Ferrer, *Fibrin coating on poly (L-lactide) scaffolds for tissue engineering.* Journal of Bioactive and Compatible Polymers, 2011. **26**(5): p. 464-477.

32. Izal, I., et al., *Culture of human bone marrow-derived mesenchymal stem cells on of poly(L: -lactic acid) scaffolds: potential application for the tissue engineering of cartilage.* Knee Surg Sports Traumatol Arthrosc, 2012.

33. Lebourg, M., J. Suay Antón, and J.L. Gomez Ribelles, *Characterization of calcium phosphate layers grown on polycaprolactone for tissue engineering purposes.* Composites Science and Technology, 2010. **70**(13): p. 1796-1804.

34. Deplaine, H., J.L.G. Ribelles, and G.G. Ferrer, *Effect of the content of hydroxyapatite nanoparticles on the properties and bioactivity of poly(l-lactide) – Hybrid membranes.* Composites Science and Technology, 2010. **70**(13): p. 1805-1812.

35. Olmedilla, M.P., et al., *In vitro 3D culture of human chondrocytes using modified epsilon-caprolactone scaffolds with varying hydrophilicity and porosity.* J Biomater Appl, 2012. **27**(3): p. 299-309.

36. Shafee, E.E. and H.F. Naguib, *Water sorption in cross-linked poly(vinyl alcohol) networks.* Polymer, 2003. **44**(5): p. 1647-1653.

37. Kanchanomai, C. and Y. Mutoh, *Low-cycle fatigue prediction model for pb-free solder 96.5Sn-3.5Ag.* Journal of Electronic Materials, 2004. **33**(4): p. 329-333.

Chapter 4: Design and validation of a bio-mechanical bioreactor for cartilage tissue culture
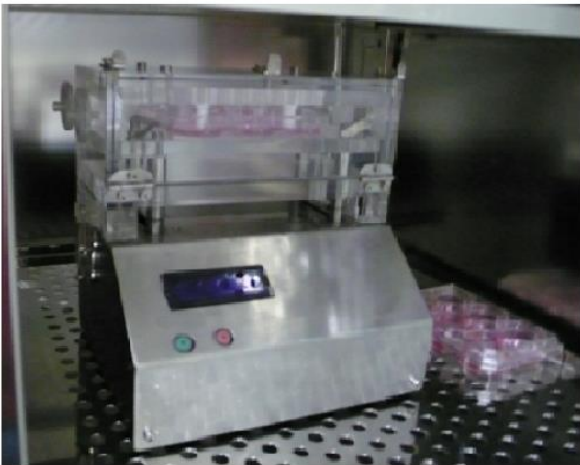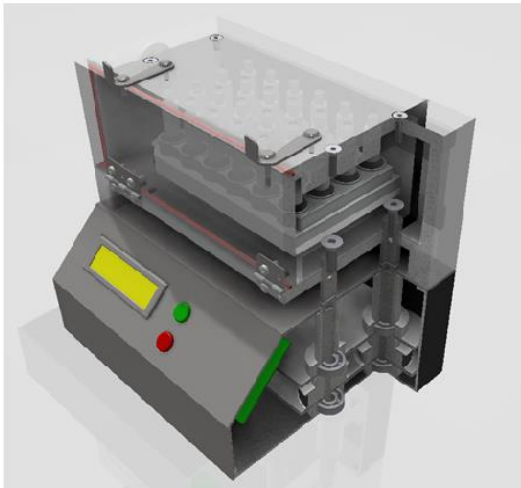
4.1 Introduction

Mechanical loading *in vivo* is essential for proper musculoskeletal development [1]. In articular cartilage the mechanical properties of the extracellular matrix (ECM) not only determine the resistance to the cyclic loading produced during motion, but also regulate the transmission of loading to the chondrocytes. The transmission of loading is transduced from the mechanosensors in the membrane and is a signaling factor that regulates the expression and translation of genes related to the synthesis of the components of ECM.

Thus, mechanical loading in vitro may simulate some of the conditions existing in vivo and may improve the synthesis of glycosaminoglycan (GAG) and mechanical properties of adult chondrocytes and mesenchymal precursors in hydrogels and semicrystalline scaffolds. Bioreactors have been thus developed for different modes of mechanical loading. The most used are designed for inducing chondrogenic differentiation through unconfined compression [2-4], direct shear stress [5], perfusion (shear stress) [6-8] or hydrostatic pressure [9-11]. Each type of those bioreactors simulates some of the conditions from different zones of cartilage. Unconfined compression resembles the conditions found in the upper zones of cartilage, where the hydrostatic pressure is the lowest in all cartilage (increases with deepness), the fluid flow is the highest (decreases with deepness) and the strain is the highest (≈50% in the surface zone, 10-20% in the medium zone). Hydrostatic pressure generates a homogeneous distribution of force and the mechanical stress is produced in the deeper zones, where there is practically no strain. Ideally, semi-confined compression would resemble all the zones at the same time but this is hard to perform in cell cultures, as this requires a permeable load plate over the load zone and impermeable boundaries around the rest of the scaffold [12].

For both compression and hydrostatic pressure in hydrogels, intermittent or dynamic application of mechanical stress [13, 14] produces higher expressions of collagen II and proteoglycan expression than static loading [15, 16], as well as better mechanical properties in mature chondrocytes. This effect is also found in differentiation of pluripotential precursors, like mesenchymal stem cells (MSCs), although in these cases the response is also determined by the 3D environment and the state of cell differentiation [2, 17-19]. Dynamic loading may also reduce hypertrophy typically found in chondrogenic differentiation of MSCs, thus improving the stabilization of the differentiated phenotype [20, 21]. In

93

unconfined compression the chondrogenic differentiation depends on the range of strain (if displacement-controlled) or stress (if force-controlled) and the applied frequency [5], typically frequencies of 1 Hz and strains of 10, being also necessary the addition of resting periods The periods of continuous cycling loading in knee, for example, rarely excess 1 h, being intercalated with resting periods during the day, which reach up to 16 h [12].

To design bioreactors for mechanical stimulation, besides the importance of parameters like biocompatibility, sterility and gas exchange [22], it is important to produce systems with accurate control of the stimulus without compromising manipulation for changing medium or taking samples, for example. In the present work a modular bioreactor for unconfined compression was designed with displacement control of samples in a 48 multi-well standard plate, that can be operated under laminar hood. The advantages of the present design are also presented.

4.2. Bioreactor design

4.2.1 Mechanical design and construction

The objective of this bioreactor is the evaluation of the influence of mechanical stimulation in cell proliferation and differentiation. So, the dawning and construction of specific equipment capable of providing the desired stimulation and their monitoring to satisfy the mechanical stimuli applied in a 3D scaffold is required. In this way, it is important to introduce minimum variations in the conventional culture methods, in order to properly evaluate the influence of the mechanical stimulus.

In this way a commercial culture plate with 48 wells as base for culture medium was used, which can be substituted by other commercial culture plates. This system is prepared for being placed in an incubation chamber with controlled temperature and humidity, and allows the change of the culture medium whenever is necessary. It is important to refer that the culture period can last up to one month, period in which the system will be working inside the incubator.

To comply with the above described requirements a schematic layout of the various components of system is shown in Figure 4.1.
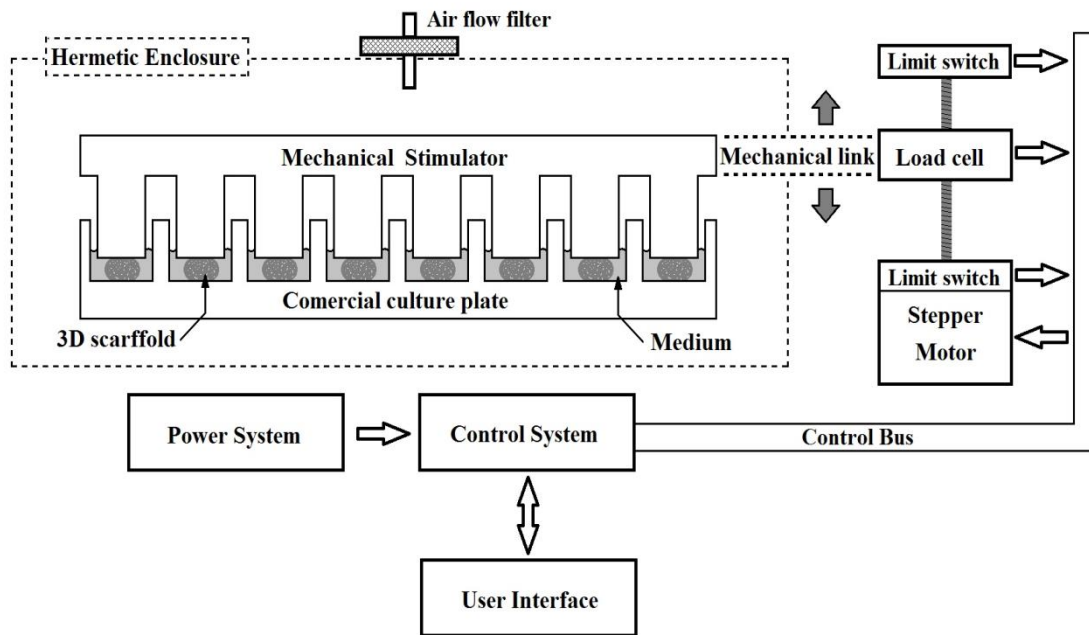
Figure 4.1 - **Block diagram of the various components and subsystems that compose the developed bioreactor.**

The culture plate will be inserted in a hermetic enclosure, in order to avoid the culture medium contamination by external agents neither during normal operation nor when changing culture medium.

The mechanical stimulator has the same format of the culture plate and shows a vertical controlled movement according to the required parameters. These movements are produced using a screw system connected to a stepper motor. In this link a load cell is placed to evaluate the force applied to the 3D scaffolds, as shown in the Figure 4.1.

The stepper motor is controlled by an electrical system based in a microcontroller, especially developed for this application that is responsible to control the mechanical stimulator in a close loop as indicated in the user interfaces.

The local user interface (using a 16x2 LCD and two buttons) provides the assay information to the user and the possibility to stop, start or change the culture medium. It should also be

noted that this interface is very simple due to security reasons, as it may be placed in various devices in the same incubator.

On the other hand, the remote interface allows controlling all equipment parameters. This interface corresponds to a software application installed in a computer that can connect to the equipment using a USB port.

Considering that the cells can be contaminated, is important to guarantee that all parts in contact directly and indirectly with the culture medium can be easily sterilized. Furthermore, to ensure that there is no air saturation of the hermetic enclosure, it is necessary to include a set of filters to provide the air flow.

The 3D mechanical project of equipment complying with the requirements described above is presented in Figure 4.2.
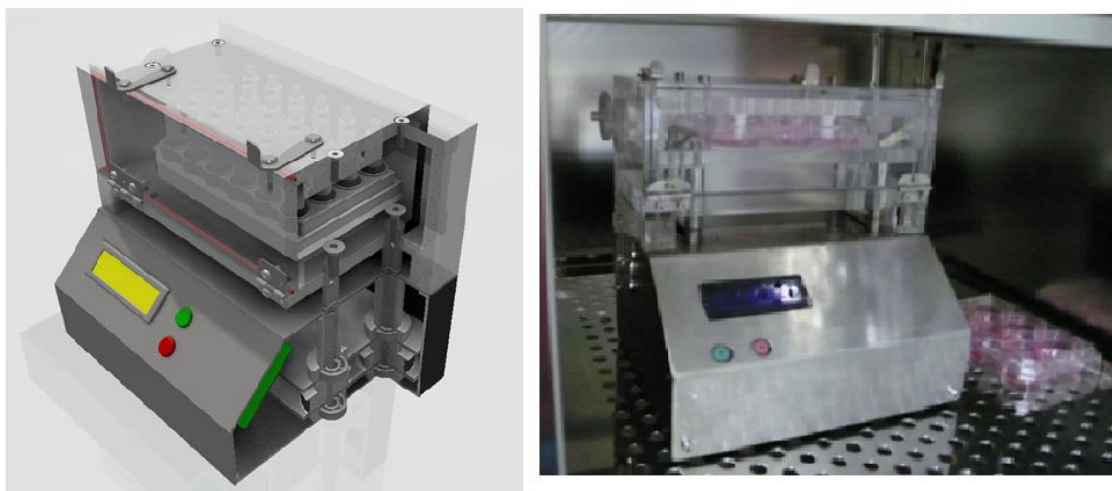
Figure 4.2 - 3D design and schematic section of the mechanical bioreactor. In the picture at the right, the prototype suitable for cell culture.

The scaffold deformation is achieved by the movement along the vertical axis of the table where the culture plate is placed, being in this way the scaffolds compressed and decompressed against an array of Teflon columns with the same format of the wells of the commercial plate. The Teflon columns are independent, i.e. it is possible to remove some of

them in order to use samples with and without compression in the same plate. In that way, a simple, compact and easily sealing design is obtained (Figure 4.2).

The movement along the vertical axis is obtained using four shafts internally threaded, inserted in a set of shafts with external threaded. The latter are interconnected by a timing belt which is also connected to a stepper motor. When the stepper motor performs one complete rotation, the external threaded shafts perform also one rotation leading to a vertical movement of the internally threaded shafts of the same dimension as the thread pitch, which in this case is 1 mm. This set up is implemented with a Nanotec ST4209S1006-B stepper motor with 400 steps of resolution per revolution, which enables a vertical movement resolution of 0.0025 mm per step.

The hermetic enclosure is detachable from the rest of equipment through two clasps, allowing to remove it to perform the exchange of the culture medium without need to remove all equipment from the incubation chamber thereby avoiding possible contaminations. All components that constitute the hermetic enclosure are made of acrylic plastics in order to allow visualizing the status of the experiment; the remaining components are made in stainless steel. On the other hand, the mechanism in the lower box that produces the movement does not need to be sterilized, being in this way fabricated in aluminium to obtain a lighter equipment.

4. 2.2 Electrical control system

The link of the control system with the various peripherals of the bioreactor is shown in the block diagram of Figure 4.2. The electrical system was specifically developed for this equipment in order to fulfil the functional requirements of the mechanical system. Further, the developed architecture was implemented using commercial electrical components.
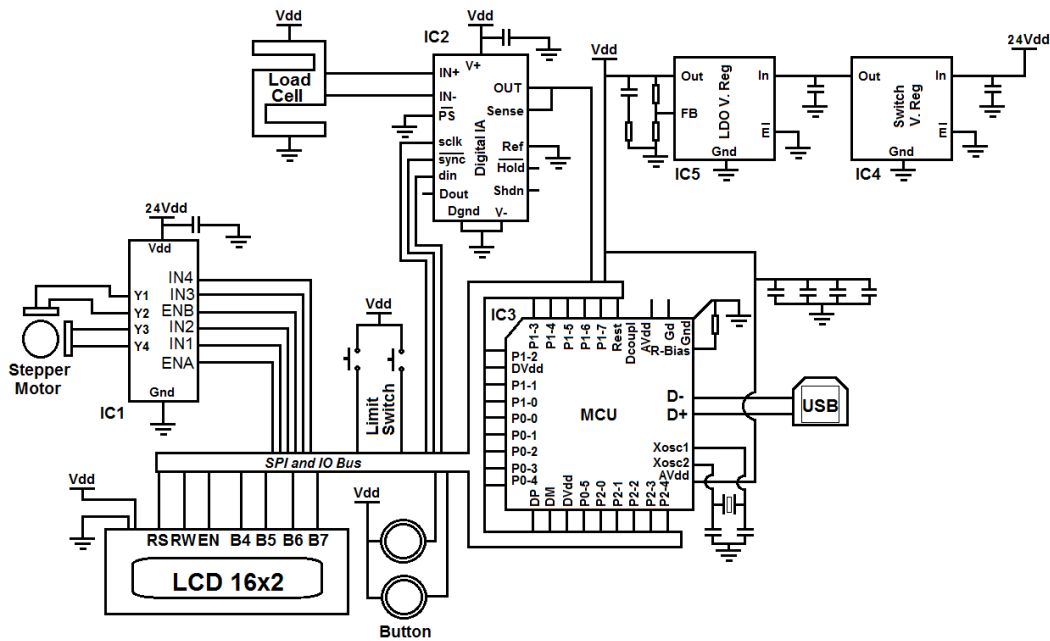
Figure 4.3 - Schematic representation of the electrical control circuit.

The schematic representation of the electrical control circuit (Figure 4.3) shown that each coil of stepper motor is connected to the dual full bridge driver integrated circuit (IC) (IC1), which allows to control the movement of the motor.

One of the main factors in the choice of this component is the operation current, as the motor needs 950 mA of nominal current. Therefore, considering that the system must be working for long periods of time, the operation voltage and the thermal dissipation become a key factor. In this way, the integrated circuit L298N (STMICROELECTRONICS) was selected as it shows an operation current up to 4 A, an operation voltage up to 46 V and a power dissipation of 25 W for a thermal resistance junction-ambient of 35 ºC/W.

The load cell is connected to a Wheatstone bridge with the output signal connected to a positive and negative input of the instrumentation amplifier (IA) with a digitally programmable gain (IC2). As IC6 was used the LTC6915 from Linear Technology with fourteen levels of programmable gain as it enables to adapt to various models of load cells. The output voltage of the IA was converted to digital using one of the 10 bits analog to digital converter (ADC) present in the micro controller (MCU) (IC3).

All components of the electrical controller circuit are controlled by an MCU, which is also responsible for the management of user interface. The MCU is the AT90USB1287 from

ATMEL. It is a low power 16 MHz 8 Bits AVR RISC-architecture with 8 channel 10 bits ADC and low-speed and full-speed USB 2.0 inside.

The IC4 is responsible for ensuring the 5 V regulated voltage to the circuit. The IC used is the LM2596 from Texas Instruments which is a switching step-down voltage regulator with 80% of efficiency. This is a quite important characteristic for the present application, as, when compared to linear regulators, less heat is produced during the long periods of use required for cell culture. As some parts of the circuit require 3.3 V, another voltage regulator IC6 is used, being in this case a low dropout line voltage regulator (LDO) NCP4682 from ON Semiconductors powered from the IC5.

4.2.3 Firmware and remote interface design

The developed circuit is based on digital components and in this way it is controlled by the MCU, for which it was necessary the development of the firmware. This firmware controls the deformation, allowing defining the oscillation frequency and deformation amplitude by the user. The system allows also defining a set of activation and repose cycles in two temporal levels (small and long cycles). Furthermore, it is possible to use a manual control to define the start point of the displacement cycle of a given experience.

As a remote interface, the Low-Speed USB protocol is implemented, due to the low transmission rate needed in this application. The remote interface of the setup is a software application developed using the open source Qt Creator platform with a cross-platform C++ development environment, which is part of the SDK for the Qt GUI Application development framework (Figure 4.4).
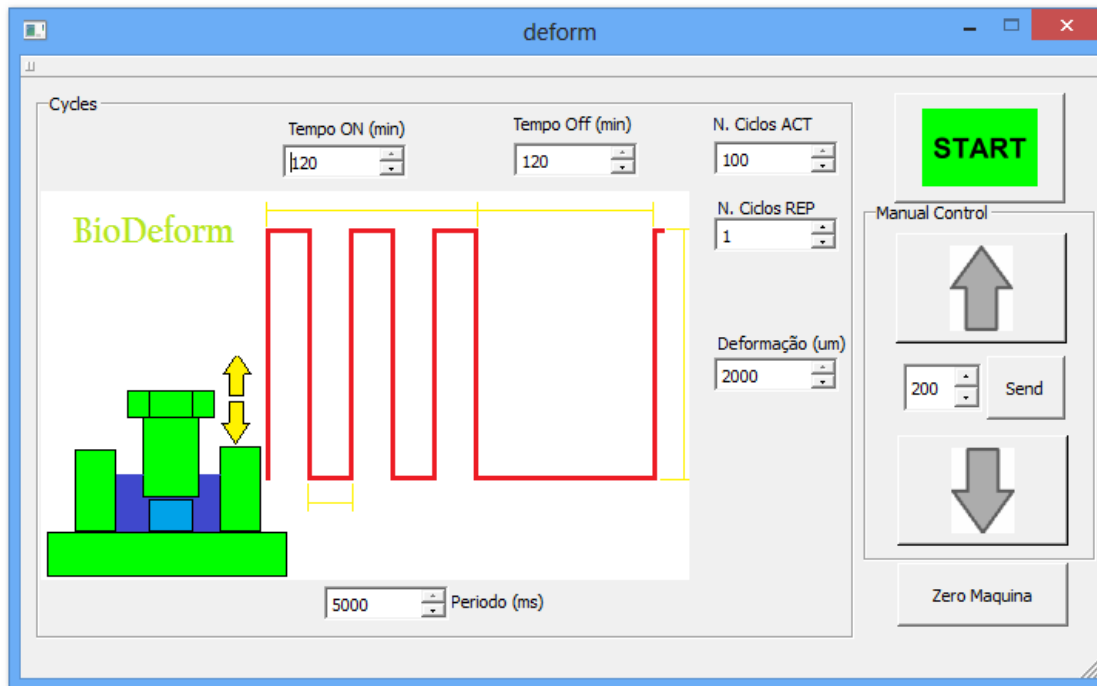
Figure 4.4 - Software layout with the needed control functions.

According to the characteristics of the developed system and of the used components, the system only allows a maximum speed of 6 mm per second. The control application provides this limitation to the user when it changes the deformation or the frequency parameter and the limit is exceeded.

4.3 Validation tests: sterility and cell cultures

Different protocols for the sterilization of the hermetic enclosure were tested, involving different times of ultraviolet light (UV), (30 min, 1hour and 2 hours, in a single step after mounting all the pieces of the hermetic enclosure. The lower box of the bioreactor was not in contact with cells and culture medium, thus it didn't need sterilization, and it simply was cleaned with Mycoplasma-Off (Minerva Biolabs). The best protocol for sterilization was performed in detail as follows, and in order to ensure sterility, more steps had to be involved and an additional UV irradiation period was needed. First, the hermetic enclosure was washed in distilled autoclaved water containing 10% of sodium hypochlorite, separated in three parts: the external case, the mechanical stimulator without the Teflon columns and the

table to hold culture plates. The stainless steel pieces and screws, and the Teflon columns may be autoclaved. After 24 h at least in sodium hypochlorite solution, the pieces are washed with sterile distilled water, dried, put under laminar flow hood and sterilized by UV rays for 2 h, directing the inner surfaces to the UV lamp. The pieces are mounted with the help of autoclaved plies and tools, and washed with EtOH 70% to ensure sterility. Once mounted, the enclosure is put in UV for an additional 1 h. After that, four commercial air filters are holed in the respective holes.

To study the viability and lack of contamination of the bioreactor, a series of tests were performed in static conditions. Approximately 10^5 KUM5 cells - a chondroprogenitor cell line used and discussed in detail in the next chapter [23] - were seeded in each well of multi-well plate, with Dulbecco's modified Eagle's medium (DMEM) 4.5 g/l (Gibgo) of glucose containing 10% Fetal Bovine Serum (FBS) (Biochrom, Merck Millipore) and tested inside the bioreactor. In half of the wells the Teflon columns were placed, and the other remained without them in order to observe if these pieces can add a source of contamination or problems. As a control, another plate was placed at the same time with the same cell number and medium conditions, out of the bioreactor.

For the first 3 days, cells in all conditions reached confluence at the same time and were passaged to new plates. For at least 2 weeks, cells in all conditions grow without proliferation changes (Figure 4.5). No contamination was observed with optic microscopy in any condition. Cells in all conditions proliferated and reached confluence at the same time, thus it could be inferred that there is no contamination affecting the cells or cell death, and that the biorreactor is totally hermetic when it is closed.
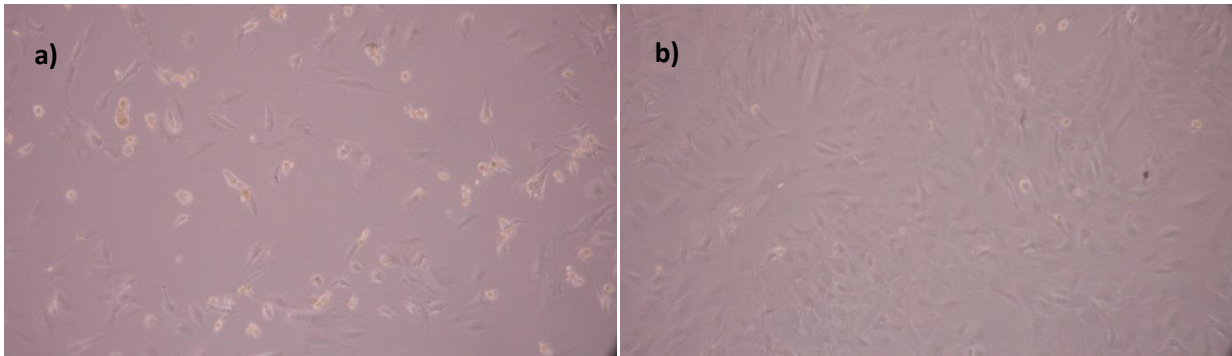
Figure 4.5 - Pictures taken with optic microscope, 10X magnification. a) Cells attached in the wells inside bioreactor, with Teflon pieces touching the medium, 1 h after seeding. b) Cells reaching confluence in the same wells after 2 weeks.

4.4 Conclusions

A bioreactor has been designed and constructed to allow dynamic compression stimulation of scaffolds immersed in culture medium into commercial culture well plates. The bioreactor is able to work in the conditions inside the incubator. The modular design allows easy cleaning and operating under laminar hood. The protocol for sterilization ensures lack of observable contaminations, which is a critical requirements for cell culture. This bioreactor will be used for the works described in the next chapter.

4.5 References

1.   Kelly, D.J. and C.R. Jacobs, *The role of mechanical signals in regulating chondrogenesis and osteogenesis of mesenchymal stem cells.* Birth Defects Res C Embryo Today, 2010. **90**(1): p. 75-85.

2.   Huang, A.H., et al., *Long-term dynamic loading improves the mechanical properties of chondrogenic mesenchymal stem cell-laden hydrogel.* Eur Cell Mater, 2010. **19**: p. 72-85.

3.   Lima, E.G., et al., *The beneficial effect of delayed compressive loading on tissue-engineered cartilage constructs cultured with TGF-beta3.* Osteoarthritis Cartilage, 2007. **15**(9): p. 1025-33.

4. Nicodemus, G.D. and S.J. Bryant, *The role of hydrogel structure and dynamic loading on chondrocyte gene expression and matrix formation.* J Biomech, 2008. **41**(7): p. 1528-36.

5. Li, Z., et al., *Chondrogenesis of human bone marrow mesenchymal stem cells in fibrin-polyurethane composites is modulated by frequency and amplitude of dynamic compression and shear stress.* Tissue Eng Part A, 2010. **16**(2): p. 575-84.

6. Xie, L., et al., *In vitro mesenchymal trilineage differentiation and extracellular matrix production by adipose and bone marrow derived adult equine multipotent stromal cells on a collagen scaffold.* Stem Cell Rev, 2013. **9**(6): p. 858-72.

7. Goncalves, A., et al., *Effect of flow perfusion conditions in the chondrogenic differentiation of bone marrow stromal cells cultured onto starch based biodegradable scaffolds.* Acta Biomater, 2011. **7**(4): p. 1644-52.

8. Mahmoudifar, N. and P.M. Doran, *Chondrogenic differentiation of human adipose-derived stem cells in polyglycolic acid mesh scaffolds under dynamic culture conditions.* Biomaterials, 2010. **31**(14): p. 3858-67.

9. Angele, P., et al., *Cyclic hydrostatic pressure enhances the chondrogenic phenotype of human mesenchymal progenitor cells differentiated in vitro.* J Orthop Res, 2003. **21**(3): p. 451-7.

10. Miyanishi, K., et al., *Effects of hydrostatic pressure and transforming growth factor-beta 3 on adult human mesenchymal stem cell chondrogenesis in vitro.* Tissue Eng, 2006. **12**(6): p. 1419-28.

11. Zeiter, S., P. Lezuo, and K. Ito, *Effect of TGF beta1, BMP-2 and hydraulic pressure on chondrogenic differentiation of bovine bone marrow mesenchymal stromal cells.* Biorheology, 2009. **46**(1): p. 45-55.

12. Wong, M. and D.R. Carter, *Articular cartilage functional histomorphology and mechanobiology: a research perspective.* Bone, 2003. **33**(1): p. 1-13.

13. Demarteau, O., et al., *Dynamic compression of cartilage constructs engineered from expanded human articular chondrocytes.* Biochem Biophys Res Commun, 2003. **310**(2): p. 580-8.

14. De Croos, J.N., et al., *Cyclic compressive mechanical stimulation induces sequential catabolic and anabolic gene changes in chondrocytes resulting in increased extracellular matrix accumulation.* Matrix Biol, 2006. **25**(6): p. 323-31.

15.   Steinmeyer, J. and S. Knue, *The proteoglycan metabolism of mature bovine articular cartilage explants superimposed to continuously applied cyclic mechanical loading.* Biochem Biophys Res Commun, 1997. **240**(1): p. 216-21.

16.   Wong, M., et al., *Chondrocyte biosynthesis correlates with local tissue strain in statically compressed adult articular cartilage.* J Orthop Res, 1997. **15**(2): p. 189-96.

17.   Huang, A.H., M.J. Farrell, and R.L. Mauck, *Mechanics and mechanobiology of mesenchymal stem cell-based engineered cartilage.* J Biomech, 2010. **43**(1): p. 128-36.

18.   Thorpe, S.D., et al., *Dynamic compression can inhibit chondrogenesis of mesenchymal stem cells.* Biochem Biophys Res Commun, 2008. **377**(2): p. 458-62.

19.   Thorpe, S.D., et al., *European Society of Biomechanics S.M. Perren Award 2012: the external mechanical environment can override the influence of local substrate in determining stem cell fate.* J Biomech, 2012. **45**(15): p. 2483-92.

20.   Vinardell, T., et al., *Hydrostatic pressure acts to stabilise a chondrogenic phenotype in porcine joint tissue derived stem cells.* Eur Cell Mater, 2012. **23**: p. 121-32; discussion 133-4.

21.   Bian, L., et al., *Dynamic compressive loading enhances cartilage matrix synthesis and distribution and suppresses hypertrophy in hMSC-laden hyaluronic acid hydrogels.* Tissue Eng Part A, 2012. **18**(7-8): p. 715-24.

22.   Obradovic, B., et al., *Gas exchange is essential for bioreactor cultivation of tissue engineered cartilage.* Biotechnol Bioeng, 1999. **63**(2): p. 197-205.

23.   Sugiki, T., et al., *Hyaline cartilage formation and enchondral ossification modeled with KUM5 and OP9 chondroblasts.* J Cell Biochem, 2007. **100**(5): p. 1240-54.

Chapter 5: Fatigue Prediction on Poly-ε-caprolactone Macroporous Scaffolds - Influence of extracellular matrix after cell culture in bioreactor
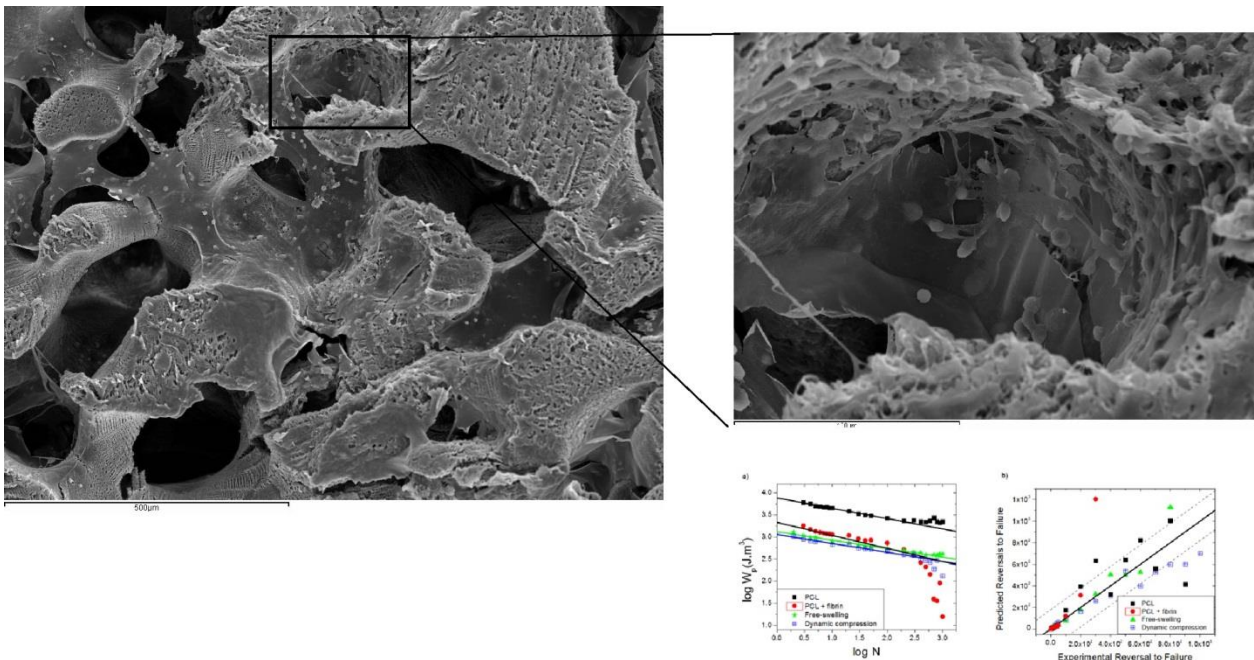
This chapter is based on the paper: **Mechanical fatigue performance of PCL-chondroprogenitor constructs after under bioreactor mechanical stimulus. Panadero, J.A., Sencadas V., Silva S.C.M., Ribeiro, C., Correia V., Gama, F.M., Gomez Ribelles, J.L., Lanceros-Mendez, S. Submitted to Journal of Biomedical Materials Research: Part A, 2014.**

5.1 Introduction

Articular hyaline cartilage is a tissue that provides low friction and load bearing features to the hips and knees. Its mechanical properties are a result of an organized ECM, containing proteins like sulphated glycosaminoglycans, which allow high water uptake [1-3]. Cartilage is an avascular tissue and their single cells, the chondrocytes, show a slow metabolism, as a consequence of limited nutrients and oxygen. Given its inability to self-repair after injury or aging, tissue engineering therapies are a valuable option for the regeneration of cartilage.

These strategies consist on growing cells in 3D native-like environments - e.g. hydrogels or polymeric scaffolds -and providing adequate stimulus, typically through growth factors and other soluble molecules, guiding the process of cell differentiation [4]. In the case of chondrogenic differentiation, in vitro cultures are performed for long periods – usually 28 days or more [5, 6]. It has been demonstrated that bioreactors that apply dynamic loading can improve differentiation, through control of both the applied mechanical loads and the cell state of differentiation. Moreover, these strategies can also serve as models for understanding the processes involved in cartilage ECM remodeling. This process can be monitored by the analysis of specific ECM markers, and also through the increase of the elastic modulus.

The cyclic mechanical loads applied to the scaffolds leads to material fatigue. Such effect, known to occur in biomaterials [7], has been rarely assessed for the constructs combining the scaffold and the ECM produced by the cells inside the pores. This can actually be quite relevant since the development of ECM can modify the fatigue resistance of the scaffold, being more representative of the mechanical scaffold performance *in vivo*. Indeed, any factor limiting water permeation through the material will contribute to apparent elastic modulus and fatigue behavior [8]. Thus, the ECM can play a role in fatigue resistance, due to its ability to retain water. Fatigue analysis can thus provide better insight and new information not only on the mechanical performance of the constructs but also on the ECM integration with the scaffold surfaces.

As seen in previous chapters, fatigue behavior of materials can be influenced by factors influencing stress-strain constitutive behavior like loading history and, polymer composition,

among others [8, 9]. As described in the previous chapters 2 and 3, the Morrow model has been successfully applied to poly-ε-caprolactone (PCL) fatigue behavior under cyclic mechanical loading and to assess the influence of water and PVA to the PCL macroporous structure [10].

To remind the reader, the model is based on the evolution of the plastic strain energy density that can be physically interpreted as the distortion energy, associated to the change in shape of a volume element and can be related to failure, in particular under conditions of ductile behavior [11].

Fibrin is a hydrogel that not only can provide mechanical resistance by water retention [12] but it is also adhesive to cells, resembling some aspects of a pericellular matrix. It has been found that in the presence of cyclic mechanical loading, fibrin hydrogels induce higher expression of chondrogenesic markers than non-adhesive hydrogels, in mesenchymal stem cell cultures [13, 14]. Further, fibrin within PCL scaffolds has a minor impact on fatigue behavior as compared with the effect of the water [8]. Therefore fibrin hydrogels can be of interest for cartilage tissue engineering.

In the present work, chondrogenic precursor cells were seeded in fibrin hydrogels formed inside PCL macroporous scaffolds and cultivated in chondrogenic medium. To simulate the physiological mechanical environment of the upper zones of cartilage, the culture was performed in a bioreactor able to produce cyclic compression by displacement control. The fatigue behavior of the constructs was analyzed overtime, and the contribution of the ECM produced during cell cultivation on the properties observed is discussed.

5.2 Materials and methods

5.2.1 Materials

Poly-ε-caprolactone (PCL, 43-50 kDa) and 1,4-dioxan were purchased from *Sigma-Aldrich*. Poly(ethyl methacrylate) (PEMA - Elvacite 2043) spheres (mean diameter of 200 □m) were purchased from *Lucite*. Fibrinogen from human plasma 50-70% protein (≥80% of protein is clottable) and thrombin from human plasma lyophilized powder, ≥2,000 NIH units/mg protein (E1%/280, 18.3) were purchased from *Sigma-Aldrich*, as well as L-Proline, TGF-β1,

ascorbic acid, dexamethasone, TriReagent and isopropanol. Coagulation factor XIII was purchased from Merck. ITS, DNAse I and PicoGreen DNA quantification kit were purchased from Invitrogen. iScript kit for reverse transcription was purchased from Biorad, Power SYBR™ Green PCR Master Mix for real-time PCR was purchased from Applied Biosystems.

5.2.2 Sample preparation

PCL (Sigma-Aldrich) scaffolds were prepared as previously described in chapter 2 and 3 [11]. Briefly, PCL was dissolved in dioxane (25% w/v) and this solution was mixed with PEMA (Lucite) microspheres (1:1 w/w). Then, the mixture was placed in Teflon Petri dishes and submerged in liquid nitrogen for a minute. Dioxane (Sigma-Aldrich) was extracted from the frozen plates with ethanol at - 20 ^{0}C for three days, changing ethanol every day. Porogen leaching was performed in ethanol at 40 ^{0}C for one day. The porous samples were cut into cylinders with 5 mm diameter and a thickness of approximately of 2 mm. Further leaching for each cylinder was performed in ethanol at 40 ℃ for nine days, changing ethanol daily, in order to assure complete removal of porogen.

5.2.3 Sample Characterization

Sample morphology and gel structure was assessed by scanning electron microscopy using a *JEOL JSM-5410* apparatus equipped with a cryogenic device. Images were taken at an accelerating voltage of 10 kV. Samples were previously immersed in water during 24 h and then frozen at -80 ℃. Then, the samples were cryo-fractured and water was sublimated during 40 min before coating with a gold thin layer.

Mechanical experiments were performed on cylindrical samples with 6 mm diameter and a height of ~2 mm in a *Shimadzu AG-IS* universal testing machine in compression mode at a test velocity of 1 mm.min^{-1} and at room temperature. In fatigue experiment, samples were submitted to a compressive-strain cycle load with a maximum strain of 15% and up to 1000 cycles, which is typically the strain range of interest as it is considered to be the maximum

magnitude of physical deformation suffered by articular cartilage [15, 16]. Strain deformation was measured by machine cross-head displacement and mechanical stress and strain parameters were obtained as an average of five measurements. All mechanical experiments were performed with the sample immersed in deionized water. In order to ensure the maximum water uptake, all samples were immersed in a water bath and placed in a chamber (Vacuum-Temp from Selecta) under 10^{-2} mmHg until the samples dropped to the bottom of the bath.

5.2.4 Cell culture in expansion medium

 PCL scaffolds were sterilized by gamma radiation at 25 kGy. An immortalized cell line with chondrogenic potential from murine bone marrow was used - KUM5 (Riken Cell Bank)[17]. Cells were expanded in DMEM 4.5 g/L glucose (Gibco) with 10% FBS and 1% penicillin/streptomycin. After passage 25, $2 \cdot 10^5$ cells were trypsinized, resuspended in 50 ul of medium and seeded in the PCL scaffolds by injecting with a chromatography syringe.

Another group of PCL scaffolds was seeded with cells resuspended in 25 µl of 5 U/ml thrombin solution with 20 mM $CaCl_2$ (supplemented with coagulation Factor XIII, final concentration 70 µM). The cells were directly injected in the scaffold with a bowel chromatography syringe at a density of 10^6 cells/scaffold. Simultaneously, 25 µl of filter-sterile fibrinogen were injected using another syringe. Scaffolds were held for 1 h to allow coagulation of fibrin and then submerged in the same culture medium used for expansion, in standard culture plates (48 wells). Cell culture was performed for 21 days at 37 ⁰C and 5% CO_2

The samples were observed in cryoSEM to analyse the fibrin effects on cell adhesion. After 1 day of cultivation, cells and scaffolds were fixed in glutaraldehyde 2.5 % for 1 h at 4 ⁰C. CryoSEM was performed in a *JEOL JSM-5410* equipment as previously indicated.

To estimate cell proliferation, three replicas were taken at days 0, 3, 6, 14 and 21, digested with proteinase K and the DNA content was quantified with a Picogreen kit, following

manufacturer instructions, using a standard curve obtained using the the lambda DNA provided in the kit.

5.2.5 Cell culture in bioreactor

PCL scaffolds were sterilized as described previously, and cells were expanded and seeded with fibrin in the scaffolds as described above. For bioreactor culture, the inoculated constructs with the fibrin clot were submerged in chondrogenic medium: DMEM 4.5 g/l glucose containing L-proline 50 µg/ml, ascorbic acid 50 µg/ml, dexamethasone 10^{-7} M, ITS+Premix 1%, penicillin/streptomycin 1% and TGF-β1 10 ng/ml. In these experiments, only the PCL/fibrin scaffolds were employed.

Constructs with cells were kept until day 14th in free-swelling conditions [18, 19]. Then, half of the samples were submitted to cyclic compression for 28 days in the bioreactor and the remaining samples were kept in free-swelling conditions. The home-made bioreactor can hold multiple samples under loading by Teflon cylinders, in a 48 well plate. Its configuration allows taking the plate under laminar hood for sample acquisition, changing the medium manually, and placing it in standard cell incubator. The loading profile was: 30 minutes with onset strain of 15% at a frequency of 1 Hz, and 90 minutes of stillness. The medium was changed every 3 days during stillness periods.

5.2.6 Fatigue trials

Following cell culture, mechanical experiments were performed on both the bioreactor–loaded and free-swelling samples, using a *Shimadzu AG-IS* universal testing machine, in compression mode, at a test velocity of 1 mm·min^{-1} and room temperature. In fatigue experiment, samples were submitted to a compressive-strain cycle load up to 1000 cycles to a maximum strain of 15% per cycle. Strain deformation was measured by machine cross-head displacement and mechanical stress and strain parameters were obtained as an average of five measurements. All mechanical experiments were performed on samples submerged in deionized water.

5.2.7 Real-time Polymerase Chain Reaction

In order to identify the cell expression of characteristic markers of several ECM components, quantitative real-time PCR was performed. PCL samples were cultured with the same medium and cell seeding conditions - including fibrin encapsulation – as those for mechanical analysis. Samples were collected after 1 and 14 days under free-swelling conditions. After 14 days, half of the samples were submitted to cyclic compression for 28 days in the bioreactor and the other half were kept in free-swelling conditions. Samples from both groups were taken (N=3). The total RNA was isolated using 1ml TriReagent [20], as follows: 0.1ml 1-bromo-3-chloropropane was added and the aqueous phase containing the RNA was taken by centrifugation at 12000 g at 4 ^{0}C for 15 min and mixed with 500ml isopropanol. After an incubation period of 10 min at room temperature and centrifugation for 10 min at 12000 g, the pellets were washed twice with 1 ml ethanol 75% and dried in a fume hood for 10 min at room temperature. The pellets were dissolved in 30 µl of RNAse-free water and treated with DNAse I to eliminate genomic DNA for 30 min. The amount and purity of total RNA was determined in a Nanodrop 1000 spectrophotometer (Thermo-Fisher). cDNA was synthesized with the iScript reverse transcription kit, following the manufacturer protocol.

For real-time PCR, the primers were purchased from Stabvida and their sequences are provided in Table 5.1. The expression of collagen type I and collagen type II was quantified. The amplification was carried in a CFX96 Real-time system, C1000 thermal cycler (Biorad), with the following protocol for all genes: amplification was performed for 40 cycles, each one consisting in denaturing at 95 ^{0}C for 5 s and annealing /extending at 60 ^{0}C for 40 s. The Ct values were obtained with Biorad CFX Manager software and used for expression analysis of target genes using the $2^{-\Delta\Delta Ct}$ calculation method [21], with β-actin as reference gene.

Table 5.1 - Sequence of primers for target genes

| Gene	Forward primer 5'-3'	Reverse primer 5'-3'	Amplicon size (bp)
β-actin	AGAGGGAAATCGTGCGTGAC	CAATAGTGATGACCTGGCCG	138
Collagen type I	AGCGGAGAGTACTGGATCG	GTTCGGGCTGATGTACCAGT	142
Collagen type II	AGAACAGCATCGCCTACCTG	CTTGCCCCACTTACCAGTGT	161

5.3 Results and discussion

5.3.1 Electron Microscopy

Poly-ε-caprolactone (PCL) exhibits a porous architecture with macropores ranging from 120 up to 200 μm obtained from the leaching of porogen spheres. The macropores are well interconnected with large pore throats and in addition the pore walls are microporous with small pores that result from dioxane crystals formed during the freeze extraction process (Figure 5.1a). This double porosity of the PCL samples favors scaffold permeability to nutrients and cell metabolic waste products and can be used to retain different active components [22-24]. However, apparent scaffold stiffness becomes smaller than in similar sponges lacking microporosity [25, 26]. Further, when fibrin is added to PCL scaffolds, the fibers becomes attached to the porous matrix walls (Figure 5.1b). When cells are seeded into this scaffolds without fibrin for 24h, they adhere to the polymer scaffold surface and display a flattened morphology with conical protrusions (Figure 5.1c) However, when the cells are encapsulated in the fibrin hydrogel inside the PCL scaffold, they take a morphology without the protrusions (Figure 5.1d)
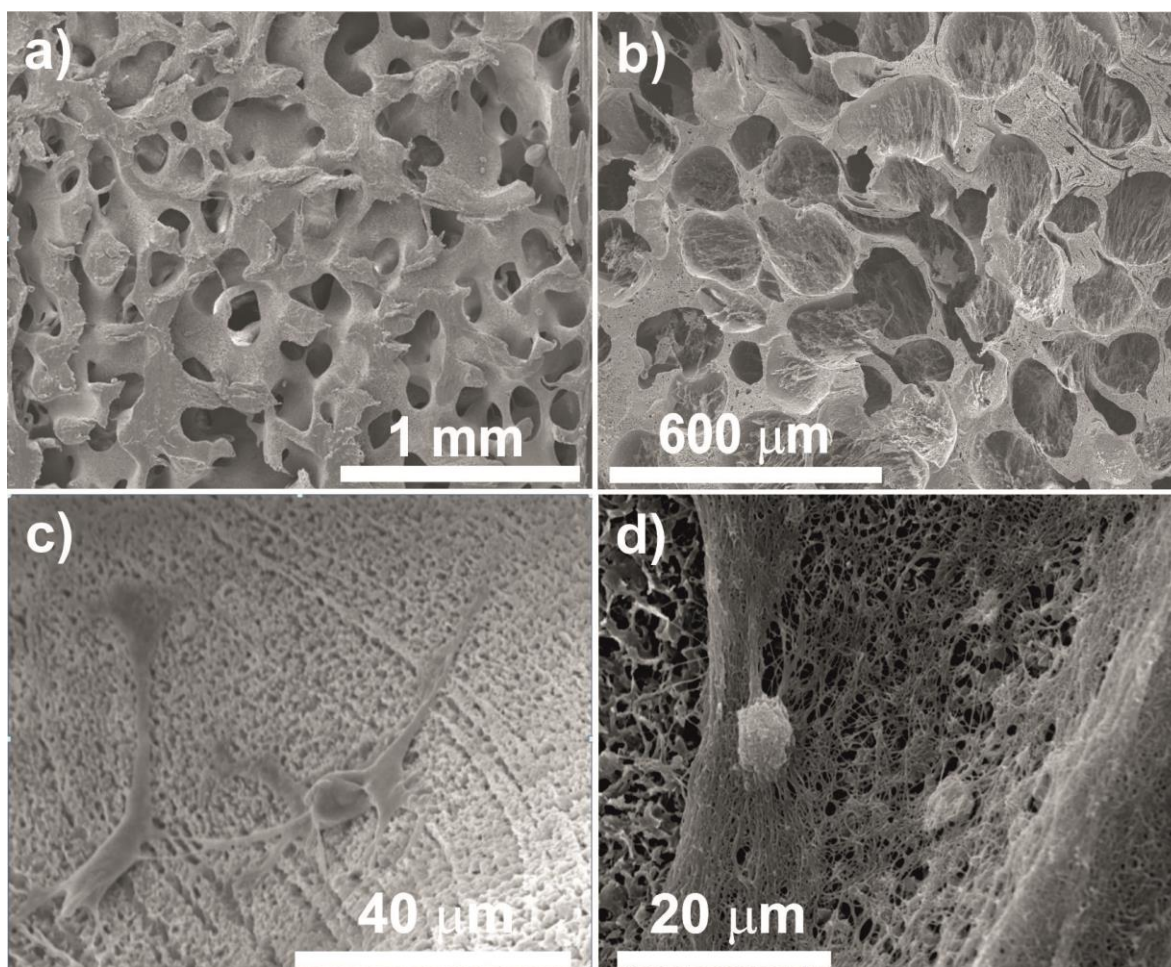
Figure 5.1 - PCL microstructure: a) pristine scaffold, b) PCL+Fibrin c) PCL without fibrin seeded with KUM5 after 1 day of cell culture, d) KUM5 encapsulated in fibrin inside the PCL scaffold, after 1 day of cell culture.

Cell attachment is different in scaffolds with and without fibrin. While cells seeded in the scaffold without fibrin attach to pore walls and spread resembling the culture in 2D monolayer [27], cells in fibrin matrix take a round shape with adhesion points in 3D.

5.3.2 Culture with Poly-ε-caprolactone at 21 days in non-differentiation medium
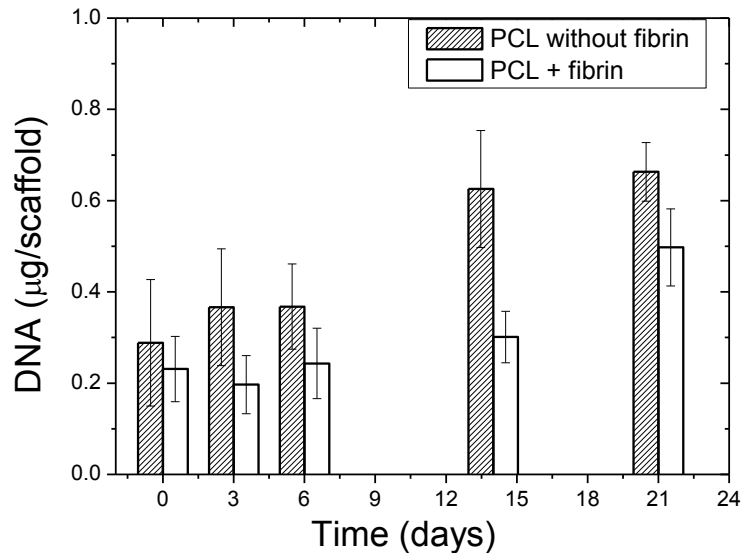

Figure 5.2 - DNA content in full scaffolds during 21 day culture period with and without fibrin.

Initially, the number of cells is similar for both conditions (Figure 5.2), but for subsequent days, fibrincontaining scaffolds present fewer cells. However, while the cell density in scaffolds without fibrin seems reach a plateau towards the end of the cultivation period, cell proliferation in the presence of fibrin accelerates at a later stage such that the number of cells in both conditions eventually tends to match. It can be speculated that fibrin limits cell growing until it is completely degraded. The effect of fibrin clot in our "in vitro" experiments must be analyzed since it mimics the physiological conditions observed when a scaffold is implanted in a cartilage defect combined with microfracture of subchondral bone. Bleeding in the zone of the implant originates a clot which fills the scaffold pores, acting as migration path for mesenchymal stem cells coming from subchondral bone [25, 28, 29]. On the other hand it has been demonstrated that fibrin encapsulation play a positive role in mechanotransduction [13, 14], possibly simulating the necessary pericellular environment for mechanosensitive cells [18] Therefore, all the assays for differentiation in this work were performed in the presence of fibrin.

5.3.3 Mechanical behavior

The differential 3D structure affects cell growing rate over time, and can affect the way mechanical loads are sensed by the cells as well, through different cytoskeleton configurations [13].

The fatigue behavior of PCL with fibrin constructs was analyzed after cell culture, both under free-swelling and loading conditions. The representative mechanical hysteresis loops obtained are presented in Figure 5.3. Lower hysteresis and lower maximum stress are noticed in each cycle for the samples under dynamic cell culture (Figure 5.1a, b and d). The polymer scaffolds elastic modulus (E) was determined for the first cycle at $\varepsilon = 5\%$ and it was observed that it increases with the incorporation of fibrin. The elastic moduli of the constructs after cell culture were compared with the elastic moduli obtained for PCL and PCL+Fibrin constructs without cell culture, in the same measuring conditions, as seen in chapter [10]. Both PCL+Fibrin groups after cell culture show a slight increase of the elastic modulus after cell cultivation. The elastic moduli after cell culture were also compared with data reported for PCL filled with a PVA gel, described in chapter 3, that hardens by freeze/thawing cycles and can serve as mechanical model of growing tissue [30, 31]. The elastic modulus of the constructs after cell culture is similar to the highest values obtained for PCL+PVA, corresponding to 6 cycles of freeze-thawing. No statistical difference in elastic modulus is observed between cell culture samples under free-swelling and cyclic loading conditions. Nevertheless, it was observed a decrease of the maximum stress after each cycle, which suggests that the material undergoes permanent deformation with increasing the number of the loading cycles during the first ~50 loading cycles, then reaching a stable plateau (Figure 5.3d).
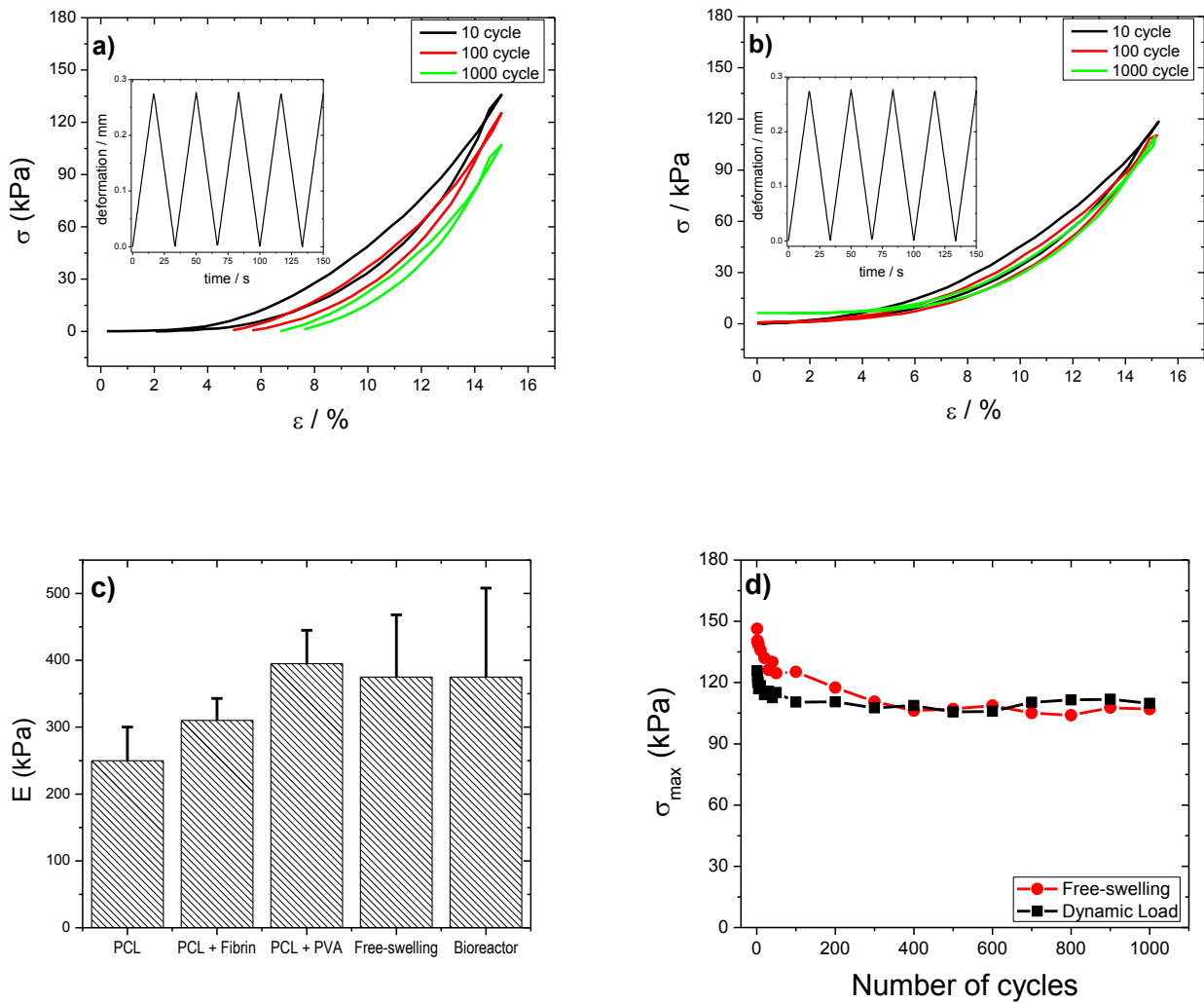
Figure 5.3 - Mechanical hysteresis loops after cell culture for a) free-swelling PCL+Fibrin and b) PCL+Fibrin in dynamic cell culture in the bioreactor; c) Elastic moduli obtained for the first cycle for the different PCL samples and d) average maximum tensile stress as a function of the number of cycles for free-swelling and dynamic cell culture in the bioreactor.

5.3.4 Morrow energy model: plastic strain energy density-life model

Under cyclic loading, the plastic strain energy per cycle is considered a measure of the amount of fatigue damage per cycle. The amount of plastic strain and the energy absorbed during cyclic loading by the material has been postulated as a basis for failure analysis. The relation between plastic strain energy density and the fatigue life can be expressed as [11] :

$$N_f^m W_p = C \tag{1}$$

where W_p is the overall equivalent behavior similar to plastic strain energy density; N_f is the fatigue life and m and C are the fatigue exponent and coefficient, respectively.

Fatigue life for PCL scaffolds immersed in water and after cell culture (free-swelling and in bioreactor) submitted to cyclic compressive loading is presented in Figure 5.4. Experimental data were fitted according to equation 2 to evaluate material response to cyclic mechanical loading before ample collapse with R > 0.98. Fitting results are presented in Figure 5.4 as solid lines and the fitting parameters are represented in Table 5.2. A decrease of fatigue exponent (slope of Figure 5.4) and coefficient (y-intercept) was observed for the samples submitted to cell culture (free-swelling and in bioreactor) and posterior mechanical compressive cyclic experiments (Table 5.2), which indicate the decrease in sample mechanical hysteresis and consequently lower energy loss observed in Figure 5.3. According to ANOVA with Tukey test, the slopes are significantly different between the PCL samples (with and without fibrin), and the samples obtained after cell culture under free-swelling and load bearing conditions, meaning that a larger number of cycles are needed after cell culture to dissipate the same energy. The constructs obtained after cell culture thus have an increased resistance to fatigue. However, the slope is higher in samples obtained in this work after cell culture than those reported for PCL+PVA.
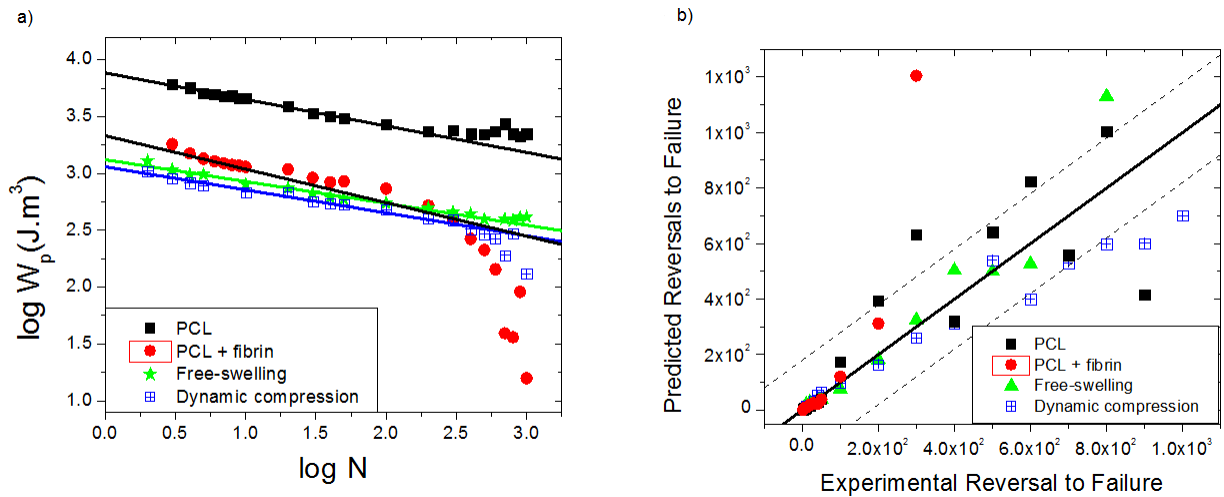
Figure 5.4 - a) Relationship between the overall equivalent behavior similar to plastic strain energy density and number of load recovery cycles for the different PCL samples after different cell culture conditions, b) Comparison of experimental and predicted fatigue behaviors, calculated according to Morrow's model.

Table 5.2 - Fitting results after Morrow's model (equation 2) for the different PCL scaffolds and after the different cell culture conditions.

Sample	m	C
PCL	0.24 ± 0.05	2500 ± 600
PCL + Fibrin	0.27 ± 0.04	2100 ± 660
PCL+PVA 6 cycles	0.16 ± 0.04	1865 ± 170
Free-swelling	0.22 ± 0.02	1445 ± 373
Bioreactor	0.20 ± 0.02	1171 ± 314

PCL constructs mechanical life cycle performance was calculated according to the fitting parameters obtained by Morrow's model (Table 5.2) and compared to the experimental results. The calculated values from the Morrow's model obtained for each sample was plotted versus the experimental ones in Figure 5.4. In this figure, perfect correlation would be represented by data points lying on the solid diagonal line, and the dashed lines on either side of the diagonal represent error bands of a factor of 10 [32]. Figure 5.4 shows that the model is

able predict successfully the load recovery cycle behavior of PCL, PCL + fibrin and PCL cell seeded under free-swelling and dynamical loading. It was previously observed that the mechanical hysteresis of PCL scaffolds and its fatigue behavior is affected by the presence of water inside of porous structure, the main contribution of material fatigue behavior being given by aqueous media that acts as plasticizer and promotes a uniform distribution of the applied stress along the sample and not only in the trabeculae of PCL [10]. Moreover, the incorporation of fibrin without cells or even PVA with different freeze/thawing cycles inside of polymer porous does not influence the fatigue material performance [30] as much as the cell culture in different conditions does.

Figure 5.4b shows that the mechanical stability of PCL scaffolds after cell seeding was increased up to 600 cycles, which is higher than the ones observed for the PCL, PCL + fibrin and PCL filled with PVA,. This result indicates that the material behavior is influenced by the presence of the ECM inside the porous scaffold and the mechanical behavior depends on factors related to the matrix generated by cells and not only on polymer elasticity and water homogenous distribution.

Failure can come from different reasons, such as physical and mechanical gaps between the scaffold and the matrix. The fatigue analysis was performed without cell fixation, in order to avoid chemical modification of the ECM and consequent artifacts on the mechanical measurements. However, these are performed in a harsh hypotonic environment, without proper nutrients and sterility, thus cells can die in the process. Although cells by themselves should not contribute to mechanical resistance of the construct, it is not known whether cell death can be affecting the ECM at the end. This problem can be addressed by evaluating matrix composition before and after the mechanical measurements.

5.3.5 Quantitative real-time Polymerase Chain Reaction
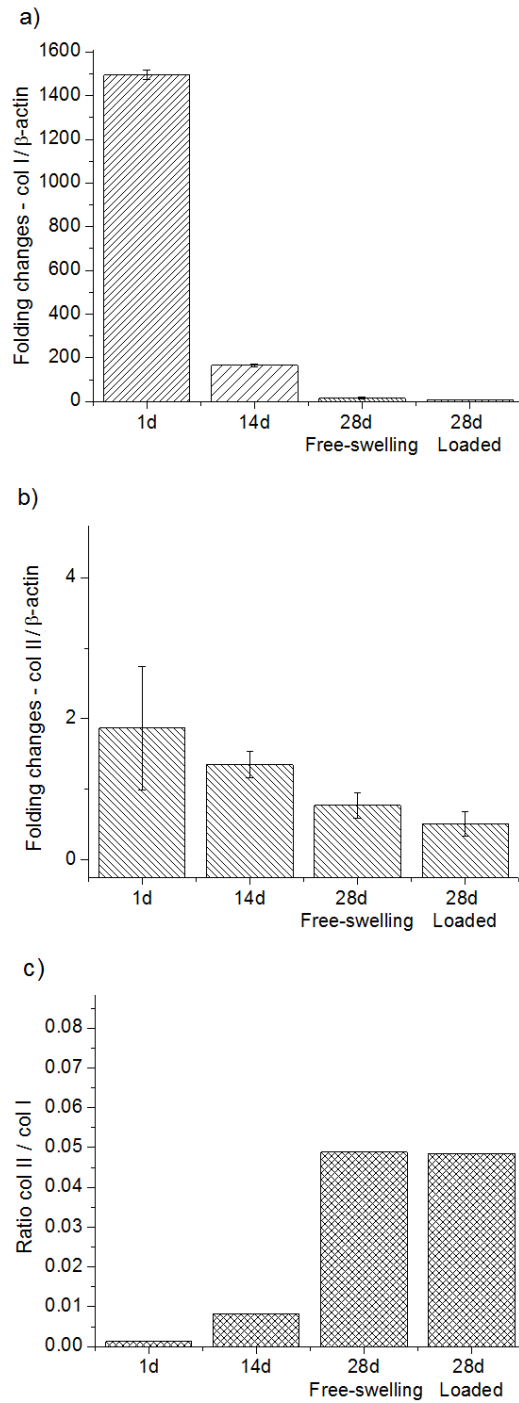
Figure 5.5 - Folding changes (initial value of 2) with respect to β-actin housekeeping gene for a) collagen type I and b) collagen type II. c) Ratio of expression between collagen type I and type II.

The expression of collagen type I strongly decrease after 14 and 28 days of cell culture, indicating a reduction on fibrous-like matrix component (Figure 5.5). However, there are no relevant changes in expression of collagen type II through time (a slight non-significative reduction, according to ANOVA contrasted with Tukey test). The ratio of expression between collagen type II and type I is subsequently increased with time, although at the end of the experiments there is still more relative expression of collagen type I than type II (ratio col II/col I is lower than 1). No differences are observed between samples under mechanical stimulus and under free-swelling conditions.

KUM5 cells are precursors from mesenchymal origin that express collagen type II even without induction of differentiation [17]. In our case, expression of collagen type II did not increase with time, suggesting that there is no induction by the specific medium nor the mechanical loads of chondrogenic trait. Nevertheless, there is a trend for reduction of collagen type I, indicating a decrease of that fibrocartilage component [33]. This result, combined with the fact that no other matrix components and no other quantitative analysis for matrix deposition were performed, does not allow concluding that a chondrogenic matrix was obtained. An accurate analysis of fibrin degradation was not carried out, but most of the fibrin should have disappeared after 14 days. The presence of fibrin and its degradation rate can have an effect in the type of matrix that is produced. Although it can be thought that a culture without fibrin could have provided insight as a negative control, the size of the pores is bigger than the diameter of cells, and the surfaces of a scaffold of these characteristics, without a pericellular matrix, could act as a 2D surface [26, 27] , introducing geometric variables that would hinder comparisons. It is important to remark that fibrin, in absence of mechanical stimuli, induces more fibrous tissues in mesenchymal cells and favor, for example, myogenesis over chondrogenesis [13]. It is possible that the initial two weeks of cell culture in the fibrin matrix without loading hinder production of collagen II, but the medium compensates some effects as the collagen type I expression is reduced. The lack of response of cells to mechanical loading could be also related with fibrin, as it has been found that cyclic loading in fibrin hydrogels provokes mesenchymal stem cells to keep undifferentiated traits at the initial stages [13]. If not all fibrin has been degraded when loading starts to be applied, or if the substitute matrix is of fibrous nature, it could be contributing to the absence of differences with dynamic loading during cell culture. This effect can be also caused by the scaffold permanent deformation.

5.4 Conclusions

Despite the biochemical composition, the produced matrix has a clear effect in modifying the fatigue properties of the constructs. Above all, presence of matrix results in different fitting values and better correlation to Morrow's model than any PCL scaffold without cells. When compared with a scaffold with the pores filled with a PVA gel (freeze-thawing 6 cycles), if the elastic modulus is the only parameter observed, samples with cells would be categorized as with the same mechanical properties than the latter. Therefore, a main conclusion and consideration can be taken, and it is valid even with the matrix conditions: Elastic modulus cannot be the only descriptor necessary to characterize mechanical functionality of in vitro constructs with cells. It remains unclear if a more chondrogenic matrix were achieved; the resistance to fatigue would improve. If in the limited conditions of this study it does, and produces different results that scaffolds without cells with and without hardened PVA, it is reasonable to think that with more chondrogenic induction the response to fatigue it would be also different to those cases.

5.5 References

1. Bobick, B.E., et al., *Regulation of the chondrogenic phenotype in culture.* Birth Defects Res C Embryo Today, 2009. 87(4): p. 351-71.
2. Csaki, C., P.R. Schneider, and M. Shakibaei, *Mesenchymal stem cells as a potential pool for cartilage tissue engineering.* Ann Anat, 2008. 190(5): p. 395-412.
3. Schulz, R.M. and A. Bader, *Cartilage tissue engineering and bioreactor systems for the cultivation and stimulation of chondrocytes.* Eur Biophys J, 2007. 36(4-5): p. 539-68.
4. Yoo, J.U., et al., *The chondrogenic potential of human bone-marrow-derived mesenchymal progenitor cells.* J Bone Joint Surg Am, 1998. 80(12): p. 1745-57.
5. Demarteau, O., et al., *Dynamic compression of cartilage constructs engineered from expanded human articular chondrocytes.* Biochem Biophys Res Commun, 2003. 310(2): p. 580-8.

6. Li, Z., et al., *Chondrogenesis of human bone marrow mesenchymal stem cells in fibrin-polyurethane composites is modulated by frequency and amplitude of dynamic compression and shear stress.* Tissue Eng Part A, 2010. 16(2): p. 575-84.

7. Ergun, A., et al., *In vitro analysis and mechanical properties of twin screw extruded single-layered and coextruded multilayered poly(caprolactone) scaffolds seeded with human fetal osteoblasts for bone tissue engineering.* J Biomed Mater Res A, 2011. 99(3): p. 354-66.

8. Mars, W.V., *Factors that affect the fatigue life of a rubber: a literature survey.* Journal of Rubber Chemistry and Technology, 2004. 77(3): p. 391-412.

9. Ince, A. and G. Glinka, *A modification of Morrow and Smith–Watson–Topper mean stress correction models.* Fatigue & Fracture of Engineering Materials & Structures, 2011. 34(11): p. 854-867.

10. Panadero, J.A., et al., *Fatigue prediction in fibrin poly-epsilon-caprolactone macroporous scaffolds.* J Mech Behav Biomed Mater, 2013. 28: p. 55-61.

11. Morrow, J.D., *Internal Friction, Damping, and Cyclic Plasticity*, in *ASTM-STP 378*1965: Philadelphia.

12. Lee, K.Y. and D.J. Mooney, *Hydrogels for Tissue Engineering.* Chemical Reviews, 2001. 101(7): p. 1869-1880.

13. Thorpe, S.D., et al., *European Society of Biomechanics S.M. Perren Award 2012: the external mechanical environment can override the influence of local substrate in determining stem cell fate.* J Biomech, 2012. 45(15): p. 2483-92.

14. Steward, A.J., et al., *Cell-matrix interactions regulate mesenchymal stem cell response to hydrostatic pressure.* Acta Biomater, 2012. 8(6): p. 2153-9.

15. Wong, B.L. and R.L. Sah, *Effect of a focal articular defect on cartilage deformation during patello-femoral articulation.* Journal of Orthopaedic Research, 2010. 28(12): p. 1554-1561.

16. Guilak, F., A. Ratcliffe, and V.C. Mow, *Chondrocyte deformation and local tissue strain in articular cartilage: A confocal microscopy study.* Journal of Orthopaedic Research, 1995. 13(3): p. 410-421.

17. Sugiki, T., et al., *Hyaline cartilage formation and enchondral ossification modeled with KUM5 and OP9 chondroblasts.* J Cell Biochem, 2007. 100(5): p. 1240-54.

18. Huang, A.H., M.J. Farrell, and R.L. Mauck, *Mechanics and mechanobiology of mesenchymal stem cell-based engineered cartilage.* J Biomech, 2010. 43(1): p. 128-36.

19. Thorpe, S.D., et al., *Dynamic compression can inhibit chondrogenesis of mesenchymal stem cells.* Biochem Biophys Res Commun, 2008. 377(2): p. 458-62.

20. Chomczynski, P., *A reagent for the single-step simultaneous isolation of RNA, DNA and proteins from cell and tissue samples.* Biotechniques, 1993. 15(3): p. 532-4, 536-7.

21. Livak, K.J. and T.D. Schmittgen, *Analysis of relative gene expression data using real-time quantitative PCR and the 2(-Delta Delta C(T)) Method.* Methods, 2001. 25(4): p. 402-8.

22. Lebourg, M., J. Suay Anton, and J.L. Gomez Ribelles, *Hybrid structure in PCL-HAp scaffold resulting from biomimetic apatite growth.* J Mater Sci Mater Med, 2010. 21(1): p. 33-44.

23. Lebourg, M., J. Suay Antón, and J.L. Gomez Ribelles, *Characterization of calcium phosphate layers grown on polycaprolactone for tissue engineering purposes.* Composites Science and Technology, 2010. 70(13): p. 1796-1804.

24. Deplaine, H., J.L.G. Ribelles, and G.G. Ferrer, *Effect of the content of hydroxyapatite nanoparticles on the properties and bioactivity of poly(l-lactide) – Hybrid membranes.* Composites Science and Technology, 2010. 70(13): p. 1805-1812.

25. Martinez-Diaz, S., et al., *In vivo evaluation of 3-dimensional polycaprolactone scaffolds for cartilage repair in rabbits.* Am J Sports Med, 2010. 38(3): p. 509-19.

26. Olmedilla, M.P., et al., *In vitro 3D culture of human chondrocytes using modified epsilon-caprolactone scaffolds with varying hydrophilicity and porosity.* J Biomater Appl, 2012. 27(3): p. 299-309.

27. Wheeldon, I., et al., *Nanoscale tissue engineering: spatial control over cell-materials interactions.* Nanotechnology, 2011. 22(21): p. 212001.

28. Lebourg, M., et al., *Cell-free cartilage engineering approach using hyaluronic acid-polycaprolactone scaffolds: a study in vivo.* J Biomater Appl, 2014. 28(9): p. 1304-15.

29. Steward, A.J., D.R. Wagner, and D.J. Kelly, *The pericellular environment regulates cytoskeletal development and the differentiation of mesenchymal stem cells and determines their response to hydrostatic pressure.* Eur Cell Mater, 2013. 25: p. 167-78.

30. Panadero, J.A., et al., *In vitro mechanical fatigue behaviour of poly-ε-caprolactone macroporous scaffolds for cartilage tissue engineering. Influence of pore filling by a poly(vinyl alcohol) gel.* Journal of Biomedical Materials Research: Part B - Applied Biomaterials, 2014. Accepted.

31. Vikingsson, L., et al., *An "in vitro" experimental model to predict the mechanical behavior of macroporous scaffolds implanted in articular cartilage.* Journal of the Mechanical Behavior of Biomedical Materials, 2014. 32(0): p. 125-131.

32. Kanchanomai, C. and Y. Mutoh, *Low-cycle fatigue prediction model for pb-free solder 96.5Sn-3.5Ag.* Journal of Electronic Materials, 2004. 33(4): p. 329-333.

33. Richter, W., *Mesenchymal stem cells and cartilage in situ regeneration.* J Intern Med, 2009. 266(4): p. 390-405.

34. Wong, M. and D.R. Carter, *Articular cartilage functional histomorphology and mechanobiology: a research perspective.* Bone, 2003. 33(1): p. 1-13.

Chapter 6: Conclusions and Future work
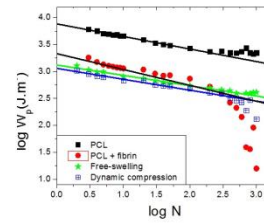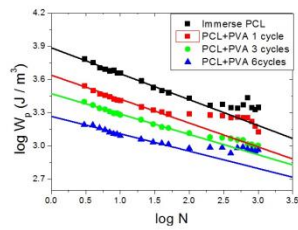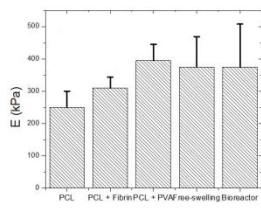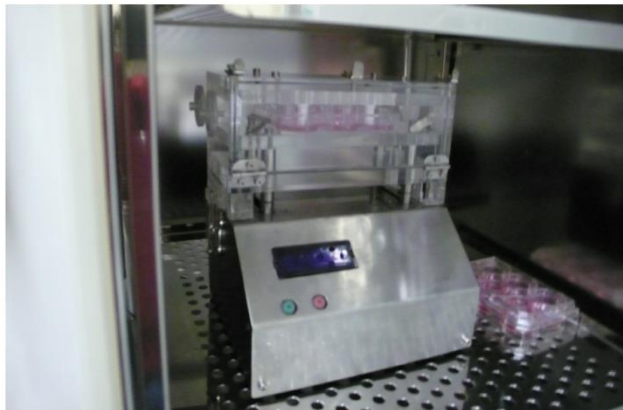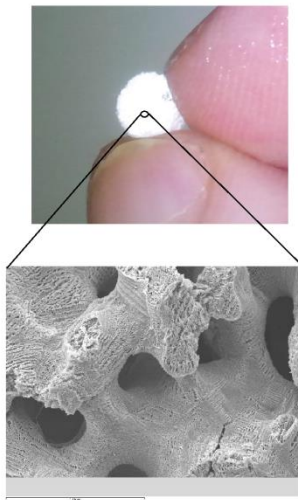
6.1 Conclusions

There is a strong need to understand the mechanical performance of scaffold biomaterials for cartilage tissue engineering, which must sustain cyclic loading in the knee. One of the properties that can provide relevant information is the resistance to fatigue.

In this work, macroporous poly-ε-caprolactone (PCL) scaffolds were produced and their fatigue behavior analyzed by the Morrow´s model. Since the behaviour of the scaffold in dry state is not representative of that in the aqueous media found *in vitro* and *in vivo* models, the analysis was also performed in water immersion. It was found that water inside the pores plays a critical effect in improving resistance to fatigue. However, a fibrin hydrogel, a usual component in knee surgery, does not influence fatigue behavior significantly

Further, a poly(vynil-alcohol) (PVA) hydrogel was introduced in the PCL scaffolds in order to simulate a growing tissue within the pores. It has been observed that fatigue resistance is improved when the stiffness of the hydrogel but, on the other hand, the experimental data deviated from the applied model after few cycles, indicating the influence of other relevant aspects not considered in this model.

Finally, a bioreactor suitable for cell culture conditions was designed and built to simulate the mechanical cyclic loading *in vivo*. The bioreactor was used to apply loading to chondrogenic precursor cell culture in PCL scaffolds with fibrin and the results were compared with free-swelling culture conditions. There were not significant differences between both culture conditions. However, relatively to mechanical resistance to fatigue, it was found that the extracellular matrix properties improved fatigue resistance of PCL scaffolds, when compared with other fillers like PVA, despite the fact that the measured elastic modulus at the first cycle was similar in all the cases.

Thus, it has been shown that fatigue analysis provides additional information to understand mechanical properties of biomaterials. The observed differences in the PCL samples tested under different conditions undoubtedly determine their fatigue behavior. The porosity of the scaffolds adds complexity to the fatigue behavior and limits the application of suitable models, as pore geometry and interconnectivity is not regular. Further, when other materials

such as PVA or an ECM are present within the PCL scaffold, the fatigue behavior is influenced due to surface interactions

Once the scaffold is implanted in a cartilage defect, with a therapy that combines microfracture of subchondral bone and scaffold implantation, the pore structure is filled first by a fibrin clot and physiologic fluids. The results obtained in this thesis show that pore filling significantly influences the mechanical behavior of the material in particular its performance under dynamic compression. Then the substitution of fibrin matrix by the extracellular matrix produced by the cells is expected to further modify the properties of the scaffold / newly formed tissue construct.

Quite unexpectedly we observed no significant differences in cell cultures under mechanical stimulus and in free-swelling, neither in mechanical properties nor in gene expression. Nevertheless this could be a feature restricted to the selected cell line that cannot be extended to human mesenchymal stem cells. Anyway, the main conclusion of this thesis is still valid: the analysis of fatigue is an interesting methodology to add to standard methods for mechanical evaluation of the scaffolds, as it provides relevant information. Samples with similar starting parameters (PCL+PVA and PCL+ECM) can behave differently under cyclic loading. Fatigue is related with the extension of pre-existing cracks in materials, but in these constructs, the reasons for fatigue can be related also with the intrinsic structural properties of the extracellular matrix and its discontinuations in the boundaries with the porous scaffold.

6.2 Future work

In order to continue with this investigation, it would be interesting to extend the fatigue analysis to different frequencies, especially from 0.1 Hz to 10 Hz, which is the typical range of loading frequencies in the human knee. Other conditions that approximate more to the knee *in vivo* environment would be important to improve the model (temperature, ionic strength of the aqueous medium, etc.). Further steps would require modifying the porosity internal geometry of the samples, in order to obtain a relation of the decrease of dissipated energy and the structure. In a broader study, it would be applicable to other materials suitable for cartilage tissue engineering.

For cell culture on *in vitro* models, it would be important to work with human primary MSCs. Other variations in culture conditions may include different medium, fibrin concentration and controls without fibrin.

In order to highlight the effects of the extracellular matrix and its interaction with the scaffolds walls, atomic force microscopy could be used to produce cyclic loading with the microcantilever tip in specific regions of the constructs.

A final stage of this investigation would relate improved models of fatigue evolution with components of the extracellular matrix. At the beginning could be enough with a broad battery of matrix markers, but the peak of the research would involve transcriptomics (or even proteomics) with mRNA chips, to correlate a complete expression data with the mechanical properties.